PHYSICAL REVIEW
LETTERS

VOLUME 4 MARCH 1, 1960 NUMBER 5

POSSIBLE NEW EXPERIMENTAL TEST OF GENERAL RELATIVITY THEORY*

L. I. Schiff
Institute of Theoretical Physics, Department of Physics, Stanford University, Stanford, California
(Received February 11, 1960)

In a paper now in process of publication,[1] it is argued that only the planetary orbit precession provides real support for the full structure of the general theory of relativity. The other two of the three "crucial tests," the gravitational red shift and deflection of light, can be inferred correctly from the equivalence principle and the special theory of relativity, both of which are well established by other experimental evidence. It is also pointed out that a terrestrial or satellite experiment that would really test general relativity theory would have either to use particles of finite rest mass in such a way that the equation of motion can be confirmed beyond the Newtonian approximation, or to verify the second-order deviations of the metric tensor from its Minkowski form.

In an attempt to devise a feasible experiment that might accomplish one of these objectives, we have calculated the properties of a spinning test particle (torque-free gyroscope). We start from the covariant equations of Papapetrou[2] for the motion of the center of mass and the spin angular momentum, generalized by inclusion of a nongravitational constraining force $\vec{F}$, and work to lowest order. The motion of the center of mass in the gravitational field of the rotating earth is then described by the Newtonian equation

$$m(d\vec{v}/dt) = -(GmM/r^3)\vec{r} + \vec{F}, \tag{1}$$

where m is the rest mass of the particle, $\vec{r}$ is its coordinate, $\vec{v} = d\vec{r}/dt$ is its velocity, G is the Newtonian gravitational constant, and M is the mass of the earth. The spin angular momentum vector measured by a co-moving observer, $\vec{S}^0$, obeys the equation

$$d\vec{S}^0/dt = \vec{\Omega} \times \vec{S}^0, \tag{2}$$

where

$$\vec{\Omega} = (\vec{F} \times \vec{v})/2mc^2 + (3GM/2c^2r^3)(\vec{r} \times \vec{v}) + (GI/c^2r^3)[3(\vec{\omega}\cdot\vec{r})\vec{r}/r^2 - \vec{\omega}]; \tag{3}$$

$I = 2MR^2/5$ is the moment of inertia of the earth of radius R, assumed to be homogeneous, and $\vec{\omega}$ is its angular velocity vector. The first term on the right side of (3) is the Thomas precession,[3] which is a special relativity effect. The other two are the lowest order effects of general relativity; the second term arises whether or not the earth is rotating, and the third term is the earth rotation effect of Lense and Thirring.[4] While the second term involves the first-order deviations of the metric tensor from its Minkowski form, which can be calculated without the use of general relativity,[1] it also depends on the equation of motion of matter of finite rest mass beyond the Newtonian approximation. It is therefore a genuine consequence of general relativity. The same is true of the third term, since in addition it depends on off-diagonal space-time components of the metric tensor.

Equations (2) and (3) may be obtained either from the standard or the isotropic form of the Schwarzschild line element, and using for the supplementary condition on the angular momentum tensor either that of Corinaldesi and Papapetrou[5] or of Pirani.[6] The equation of motion of the spin in the nonrotating, earth-centered co-

ordinate system looks quite different in these four cases, but they all agree when expressed in terms of the spin measured by a co-moving observer. It should also be remarked that the corrections to Eq. (1) that arise from the spin are unobservably small in any realizable situation.

It follows at once from the form of Eq. (2) that the magnitude of the spin angular momentum measured by a co-moving observer is constant in time. Thus if the moment of inertia of the spinning particle does not change, the angular velocity of rotation is constant, and the spinning particle behaves like a clock which can be set to any desired frequency. This frequency exhibits Doppler and gravitational shifts when observed from outside, just like that of a more conventional clock. It is possible that its frequency stability could be made to compare favorably with those of other types of precision clocks. It also follows from (2) that a number of spinning particles with various magnitudes and directions for their angular momentum vectors maintain fixed angles of these vectors with respect to each other. The vector $\vec{\Omega}$, which in general is not constant, is their common angular velocity of precession with respect to the external "fixed stars"; in comparing their directions with the outside world, a correction must of course be made for aberration whenever $\vec{v} \neq 0$.

If a spinning particle is in free fall, as in a satellite, then $\vec{F} = 0$. For an orbit in the earth's equatorial plane, for example,

$$\vec{\Omega} = (3GM/2c^2r)\vec{\omega}_0 - (2MGR^2/5c^2r^3)\vec{\omega}, \qquad (4)$$

where $\vec{\omega}_0 = (\vec{r}\times\vec{v})/r^2$ is the instantaneous orbital angular velocity vector of the particle. The minus sign in Eq. (4) deserves some comment. The third term of Eq. (3) tends to cause a spinning particle to precess in the same direction as the rotating earth at the poles ($\vec{r}$ parallel or antiparallel to $\vec{\omega}$), but in the opposite direction at the equator ($\vec{r}$ perpendicular to $\vec{\omega}$). This is physically reasonable if we think of the moving earth as "dragging" the metric with it to some extent. At the poles, this tends to drag the spin around in the same direction as the rotation of the earth. But at the equator, since the gravitational field falls off with increasing r, the side of the spinning particle nearest the earth is dragged more than the side away from the earth, so that the spin precesses in the opposite direction.

If the center of mass of the spinning particle is constrained to remain at rest with respect to the rotating earth, as in an earth-bound laboratory,[7] then

$$\vec{v} = \vec{\omega}\times\vec{r}, \quad d\vec{v}/dt = \vec{\omega}\times\vec{v}. \qquad (5)$$

The required constraining force $\vec{F}$ can then be found from (1) and (5), and substituted into (3). When the particle is at the surface of the earth at latitude λ, the precession angular velocity may be written in the form

$$\vec{\Omega} = [(4gR/5c^2)(1+\cos^2\lambda) - (\omega^2R^2/2c^2)\cos^2\lambda]\vec{\omega} + (4g\sin\lambda/5\omega c^2)(\vec{\omega}\times\vec{v}), \qquad (6)$$

where $g = GM/R^2$ is the acceleration of gravity at the surface of the earth. Only the square bracket term in Eq. (6) gives rise to a secular precession of the spin axis, and the second part of it is very small compared to the first. Thus to good approximation, a particle with spin axis perpendicular to the earth's axis precesses at the rate $2\pi(4gR/5c^2)(1+\cos^2\lambda) = 3.5\times10^{-9}(1+\cos^2\lambda)$ radians per day. It also follows from Eq. (3) that the corresponding effects caused by the sun and moon are negligibly small in comparison.

A secular precession of 6×10^{-9} radian per day would be very difficult, but perhaps not impossible, to observe. Professor W. M. Fairbank and Professor W. A. Little of this department are exploring the possibility of using for this purpose a gyroscope that consists of a superconducting sphere supported by a static magnetic field.[8] Such a gyroscope would also be of interest as a device for performing experiments in low-temperature physics. If it could be made to operate exceedingly well, it might in addition be used for an experimental test of Mach's principle, by comparing the orientation of its axis with a field of "fixed stars" over a period of a year or so. Most of the experimental difficulties that seem to arise with a high-precision gyroscope are greatly reduced if the gyroscope does not have to be supported against gravity. This, together with the fact that ω_0 is generally much larger than ω, suggests that experiments of this type might be more easily performed in a satellite than in an earth-bound laboratory.

A full account of this work will be submitted shortly for publication in the Proceedings of the National Academy of Sciences.

---

*Supported in part by the U. S. Air Force through the Air Force Office of Scientific Research.

[1]L. I. Schiff, Am. J. Phys. (to be published).
[2]A. Papapetrou, Proc. Roy. Soc. (London) A209, 248 (1951).
[3]L. H. Thomas, Phil. Mag. 3, 1 (1927).
[4]J. Lense and H. Thirring, Phys. Z. 29, 156 (1918).
[5]E. Corinaldesi and A. Papapetrou, Proc. Roy. Soc. (London) A209, 259 (1951).
[6]F. A. E. Pirani, Acta Phys. Polon. 15, 389 (1956). Our Eqs. (2) and (3) are generalizations of some of the results derived by Pirani.
[7]This type of experiment was suggested to the author by W. M. Fairbank.
[8]I. Simon, J. Appl. Phys. 24, 19 (1953); J. Instr. Soc. Am. 1, No. 9, 79 (1954).

BUMPY TORUS*

Gordon Gibson,† Willard C. Jordan,‡ and Eugene J. Lauer
Lawrence Radiation Laboratory, University of California, Livermore, California
(Received February 1, 1960)

Magnetic field configurations resulting from various coil arrangements are being used for thermonuclear studies. In the absence of particle interactions, charged particles which occupy certain regions of velocity space are contained indefinitely provided the particles behave adiabatically. However, there are regions in velocity space in which particles are not contained; e.g., in the mirror machine if the velocity vector of a charged particle makes a sufficiently small angle with the magnetic field the particle escapes through a mirror.[1] Hence, the mean containment time is limited to approximately the time, τ_S, for small-angle scattering to cumulate to a large angle insofar as multiple scattering is the dominant loss mechanism.

A uniformly wound torus would eliminate the end losses; however, another difficulty is introduced. Because of the drift of the charged particles resulting from the gradient of the magnetic field, the particles rapidly impinge on the walls of the device.

A simple case to illustrate the drift motion both in a magnetic mirror machine and in the torus is one where the velocity, v, of the particle is normal to the magnetic field, H, and the longitudinal gradient of the field is zero. The magnetic moment, μ, of the particle motion is an adiabatic invariant[2]; therefore $\mu = W_\perp/H = \frac{1}{2}mv_\perp^2/H$ = constant, and if the particle's energy, W, is a constant the particle's guiding center moves along a path defined by H = constant. The particle drifts are illustrated in Fig. 1.

A rotational transform[3] tends to reduce the loss due to drifts in the torus. However, the rotational transform may be ineffective if the particle motion along the field lines is slow (relative to the drift velocity), with the result that the containment time would again be limited to approximately the scattering time τ_S. The electric field and other phenomena associated with a dense plasma would also affect the containment time.

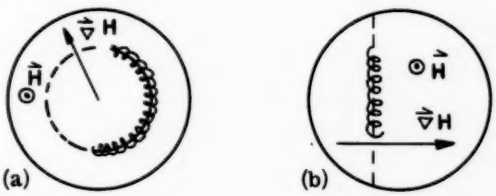

FIG. 1. Particle drift paths. (a) Mirror machine cross section, median plane. (b) Uniformly wound torus cross section.

In this paper the single-particle motion in the magnetic field created by a circular array of circular current loops is investigated (see Fig. 2). The extent to which this geometry would have the advantage of closed precessional sur-

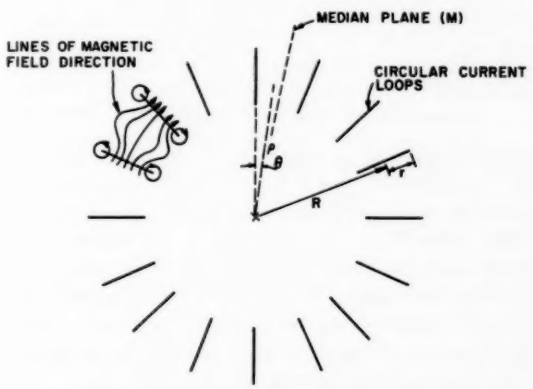

FIG. 2. The bumpy torus geometry and field magnitudes. The symmetry plane, S, is the plane of the sheet of paper.

faces which would not intersect the walls [see Fig. 1(a)], and would also eliminate end effects,[4] is investigated. Because of the complexity of a 3-dimensional calculation, the results in this paper are limited to an investigation of the intersection of the precessional surfaces with the symmetry plane containing the torus. The single-particle model is of special interest during the plasma buildup stage in the high-energy injection schemes.[5,6] The stability of a plasma has not been investigated theoretically for this geometry; of course if a plasma would build up, the cooperative effects could be observed experimentally.

It is assumed that the following quantities are constants of the motion: (1) the kinetic energy, W; (2) the magnetic moment, $\mu = W_{\perp}/H$; and (3) the action integral, $J = \int p_{\parallel} dl$, evaluated over a period (as defined later) of the longitudinal motion, where $p_{\parallel}$ is the component of the momentum parallel to the field and dl is the element of path length parallel to the field.[7]

The IBM 650 is being used to calculate (1) the magnitude of the magnetic field, (2) the direction of the magnetic field, and (3) the action integral for particular values of the magnetic moment and starting coordinates.

The code is set up to calculate these quantities in the symmetry plane S (see Fig. 2) for N equally spaced circular current loops (current I) with a ratio of major radius divided by current loop radius, R/r. Because of the symmetry it is only necessary to investigate the region between a median plane and the plane of an adjacent current loop.

Taking account of the constancy of the kinetic energy and of the magnetic moment, the action integral may be written as

$$J = mv \int \left(1 - \frac{H}{H_0} \sin^2\delta\right)^{1/2} dl,$$

where mv is the momentum, H_0 is the initial field magnitude, and δ is the initial angle that the velocity makes with the field direction. For a given value of μ, this integral is calculated as a function of the radial position of the starting point in the median plane, M. The integrals are stopped either at the turning point where $v_{\parallel}$ has decreased to zero or at the plane of the adjacent coil if there is no turning point.[8]

Figure 3 shows the results of the action integral calculations for seven values of μ and also some of the field magnitude calculations that

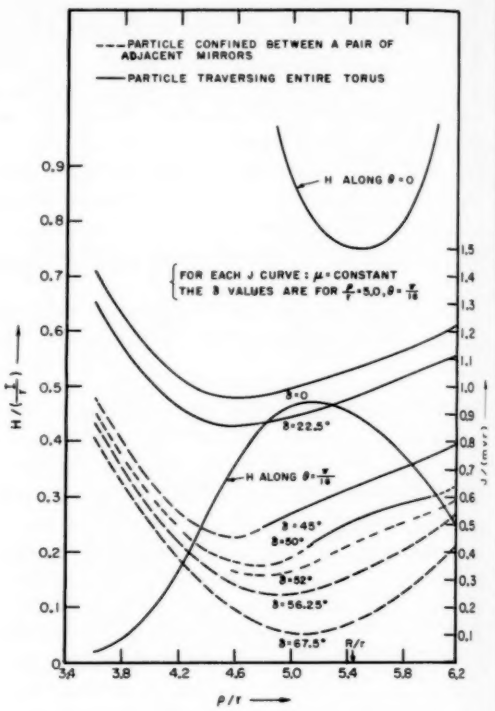

FIG. 3. Adiabatic invariants and field magnitudes for a bumpy torus with $N = 16$ and $R/r = 5.44$.

have been obtained for the case of $N = 16$ and $R/r = 5.44$. All of the action integral curves have a minimum (for $J \neq 0$). Choosing a particular curve of μ = constant, then for a chosen value of J the two values of ρ (inner and outer), where the precessional surface intercepts the plane of symmetry S, are uniquely determined. It is most unlikely that these surfaces are not closed outside of the S plane; however, a 3-dimensional calculation is required for a rigorous proof.

For the particular case of precession in the median plane M, $J = 0$ and the intercepts of the precessional surface are not defined. However, as shown above, the precession for this special case is constrained to a path along which H = constant. The plot of H vs ρ/r in the plane S has a maximum (this must be a maximum for displacements out of the plane S also). Thus, inner and outer intercepts for the precessional curve (which must be closed) with the plane of symmetry S may be found from the curve of H vs ρ in the median plane. In the limit as μ approaches the value characteristic of a particle trapped in

the median plane (holding the kinetic energy constant), the intercepts predicted by the J curves appear to approach those predicted by the median-plane H curve as they should.

In case $v_{\parallel}$ is nearly zero at a mirror (transition from dashed to solid lines in Fig. 3), J does not necessarily remain constant in time (see footnote[8]). Such a particle has $v_{\perp} \simeq v$ = constant and so follows a closed precessional curve for which H = constant in the plane of the coil (i.e., at $\theta = 0$).

Another special case is for $\mu = 0$. In this instance J is proportional to the length of the field line (over the path of integration), and since J is shown to have a minimum value in the S plane this is certainly a minimum with respect to displacements out of the S plane also. Hence, these precessional surfaces are closed.

Scattering can change the value of μ suddenly so that a vertical transition occurs in Fig. 3 from one of the μ = constant curves to another at a nearly constant ρ. After the transition the particle is constrained to the new precessional surface associated with the new values of μ and J until another scattering occurs. Since the J vs ρ curves do not all have the same shape and since their minima do not all occur at a single value of ρ, scattering can result in a new type of diffusion, that is, the particles can diffuse onto larger and larger diameter precessional surfaces. (This diffusion is independent of the orbit diameter.) It is planned to investigate different values of N and R/r. Increasing N and R/r proportionally should enable one to approach the degenerate case of a linear series of mirror machines and hence reduce the effect of this new type of diffusion. Initial results with $N = 4 \times 16$ or 64 and $R/r = 4 \times 5.44$ or 21.76 indicate that the minimum number of 90° changes in pitch angle of the velocity that can change the diameter of the precessional surfaces by an amount equal to the coil radius is approximately three for particle positions such that the distance from the axis is $\geq r$. Hence it is expected that the mean time for this change is about $3^2\tau_S$, or $9\tau_S$.

We are grateful for the use of the results of T. G. Northrop and E. Teller prior to publication. This work was carried out with the support and encouragement of C. M. Van Atta. The numerical work was done by J. L. Brady, T. H. Haratani, and B. Williams.

---

*This work was done under the auspices of the U. S. Atomic Energy Commission.

†Visiting from Westinghouse Atomic Power Department, Pittsburgh, Pennsylvania.

‡Visiting from Bendix Aviation Corporation, Research Laboratory Division, Detroit, Michigan.

[1]E. Fermi, Phys. Rev. 75, 1169 (1949).

[2]H. Alfvén, Cosmical Electrodynamics (Oxford University Press, New York, 1948), p. 21.

[3]L. Spitzer Jr., Phys. Fluids 1, 253 (1958).

[4]B. B. Kadomtsev, Plasma Physics and the Problem of Controlled Thermonuclear Reactions (Akad. Nauk. USSR, 1958), Vol. III, p. 285. A recent translation of this Russian paper indicates that G. I. Budker independently has suggested the possibility of stabilizing drifts by means of a "corrugated field." In this paper Kadomtsev analyzes field configurations resulting from linear series of mirror machines connected by uniform field "sleeves."

[5]A. Simon, Phys. Fluids 1, 495 (1958).

[6]G. Gibson, W. A. S. Lamb, and E. J. Lauer, Phys. Rev. 114, 937 (1959).

[7]T. G. Northrop and E. Teller have recently shown that the particle drifts are such as to conserve the action integral for a general mirror-type field: University of California Radiation Laboratory Report UCRL-5615, 1959 (unpublished). This has also been proven by Kadomtsev (see reference 5).

[8]The justification for this assumption is that it makes J approach the same value in two limiting cases (holding the kinetic energy and the magnetic moment constant): (1) for a particle that is trapped between two adjacent mirrors as the turning point approaches the mirror, and (2) for an untrapped particle as $v_{\parallel}$ at the mirror approaches zero. A more detailed analysis of this case should be made because the longitudinal period becomes very long as the above limit is approached, and the action integral theorem is not proven for this case.

EVIDENCE FOR THE QUANTIZATION OF CIRCULATION IN LIQUID HELIUM II*

C. E. Chase
Lincoln Laboratory, Massachusetts Institute of Technology, Lexington, Massachusetts
(Received January 29, 1960)

According to the theory of Onsager[1] and Feynman,[2] rotating liquid helium II should contain an array of vortex lines arranged parallel to the axis of rotation and approximately evenly distributed throughout the liquid; the circulation around these lines should be quantized in multiples of h/m, where m is the mass of the helium atom. The lowest energy state of this system would arise when each line had only one quantum of circulation associated with it; the number of lines per square centimeter crossing a plane normal to the axis of rotation would then be $2\omega m/h$. Although there is some experimental evidence in favor of this model,[3,4] the actual quantization of the circulation has not yet been established in an entirely convincing manner.[5] This Letter reports preliminary measurements of the effect of rotation upon the critical heat current W_c in a channel of moderate dimensions. The most straightforward interpretation of the results of these experiments suggests that quantized circulation is indeed a property of the rotating state, although the possibility of some other explanation cannot be positively excluded at this time.

The apparatus (Fig. 1) consists of a thin-walled stainless steel tube C, 0.262 cm in diameter by 5.16 cm long, one end of which is attached to a chamber A containing a heater H and a resistance thermometer T_1; the other end opens into the helium bath, where a second thermometer T_2 is located. The entire assembly is surrounded by a vacuum jacket D. Heat currents are generated by the heater H, and the resulting temperature gradient is measured by observing the difference between T_1 and T_2 on a 33-cycle differential thermometer bridge. C is packed with 70 stainless steel wires, 0.025 cm in diameter, producing a large number of small parallel channels of irregular cross section (these wires have been omitted from the figure for clarity). The apparatus can be rotated about the axis shown in the figure at any speed up to about 6 rad/sec by means of a variable-speed motor mounted outside the cryostat. Critical heat currents were measured by an ingenious method proposed by Vinen.[6] This method depends upon the fact that, when a heat current is switched on in undisturbed liquid helium, mutual friction only appears after a time τ of the order of several seconds, but that this time is greatly reduced if a heat current W_1 greater than the critical value is initially present. By measuring τ as a function of W_1, it is thus possible to determine W_c with a precision limited only by the size of the increments in W_1 used in the experiment. In the present case the resulting uncertainty in W_c was usually ± 0.001 watt/cm^2, although it was occasionally twice as large. Further experimental details will be given in a later publication.

In Fig. 2 the critical heat current at 1.41°K is plotted as a function of $\omega^{1/2}$. The various symbols refer to different runs; vertical lines through the points indicate the experimental uncertainty. Open symbols represent points taken upon increasing the angular velocity to the indicated values, whereas points represented by solid symbols were taken after ω had been re-

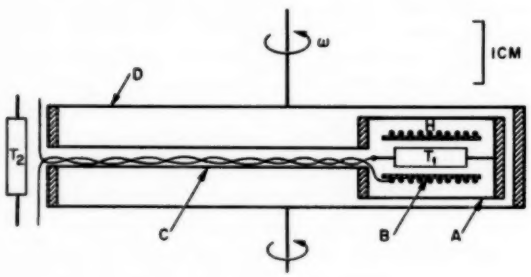

FIG. 1. The apparatus.

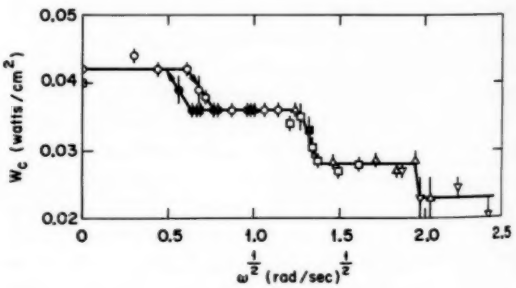

FIG. 2. Critical heat current at 1.41°K as a function of the square root of the angular velocity. Open symbols—increasing ω; solid symbols—decreasing ω.

duced from a higher value. It should be noted that, as ω is increased, W_c drops in a series of fairly sharp steps equally spaced along the abscissa. There appears to be some hysteresis at the first step, as indicated by the arrows; no such phenomenon has yet been observed at higher angular velocities, but detailed measurements have not been carried out there.

Vinen's[6,7] studies of mutual friction led him to propose that a heat current generates turbulence in the superfluid component, and that this turbulence takes the form of a tangled mass of vortex line. He further suggested that the critical heat current results from a competition between the mechanisms responsible for generation of vortex line and its annihilation at the walls of the channel. If these ideas are correct, it is plausible that the presence of vortex lines produced by rotation would alter the balance between these mechanisms in favor of the growth of turbulence, and thus decrease W_c. A reduction in W_c would then correspond to an increase in the amount of vortex line present in the channel, and the fact that this reduction takes place abruptly at certain angular velocities would indicate that the amount of vortex line present increases in discrete steps. This suggests that within a given range of angular velocities only certain configurations of vortex lines are stable, and that for rates of rotation smaller than that corresponding to the first step in Fig. 2 no vortex lines are present at all. It is unlikely that such a situation would arise unless the circulation were strictly quantized, for otherwise the circulation around each line could vary continuously so that the necessary boundary conditions were satisfied at any angular velocity. It appears that the number of stable configurations is in fact limited by the requirement that they must rotate with the same angular velocity as the apparatus, each line moving in the velocity field of its neighbors and of the images in the channel walls; otherwise the lines would be rapidly annihilated at the walls or driven out the ends of the channel.

If the circulation around each line is h/m, the equilibrium separation of vortex lines in a large volume of liquid rotating at an angular velocity ω is $l=(h/2\omega m)^{1/2}$. At the angular velocity of the first step, 0.4 ± 0.15 rad/sec, this separation is 0.034 ± 0.005 cm, which is comparable with, although somewhat larger than, the average width of the interstices between the wires of which the channel is composed. The values of l at the second and third steps are 0.017 ± 0.001 cm and 0.011 ± 0.0002 cm, respectively. Inasmuch as these lengths are in the ratio $1:\frac{1}{2}:\frac{1}{3}$, it is tempting to suppose that the steps correspond to the appearance of one, two, and three parallel rows of vortex lines along the channel. Unfortunately, it does not appear that such simple configurations would be stable against small disturbances or would rotate with the required angular velocity, unless they are constrained by friction with the top and bottom walls of the channel.

The interpretation of these measurements would be much clearer if a single channel of simple geometry were employed. Similar experiments are therefore being carried out in a rectangular channel of dimensions 0.041×0.109 cm. Preliminary results with this apparatus are in full agreement with those described above.

The author is grateful to Dr. E. Maxwell, Dr. D. Douglass, and G. Myers for many helpful discussions.

---

*The work reported in this paper was performed by Lincoln Laboratory, a center for research operated by Massachusetts Institute of Technology with the joint support of the U. S. Army, Navy, and Air Force.

[1]L. Onsager, Suppl. Nuovo cimento 6, 249 (1949).

[2]R. P. Feynman, Progress in Low-Temperature Physics, edited by J. C. Gorter (North-Holland Publishing Company, Amsterdam, 1955), Vol. 1, Chap. 2, p. 36 ff.

[3]H. E. Hall and W. F. Vinen, Proc. Roy. Soc. (London) A238, 204 (1956); A238, 215 (1956).

[4]H. E. Hall, Proc. Roy. Soc. (London) A245, 546 (1958).

[5]W. F. Vinen, Nature 181, 1524 (1958); Physica 24, 13 (1958).

[6]W. F. Vinen, Proc. Roy. Soc. (London) A240, 128 (1957).

[7]W. F. Vinen, Proc. Roy. Soc. (London) A242, 493 (1957); A243, 400 (1957).

PLASMA TRAPPING IN CUSPED GEOMETRIES*

Harold Grad
Institute of Mathematical Sciences, New York University, New York, New York
(Received November 10, 1959)

The question of the trapping of particles in cusped magnetic containment configurations has been recently examined.[1] The purpose of this Letter is to make accessible and extend certain early results which bear on this problem.[2] The trapping problem is, clearly, very closely related to the question of containment. The latter problem has been treated in some detail for the cusped geometry[3] (high $\beta \equiv 2\mu_0 p/B^2$) and to a lesser extent for the picket fence[4] (low β). The possibility of creating a cusped plasma by injection using a plasma gun has been described several times[5] and has been tried experimentally on a small scale with inconclusive results.[6]

The mechanisms are different for trapping of a single particle (i.e., a low-β stream) or a high-β cohesive plasma burst; we consider first the simpler single-particle mechanism (this has been termed impossible; see reference 1).

We consider a two-dimensional cusped configuration as shown in Fig. 1. In this simplified model the magnetic field is assumed to be totally excluded and a particle orbit consists of straight-line segments joined by helical arcs. Sufficiently close to a cusp, the orbit has the adiabatic invariant[7] (see Fig. 1 for notation),

$$\mu^* = 2mvd + \pi m^2(v^2+w^2)/eB. \qquad (1)$$

The value of μ^* will be essentially constant while a particle is close to a cusp, but it will change its value when the particle crosses the device and approaches a second cusp. The simplest containment theory[8] is based on the assumption of a complete loss of memory on traversing the apparatus. In other words, the distribution function of particles approaching a cusp is Maxwellian without any gap in a loss-cone. A refinement of this theory takes into account a certain amount of persistence in two successive values of μ^*.[2] Turning to the injection problem, we see that a complete loss in memory of the value of μ^* yields complete trapping of all injected particles. They will enjoy a lifetime which is, on the average, the same as that of any particle in the plasma, whether recently injected or not. It is only those particles with a good memory which cross to the opposite cusp and escape after but a single transit.

A simple computation of this persistence effect (based on a calculation of the last encounter made with the original cusp before crossing to the opposite side) shows that all particles are trapped which are injected within a "trapped zone" (see Fig. 1) of width

$$2\delta = 2\lambda\left(1 - \frac{\pi}{16}\frac{\lambda}{L}M^3\right)^{1/2}, \qquad (2)$$

where $\lambda = m(v^2+w^2)^{1/2}/eB$ is the Larmor radius and $M = u/(v^2+w^2)^{1/2}$ is the injection "Mach number." To be trapped, the guiding center of an approaching particle should be within a distance δ of the cusp axis. With λ/L fixed, there are no trapped particles when M is sufficiently large. The maximum width of the trapped zone is twice the Larmor radius. For most efficient trapping, the beam width should not exceed the Larmor radius. This formula is an approximation which is valid when either M or L/λ is large.

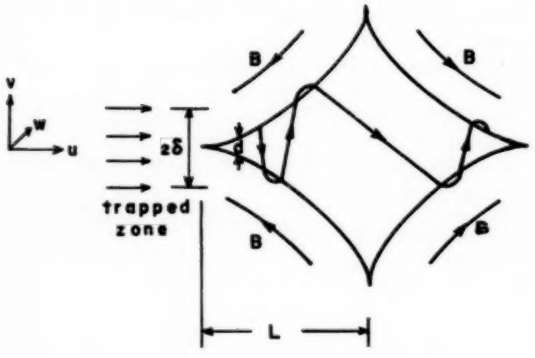

FIG. 1. Two-dimensional cusped geometry.

A similar (but much more intricate) analysis can be performed for the case of axial injection through a point cusp in a three-dimensional geometry (Fig. 2). The maximum size of the trapped zone is in this case a disk of area $\pi\delta^2 \sim L\lambda$; this area has the same order of magnitude as the total trapping area offered by the line-cusp which can be analyzed two-dimensionally as above. An appreciable fraction of those particles which approach the point cusp within the distance δ will be trapped provided that $M = u/(v^2+w^2)^{1/2}$

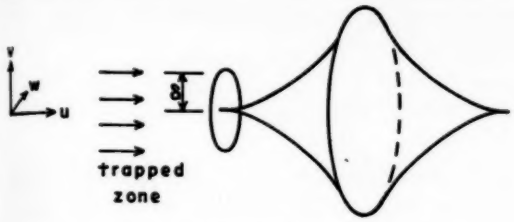

FIG. 2. Three-dimensional cusped geometry.

is smaller than some numerical factor times $(L/\lambda)^{7/6}$.

The problem of computing the trapping of a high-β plasma burst which can alter the magnetic field is much more difficult. A simple fluid-like theory can be developed for the smooth motion of a plasma in a magnetic channel.[9] If we are guided by the similar problem in ordinary fluid dynamics, we can expect complicated phenomena such as shocks (as in a diffuser with supersonic entrance velocity), jet detachment (since the magnetic walls curve away sharply), vortices in the dead space surrounding the jet. Peculiar to the magnetic channel problem, it has been shown that there is no stable transition between subsonic and supersonic regions.[9] Thus the entry of the plasma into the low-field region is a complex matter. At the far end, one cannot conclude (as is done in reference 1), merely from the fact that the magnetic pressure is higher than the energy density in the beam, that the beam will be turned back. For one thing, in the direction parallel to the magnetic field, the Maxwell stress is a tension, not a pressure. It is easy to construct flows of arbitrarily low energy density which can pass through a mirror region, and there is reason to believe that an energetic supersonic jet of this type can be stable.[9]

Theoretical analysis of this entire problem would be a huge task. Fortunately, certain simple experimental expedients should guarantee a large degree of trapping. For example, the cusped configuration can be made slightly asymmetric by misaligning the two coils. The incoming jet will then miss the opposite cusp and be trapped. Or else, two streams can be injected from opposite ends.[10] It should be remarked that a certain amount of trapped transverse magnetic field in the jets is helpful to make them collide instead of passing through one another as has been observed with "plasmoids." Otherwise one might be able to depend on the "two-stream" instability to break up the jets. Again, too much symmetry is undesirable since it might lead to a spurt sideways through the cusped diametral plane, but a slight misalignment (either in direction or in timing) would probably mitigate this effect.

Generally speaking, trapping is apt to be quite efficient in any apparatus with a large approximately field-free region (even in a mirror machine[2]), especially if there is no high degree of symmetry. It is possible that both the high-β and low-β injection techniques could prove to be useful, the first to create a plasma and the second to maintain it against cusp losses for the required time.

---

*The work presented in this paper is supported by the U. S. Atomic Energy Commission Computing and Applied Mathematics Center, Institute of Mathematical Sciences, New York University.

[1]J. L. Tuck, Phys. Rev. Letters 3, 313 (1959), where this is referred to as "entropy trapping."

[2]H. Grad, Atomic Energy Commission Report TID-7520, 1956 (unpublished), p. 148.

[3]A concise summary is given by J. Berkowitz et al., Proceedings of the Second United Nations International Conference on the Peaceful Uses of Atomic Energy, Geneva, 1958 (United Nations, Geneva, 1958), Vol. 31.

[4]Hartland Snyder (private communication, 1955).

[5]For example, see H. Grad, Atomic Energy Commission Report NYO-7969, 1957 (unpublished).

[6]D. Finkelstein, G. A. Sawyer, and T. F. Stratton, Phys. Fluids 1, 188 (1958).

[7]Reference 3, Appendix. The formula quoted there is in error.

[8]H. Grad, Atomic Energy Commission Report TID-7503, 1955 (unpublished), p. 319. See also reference 3.

[9]H. Grad, Bull. Am. Phys. Soc. 3, 288 (1958). This theory can easily be generalized to include plasma and field intermingled.

[10]This proposal, with the two "guns" an integral part of the apparatus rather than external, is being carried out by a group at Stevens Institute.

STUDY OF PHYSICS AND CHEMISTRY OF SURFACES FROM FRUSTRATED TOTAL INTERNAL REFLECTIONS

N. J. Harrick
Philips Laboratories, Irvington-on-Hudson, New York
(Received February 3, 1960)

It has been suggested[1] that the physics and chemistry of surfaces of optically transparent materials, particularly semiconductors, may be studied through the analysis of the spectrum of totally internally reflected radiation. This seems feasible since it is known that the totally reflected radiation actually penetrates the surface into the rarer medium to a depth given by

$$x_{1/2} = \frac{0.693\lambda_1}{2\pi(\sin^2\theta - n_{21}^2)^{1/2}}.$$

Here λ_1 is the radiation wavelength in the denser material, θ the angle of incidence, and n_{21}, which is less than unity, is the relative index of refraction.[2] The penetration depth is about one-tenth of a wavelength except near the critical angle; where $\sin\theta \simeq n_{21}$, the penetration depth becomes large. Goos and Hänchen[3] demonstrated this effect in a remarkable experiment where they actually measured a displacement, proportional to the penetration depth, of the internally reflected beam compared to metallic reflection as shown in the insert of Fig. 1(a).

It is the purpose of this note to give experimental evidence indicating that infrared radiation which penetrates the surface interacts with impurities on the surface at molecular resonance frequencies and that this interaction is comparable to what would be observed in a transmission measurement for impurity films on the surface thinner than a penetration depth. Since there is a prohibitive power loss in transmission through several separated layers whereas internal reflections are total, the reflection technique has the obvious advantage over transmission measurements where many encounters with the surface are necessary in order to gain sensitivity.

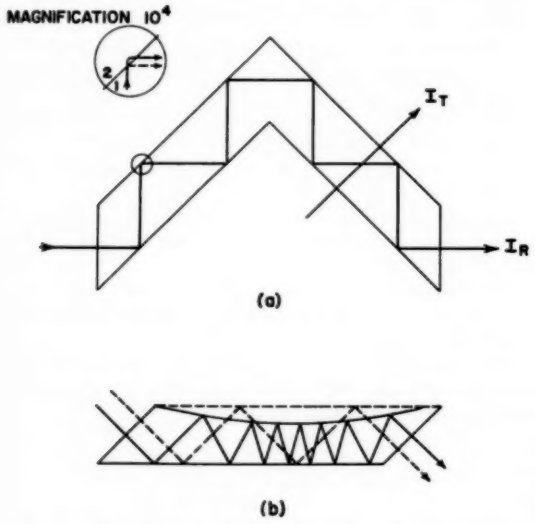

FIG. 1. Sample shapes for total internal reflection measurements.

The sample[4] used is shown schematically in Fig. 1(a) where the angle of incidence is 45 degrees. It was cut, ground, and diamond-polished in one piece from 30 ohm-cm, p-type germanium. The entrance face had dimensions of about 1/4 in. $\times$3/4 in. It should be noted that after eight reflections the exit beam is axial with the entrance beam, which simplifies the optics of the infrared spectrometer. With narrow spectrometer slits, thin samples can be used and the number of reflections can thereby be increased for the same length of sample. Figure 1(b) shows how the number of reflections can be increased by curving the surface in an appropriate way. On each reflection the angle of incidence is increased. Care has to be taken so that the angle of incidence is not decreased beyond the critical angle when the beams would be lost. To see if this technique might work, known impurities were placed on the surface and their spectra were analyzed with the aid of a Perkin-Elmer Model 12C spectrometer.

The sample shown in Fig. 1(a) was mounted in a cell so that all of the surfaces except the entrance and exit faces could be exposed to a liquid or a gas. Figure 2 compares the spectrum of the sample with no impurities intentionally added to the surface to that observed when water surrounded the sample. The 3- and 6-micron water absorption bands are clearly visible in the latter case. When the signal strength of the 3-micron band was compared to that observed in a transmission measurement through a thin film of water, the depth of penetration was determined to be about 0.15 micron, assuming a comparable strength of interaction in the transmission and

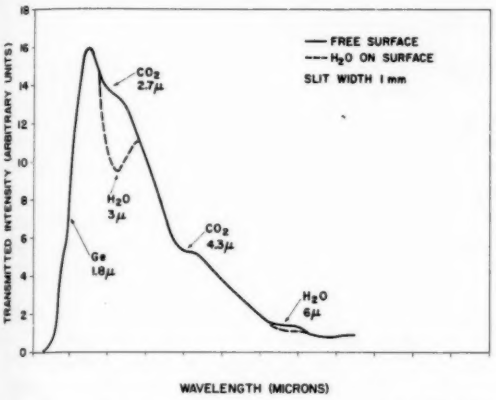

FIG. 2. Spectra of beam I_R of Fig. 1(a). The lines attributed to CO_2 indicate its presence in the atmosphere.

reflection measurements. This depth of penetration compares favorably with that calculated from theory.

A series of measurements was next made on the 3.4-micron polyethylene line. The polyethylene was dissolved in xylene to a dilution of 0.04% by weight and sprayed on the surface of the sample. The signal from transmission and reflection could be directly compared by analyzing the spectra from I_T and I_R in Fig. 1(a). The results of these measurements are shown in Fig. 3. The signal in the reflection beam does not increase with film thickness beyond a certain film thickness. The transmission signal, however, increases with thickness. For a film thickness of less than about 0.5 micron, the signal from eight reflections is greater than that from two transmissions. When we compare two reflections to two transmissions we see that the signal strengths are comparable for a film thickness less than about 0.16 micron which is also the thickness beyond which the signal strength in the reflection measurements does not increase. This is thus a measure of the penetration depth of the radiation in the rarer medium. Figure 4 shows the penetration depth of the polyethylene-germanium system, whose indices of refraction are 1.5 and 4, respectively, as a function of angle of incidence as computed from the formula in the first paragraph. We see that depth determined experimentally falls right on the theoretical curve.

These results indicate that the radiation which penetrates into the rarer medium does interact with the surface impurities at molecular resonance and that the interaction strength is comparable to that occurring in transmission meas-

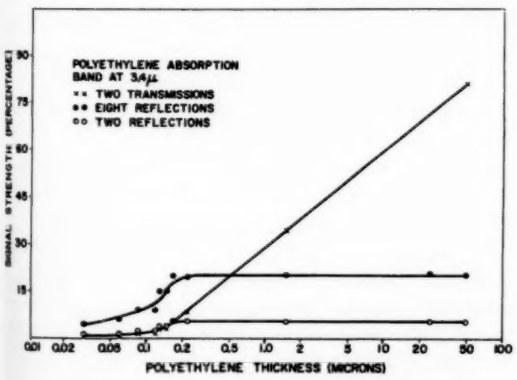

FIG. 3. Comparison of the signal strength for transmission and reflection beams, I_T and I_R of Fig. 1(a), for the polyethylene absorption line at 3.4 microns. The spectrometer slit width was 0.5 mm for these measurements.

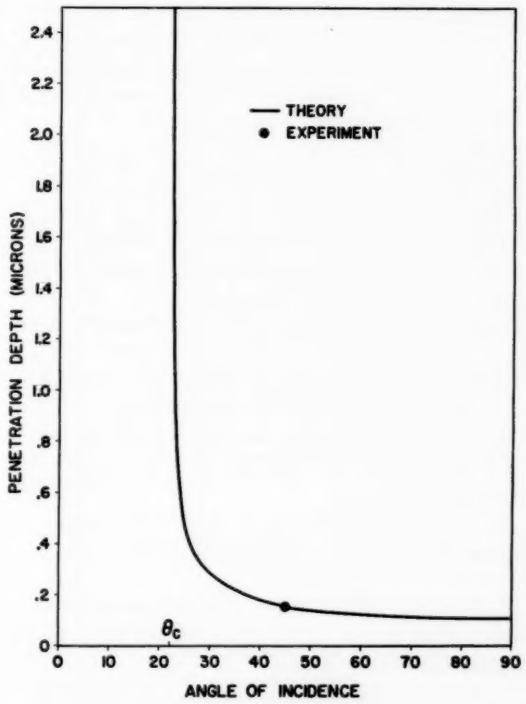

FIG. 4. The penetration depth versus angle of incidence for total internal reflection at the germanium-polyethylene interface. The experimental point is obtained from the experimental data of Fig. 3.

urements for films whose thicknesses are equal to or less than the penetration depth. Furthermore, this interaction does not represent just a power loss at resonance resulting from an increase in the refractive index in the polyethylene, and thus upsetting the condition of total internal reflection at the germanium-polyethylene interface. If this were the case, the reflected radiation would always penetrate the whole of the polyethylene film and any radiation not absorbed would be reflected from the polyethylene-air interface and the signal strength would always increase with film thickness. Near the critical angle such an effect could undoubtedly be observed.

Our results indicate that through the use of a more sensitive spectrometer and more reflections this technique should indeed work in the study of surface chemistry and we expect that it should be possible to detect one to ten atomic layers. Furthermore, such a technique should be valuable in the study of thin films.

---

[1]Discussion by N. J. Harrick following paper by R. P. Eischens at Second Conference on Semiconductor Surfaces, Naval Ordnance Laboratories, White Oak, Maryland, December, 1959 [J. Phys. Chem. Solids (to be published).] It was brought to the author's attention after the work described here was completed that Dr. J. Fahrenfort of the Royal Dutch Shell Laboratories, Amsterdam, has described what appears to be a similar technique to observe the spectra of organic materials on silver chloride at the Fourth International Congress on Molecular Spectroscopy, Bologna, September, 1959 (unpublished).

[2]Julius A. Stratton, Electromagnetic Theory (McGraw-Hill Book Company, Inc., New York, 1941).

[3]F. Goos and H. Hänchen, Ann. Phys. 1, 333 (1947).

[4]Semiconductor samples similar to these have been used in the study of other properties of semiconductor surfaces. N. J. Harrick, J. Phys. Chem. Solids 8, 106 (1959). N. J. Harrick, J. Opt. Soc. Am. 49, 376 (1959).

MECHANISM OF ANTIFERROMAGNETISM IN CHROMIUM

A. W. Overhauser and A. Arrott
Scientific Laboratory, Ford Motor Company, Dearborn, Michigan
(Received January 6, 1960)

An experiment is proposed which may in principle distinguish between three mechanisms of antiferromagnetism, one of which may obtain in chromium. Corliss, Hastings, and Weiss[1] have observed that each magnetic superstructure reflection in the neutron diffraction of a Cr single crystal is split into six spots equidistant from the reciprocal lattice point and which lie along [100] type directions from that point. This result can be interpreted in several ways:

A. Cr has basically a Néel type antiferromagnetic structure, but with periodic antiphase domains.[1]

B. The localized spins lie in a (100) plane and spiral with a fixed period in the direction perpendicular to the plane.[2]

C. The localized spins are oriented by their interaction with a static spin density wave in the conduction electron gas.[3]

Each antiferromagnetic domain (or group of antiphase domains for case A) contributes to two of the six magnetic reflection spots associated with a given reciprocal lattice point. That all six spots occur [and, for example, have equal intensity at the (1, 1, 1) point] indicates that the unit vector $\vec{\lambda}$ characteristic of a given domain (as defined below) is parallel or antiparallel to one or the other of the three [100] type axes on a statistically equal basis. For the three models under consideration, $\vec{\lambda}$ is:

A. perpendicular to the antiphase domain boundaries;

B. parallel to the axis of the spiral;

C. parallel to the wave vector of the spin density wave.

An experiment of potentially great interest it to cool a single crystal of Cr through the Néel point to low temperature in a large magnetic field parallel to a [100] crystal axis, and then to study the relative intensities of the six magnetic reflection spots. If the applied field is sufficient to upset the statistical equality of the three [100] axes with regard to $\vec{\lambda}$, the relative intensities of the spots will be modified, and should allow one to distinguish between mechanisms A, B, and C, or at least between C and A or B. Such field-cooling effects may reasonably be anticipated.

Magnetic dipole-dipole interactions contribute

an energy dependent on the angle between $\vec{\lambda}$ and the axis $\vec{s}$ of spin alignment. Usually the most favorable orientation is $\vec{\lambda}$ perpendicular to $\vec{s}$, as is observed to be the case for Cr.[1] The spin axis $\vec{s}$ will in turn be correlated with a magnetic field $\vec{H}$ if the sample is cooled through the Néel point with $\vec{H}$ applied. (It is helpful to recall that magnetocrystalline anisotropy is zero at the Néel point, so that $\vec{s}$ is free to adjust according to the direction of $\vec{H}$.)

Consider now an antiferromagnet conforming to model A or B. It is well known that the magnetic susceptibility of such a system is a maximum when $\vec{s}$ is perpendicular to $\vec{H}$. Consequently $\vec{s}$ will align parallel to one of the two [100] axes perpendicular to $\vec{H}$. Subsequently, for case A, $\vec{\lambda}$ will be formed either parallel to $\vec{H}$ or parallel to the other [100] axis perpendicular to $\vec{H}$. For case B, $\vec{\lambda}$ will be parallel to $\vec{H}$ since the spiral rotation of $\vec{s}$ sweeps through the plane perpendicular to $\vec{H}$. For mechanism C, however, the susceptibility is a maximum when $\vec{s}$ is parallel to $\vec{H}$.[4] A brief explanation is as follows. The axis of quantization of the static spin density wave is free to precess around the applied field direction. This precession gives rise to a large rotating effective (exchange) field H_1 (in the sense of a magnetic resonance experiment) which depolarizes the localized magnetic moments (similar to the effect of resonance saturation). As a result, the maximum susceptibility occurs when $\vec{s}$ is parallel to $\vec{H}$. Subsequently, magnetic dipole-dipole interactions favor $\vec{\lambda}$ being perpendicular to $\vec{H}$. The relative intensity of the two neutron reflection spots parallel to $\vec{H}$ from, say, the (1, 1, 1) reciprocal lattice point compared to that of the four spots perpendicular to $\vec{H}$ are:

No field,		1:1;
field-cooled,	A.	2:1,
	B.	1:0,
	C.	0:1.

The foregoing intensity ratios would allow one to distinguish between the three mechanisms considered. However, these ratios apply only if domain orientation adjustment resulting from the field-cooling effect is complete. Very likely, magneto-elastic effects associated with domain formation will permit only partial correlations between $\vec{\lambda}$ and $\vec{H}$. In such an event it would be difficult to distinguish between A and B. However, one should still be able to distinguish between C and A or B since the intensity ratio becomes smaller than unity in the former case and larger than unity in the latter.

Whether or not mechanism C operates in Cr is of particular interest because some remarkable properties of Cr, in addition to the splitting of the neutron reflections, can be explained by this model. Shull and Wilkinson[5] have observed that the Néel point of a powdered Cr sample is 45% higher than that of bulk Cr. This result has been confirmed by Corliss, Hastings, and Weiss.[1] Such an effect can be explained as follows. It must be remembered that the wavelength of the static spin density wave (as determined by the splitting of the neutron reflections) differs by about 7% from the lattice constant. Consequently a significant fraction of the localized spins in an antiferromagnetic domain will lie near nodes of the wave and will contribute little to the condensation energy of the antiferromagnetic state. If it were possible for a domain to terminate spatially whenever the nodes of the wave begin to fall near lattice sites, and for a new domain to begin having a more propitious correlation between the phase of its wave and the lattice sites, the condensation energy and the Néel temperature could be increased by as much as a factor of two (neglecting domain wall energies, etc.). Consequently the observed effect is easily accounted for, provided one assumes that mechanical imperfections present in the powdered specimens provided a mechanism for nucleating (and stabilizing) appropriately small antiferromagnetic domains. This explanation seems all the more likely since Hastings[6] has pointed out that the neutron reflections would not be split if the domain size were small enough to explain the appreciably higher Néel temperature. Indeed, the magnetic reflections from his powdered specimens were not split.[6] The behavior of a particular sample may well be a function of its metallurgical history.

---

[1] L. M. Corliss, J. M. Hastings, and R. J. Weiss, Phys. Rev. Letters 3, 211 (1959).

[2] T. A. Kaplan, Phys. Rev. 116, 888 (1959).

[3] A. W. Overhauser, Phys. Rev. Letters 3, 414 (1959); J. Phys. Chem. Solids (to be published).

[4] A. W. Overhauser (to be published).

[5] C. G. Shull and M. K. Wilkinson, Revs. Modern Phys. 25, 100 (1953).

[6] J. M. Hastings (private communication).

NEW MECHANISM OF ANISOTROPIC SUPEREXCHANGE INTERACTION

Tôru Moriya*
Bell Telephone Laboratories, Murray Hill, New Jersey
(Received January 25, 1960)

Anisotropic exchange interaction as a combined effect of spin-orbit coupling and exchange interaction has been discussed by several authors.[1] These previous studies, however, were restricted to the so-called pseudo-dipolar coupling which is of second order in the spin-orbit coupling. The purpose of the present note is to provide a mechanism for an interaction of the form:

$$\vec{D}\cdot[\vec{S}_1\times\vec{S}_2], \tag{1}$$

which is linear with respect to the spin-orbit coupling, important in magnetic crystals of low symmetry, and generally much larger than the pseudo-dipolar coupling treated so far. Such an interaction was first suggested from purely symmetry grounds by Dzialoshinski.[2]

The theory is an extension of the superexchange theory to include the effect of spin-orbit coupling. A new formalism recently developed by Anderson[3] is used throughout the calculation. The one-electron states localized on the cations are expressed by Wannier functions and the one-electron Hamiltonian consists of the energy of the localized states and the transfer terms among them. We denote the two degenerate wave functions localized at the position R as follows:

$$\Psi_{n\uparrow}(r-R),\ \Psi_{n\downarrow}(r-R),$$

where $\uparrow$ and $\downarrow$ mean the spin almost up and almost down, respectively. Because of the spin-orbit coupling the spin-up and spin-down states are mixed in these wave functions. The one-electron terms of the Hamiltonian are written as

$$\begin{aligned}E=\sum_R\sum_n\sum_\sigma \epsilon_n(R)\alpha_{n\sigma}^*(R)\alpha_{n\sigma}(R)+\sum_{R\neq R'}\sum_{n,n'}\Big[&b_{n'n}(R'-R)\{\alpha_{n'\uparrow}^*(R')\alpha_{n\uparrow}(R)+\alpha_{n'\downarrow}^*(R')\alpha_{n\downarrow}(R)\}\\&+C_{n'n}^{\,z}(R'-R)\{\alpha_{n'\uparrow}^*(R')\alpha_{n\uparrow}(R)-\alpha_{n'\downarrow}^*(R')\alpha_{n\downarrow}(R)\}\\&+C_{n'n}^{\,-}(R'-R)\alpha_{n'\uparrow}^*(R')\alpha_{n\downarrow}(R)+C_{n'n}^{\,+}(R'-R)\alpha_{n'\downarrow}^*(R')\alpha_{n\uparrow}(R)\Big],\end{aligned} \tag{2}$$

where

$$\begin{aligned}b_{n'n}(R'-R)+C_{n'n}^{\,z}(R'-R)&=\int\Psi_{n'\uparrow}^*(r-R')H_1\Psi_{n\uparrow}(r-R)d\tau,\\ b_{n'n}(R'-R)-C_{n'n}^{\,z}(R'-R)&=\int\Psi_{n'\downarrow}^*(r-R')H_1\Psi_{n\downarrow}(r-R)d\tau,\\ C_{n'n}^{\,-}(R'-R)&=\int\Psi_{n'\uparrow}^*(r-R')H_1\Psi_{n\downarrow}(r-R)d\tau,\\ C_{n'n}^{\,+}(R'-R)&=\int\Psi_{n'\downarrow}^*(r-R')H_1\Psi_{n\uparrow}(r-R)d\tau,\end{aligned} \tag{3}$$

and

$$H_1=\frac{p^2}{2m}+V(r)+\frac{\hbar}{2m^2c^2}\vec{S}\cdot[\mathrm{grad}V(r)\times\vec{p}],$$

$$C_{n'n}^{\,\pm}(R'-R)=C_{n'n}^{\,x}(R'-R)\pm iC_{n'n}^{\,y}(R'-R).$$

$\alpha_{n\uparrow}^*(R)$ and $\alpha_{n\uparrow}(R)$ are creation and annihilation operators of electrons in the state represented by $\Psi_{n\uparrow}(r-R)$, etc. The most important contribution to the superexchange arises from the configuration mixing of polar states due to the transfer terms of (2). The second order per-

turbation gives not only the ordinary isotropic coupling (b^2 terms) but an anisotropic coupling coming from bC terms: C^2 terms are much smaller than bC terms and make a contribution to the usual pseudo-dipolar coupling. We shall consider as an example the case of one electron per atom with the ground orbital state assumed to be nondegenerate, i.e., the orbital moment is quenched. The second order bC terms are calculated by using the relations:

$$\alpha_{n\uparrow}^{*}(R)\alpha_{n\uparrow}(R)-\alpha_{n\downarrow}^{*}(R)\alpha_{n\downarrow}(R)=2S_z(R),$$

$$\alpha_{n\uparrow}^{*}(R)\alpha_{n\downarrow}(R)=S_+(R),$$

and

$$\alpha_{n\downarrow}^{*}(R)\alpha_{n\uparrow}(R)=S_-(R),$$

for the occupied (ground) states. The empty states do not take part in the second order coupling. The result is as follows:

$$E_{R,R'}^{(2)}=\vec{D}^{(2)}\cdot[\vec{S}(R)\times\vec{S}(R')], \tag{4}$$

where

$$\vec{D}^{(2)}=\frac{4i}{U}[b(R-R')\vec{C}(R'-R)-\vec{C}(R-R')b(R'-R)], \tag{5}$$

the transfer integrals being those between the ground states of the ions at R and R', and U being the energy required to transfer an electron from an ion to its nearest neighbor, thus making a polar state. The transfer integrals b and C are calculated by using a perturbation method assuming that the orbital level separation in an ion is larger than the spin-orbit coupling. The b terms are the ordinary transfer integrals without spin-orbit coupling and the C terms are obtained, up to the first order in the spin-orbit coupling, as follows:

$$\vec{C}(R'-R)=-\tfrac{1}{2}\lambda\Big\{\sum_{m'}\frac{\vec{l}_{m'n'}^{*}(R')}{\epsilon_{m'}(R')-\epsilon_{n'}(R')}b_{m'n}(R'-R)+\sum_{m}\frac{\vec{l}_{mn}(R)}{\epsilon_{m}(R)-\epsilon_{n}(R)}b_{n'm}(R'-R)\Big\}+\vec{c}(R'-R), \tag{6}$$

where n, n' represent the ground orbitals and m, m' the excited orbitals, $\vec{l}_{mn}(R)$ the matrix element of the orbital angular momentum of the ion at R, λ the spin-orbit coupling constant, and

$$\vec{c}(R'-R)=\frac{\hbar}{4m^2c^2}\int\varphi_{n'}^{*}(r-R')[\mathrm{grad}V(r)\times\vec{p}]\varphi_n(r-R)d\vec{r}, \tag{7}$$

$\varphi_n(r-R)$ being the ground orbital wave function.

From the third order perturbation, which includes transfer terms b and C between a singly occupied and an empty Kramers' doublet and the intra-atomic exchange interaction, we get the same type of coupling as (4). This term is J/U (J being the intra-atomic exchange energy) times as small as the second order term (4) as in the case of the ordinary superexchange.

The direct exchange coupling also has an anisotropic part of the form (4). The coupling constant is given by

$$\vec{D}_{ex}=-i\lambda\Big\{\sum_{m}\frac{\vec{l}_{mn}^{*}(R)-\vec{l}_{mn}(R)}{\epsilon_m(R)-\epsilon_n(R)}J(nn'mn')-\sum_{m'}\frac{\vec{l}_{m'n'}^{*}(R')-\vec{l}_{m'n'}(R')}{\epsilon_{m'}(R')-\epsilon_{n'}(R')}J(nn'nm')\Big\}, \tag{8}$$

where

$$J(nn'mm')=\iint\varphi_n^{*}(r_1-R)\varphi_{n'}^{*}(r_2-R')\frac{e^2}{r_{12}}\varphi_m(r_2-R)\varphi_{m'}(r_1-R')d\vec{r}_1d\vec{r}_2.$$

It is interesting to note that all the terms treated above which are linear in the spin-orbit coupling have the form (1). This coupling vanishes when the symmetry of the crystal is high. For example, when there is only one magnetic ion in a unit cell and there is a center of inversion, or when there are two magnetic ions in a unit cell and a center of inversion is located halfway between them, this coupling vanishes. When the crystal symmetry is low, however, this coupling may be the most important anisotropic coupling between the spins. Though quantitative calculation of this coupling is very complicated,

we can estimate the order of magnitude in relation to the isotropic superexchange. As is easily seen, all the three contributions to $\vec{D}$ treated above are roughly $(\Delta g/g)$ times the corresponding contributions to the isotropic superexchange interaction.[4] Though there may be some reduction of the magnitude, depending on the crystal structure, this coupling may well be $(g/\Delta g)$ times as big as the pseudo-dipolar anisotropic exchange. Extension of the theory to the case of many electrons per ion is generally complicated. We may expect the above rough order estimation is also valid in this case provided the orbital moment is quenched.

The possible existence of this type of coupling was first pointed out by Dzialoshinski[2] from symmetry considerations on some trigonal weak ferromagnets, α-Fe_2O_3, $MnCO_3$, and $CoCO_3$, though its origin was not clarified. Our mechanism gives the right orders of magnitude to explain the magnetic moments of α-Fe_2O_3, $MnCO_3$, and CrF_3.

This coupling is important not only in weak ferromagnetism but also in determining the spin arrangement in antiferromagnets of low symmetry. As an example we shall consider $CuCl_2 \cdot 2H_2O$, one of the most widely studied antiferromagnets. Because of the low crystal symmetry (space group is V_h^7) there is a coupling of the type (1) between the corner ion and the base-center ion; this type of coupling is absent between two ions both at the corner (base-center) sites. The magnitude of the coupling estimated from Δg is about 10% of the superexchange interaction and $\vec{D}$ is parallel to the b axis. Therefore, the antiferromagnetic spin arrangement in this crystal may be different from the one accepted at present, i.e., alternating ferromagnetic layers in the ab plane with the moment pointing in the a direction. We propose instead the arrangement shown in Fig. 1. The c component of a spin may be about 10% of the a component. We expect that this spin arrangement may give a more consistent understanding of the proton resonance data both above and below the Néel temperature[5] and the neutron diffraction data[6] for the position of the protons. Further details and related topics will be published later.

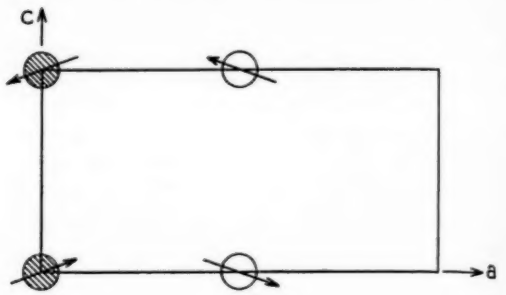

FIG. 1. A proposed spin arrangement in antiferromagnetic $CuCl_2 \cdot 2H_2O$. The spins are in the ac plane. The black and the open circles represent the ions at the positions 0, 0, 0 and $\frac{1}{2}, \frac{1}{2}, 0$, respectively.

I should like to thank Dr. P. W. Anderson for his continuous interest in this work.

---

*On leave of absence from Tokyo Metropolitan University, Tokyo, Japan.

[1]J. H. Van Vleck, J. phys. radium 12, 262 (1951); T. Moriya and K. Yosida, Progr. Theoret. Phys. (Kyoto) 9, 663 (1953); T. Nagamiya, K. Yosida, and R. Kubo, Advances in Physics, edited by N. F. Mott (Taylor and Francis, Ltd., London, 1955), Vol. 4, p. 1.

[2]I. Dzialoshinski, J. Phys. Chem. Solids 4, 241 (1958).

[3]P. W. Anderson, Phys. Rev. 115, 2 (1959).

[4]A part of $\vec{D}^{(2)}$ given by (5) which include $\vec{c}(R'-R)$ should be omitted from this order estimation. This term is more difficult to estimate than the others. A rough order estimation may be given by (spin-orbit coupling energy/ionization energy) times superexchange energy.

[5]N. J. Poulis and G. E. G. Hardeman, Physica 18, 201 (1952); J. Itoh, R. Kusaka, Y. Yamagata, R. Kiriyama, and H. Ibamoto, Physica 19, 415 (1953).

[6]S. W. Peterson and H. A. Levy, J. Chem. Phys. 26, 220 (1957).

EFFECTS OF FAST-NEUTRON IRRADIATION ON NICKEL THIN FILMS

I. Teodorescu and A. Glodeanu
Institute for Atomic Physics, Bucharest, Roumania
(Received February 8, 1960)

In order to obtain more precise information concerning the processes and defects produced in solids as a result of fast-particle irradiation such as those described by Seitz,[1] Seitz and Koehler,[2] and Brinkman,[3] we have irradiated thin films of nickel with fast neutrons.

The films were evaporated in vacuum (10^{-5} mm Hg) on glass and quartz substrates, the thickness of the films being 200-800 A; the evaporation was carried out at different temperatures of the substrates in order to obtain different stages of the crystalline structure. During the irradiation, the samples were sealed in vacuum (10^{-4} mm Hg) or in oxygen. For each of the series of the irradiated samples, one test sample was put aside for purposes of comparison. The irradiation was made for 3.38×10^{17} *nvt* and 9.45×10^{15} *nvt* at the temperatures $T = 59°C$ and $T = 45°C$, respectively. Before and after the irradiation, the saturation magnetization and coercive force of the samples were measured. The structure of the films was studied with the aid of the electron microscope and by electron diffraction.

The technique of obtaining the films and the methods of studying them have been described previously.[4]

As a result of fast-neutron irradiation, the thin films of nickel were transformed from face-centered cubic lattices with $a = 3.52$ A into close-packed hexagonal lattices with $a = 2.62$ A, $c = 4.36$ A. This transformation took place in the whole film for samples irradiated to 3.38×10^{17} *nvt*. For samples irradiated to 9.45×10^{15} *nvt* we obtain a mixture of two phases: face-centered cubic lattice and close-packed hexagonal lattice. The allotropic transformation took place only for samples irradiated in vacuum; the samples irradiated in oxygen were strongly oxidized and the oxidized film thus formed prevented the allotropic transformation into a hexagonal lattice. Such a phase change requires a volume enlargement and this is not possible.

All the irradiated samples show great changes in magnetic properties. The magnetic properties disappear for the samples which are completely transformed into close-packed hexagonal lattices (the magnetization falls from $4\pi I_S = 4000$ gauss to $4\pi I_S < 6$ gauss, and the coercive force falls from $H_c = 240$ oe to $H_c = 0$ oe).

The samples, which are in part transformed into hexagonal lattices, show a drop in magnetization of about 30-50% and their coercive force increases to a certain extent; there are cases in which it does not vary at all. The increase in the coercive force is due to the large stresses which appear in the mixture of the phases.

The samples irradiated in oxygen exhibited a drop in magnetization because the proportion of pure nickel phase was small and the oxidation correction could not be made in the case of strong oxidation. That is the explanation of the fact that the calculated magnetization is not the observed one. The coercive force also grows slightly as a result of the stresses.

The samples irradiated in oxygen showed another phenomenon: those samples, which at the beginning had a less ordered structure, presented after the irradiation a more ordered one and the hysteresis cycle was more rectangular. The ordered samples were disordered during irradiation and the hysteresis cycle was more rounded.

The results of magnetic measurements, electron diffraction, and electron microscopy were all in agreement.

In Fig. 1(a) we give the electron diffraction pattern for face-centered cubic nickel (nonirradiated). In Fig. 1(b) we give the electron diffraction pattern of nickel after irradiation, showing that the transformation into a close-packed

FIG. 1. Electron diffraction patterns of Ni. (a) Face-centered cubic (nonirradiated). (b) Close-packed hexagonal (after irradiation). (c) A mixture of the two phases.

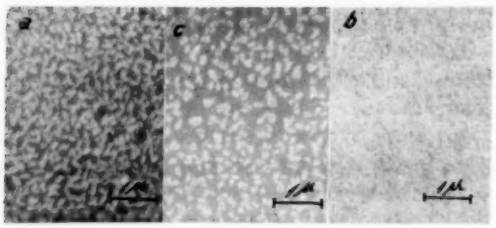

FIG. 2. Electron microscope pictures of the same samples.

hexagonal lattice had taken place. In Fig. 1(c) a mixture of the two phases of hexagonal and cubic lattice is shown.

In Fig. 2 the results of the electron microscopy for the same samples are given.

The results may be explained if we assume the following: (1) Thermal spikes were formed and their dimensions were $\sim 10^5$ atoms. (2) In the region where a thermal spike was formed, the lattice lost its meaning as the metal had a temperature above its melting point. Let us consider this as a disordered state. (3) After the thermal spike was created, the metal underwent a process of sudden annealing.

On the basis of these hypotheses, the phase transformation may be explained in the following way: During irradiation, thermal spikes are created followed by sudden annealings. Since the annealing period is too short, it is not possible to return to the initial state of order (face-centered cubic lattice); instead, there is an intermediate state, i, e., the hexagonal close-packed nickel.

The samples irradiated in oxygen do not show the transformation phase because their volume has been prevented from varying.

The authors would like to express their gratitude to Miss C. Moţoc and G. Alanz for their help during the irradiation.

[1]F. Seitz, Discussions Faraday Soc. 5, 271 (1949).
[2]F. Seitz and J. S. Koehler, in Solid State Physics, edited by F. Seitz and D. Turnbull (Academic Press, New York, 1956), Vol. 2.
[3]J. A. Brinkman, J. Appl. Phys. 25, 961 (1954); Am. J. Phys. 24, 246 (1956).
[4]A. Glodeanu and I. Teodorescu, Studii şi Cercetări de Fizică, No. 4, 1956 (to be published).

FERROMAGNETIC RELAXATION MECHANISM FOR M_z IN YTTRIUM IRON GARNET*

M. Sparks and C. Kittel†
Department of Physics, University of California, Berkeley, California
(Received February 8, 1960)

Yttrium iron garnet (YIG) is an ideal crystal for studies of ferromagnetic resonance and relaxation. The outstanding attributes of YIG are (A) cubic structure; (B) excellent insulator; (C) all magnetic ions identical and in an S state; and (D) no detectable magnetic disorder. Spencer and LeCraw[1] have reported ferromagnetic relaxation measurements on highly-purified YIG at low temperatures. Their work, together with that with Fletcher,[2] is the first to distinguish in a ferromagnet the relaxation of the magnetic moment component parallel to the static magnetic field. Their best experimental estimate of $1/T_1$ at 9.34 kMc/sec between 2 and 30°K is fitted roughly, after correction for impurity relaxation, by

$$1/T_1 \cong 1\times 10^5 T \text{ sec}^{-1}, \qquad (1)$$

with T in deg K; below 5°K the experimental curve flattens out above the values given by (1). We propose here an explanation of a significant part of the observed relaxation, giving first a brief summary of the likely course of the entire relaxation process, as well as one can tell at present.

In the absence of special paramagnetic impurities, the linewidth is believed[3] to arise from the mixing of the uniform precession (by static surface and volume imperfections) with spin wave modes degenerate with the uniform precession. These degenerate spin waves, which we call S modes, then relax by Raman scattering of thermal magnons through the magnetic dipole interaction. The rate of this process determines T_1, provided that the coupling between the uniform and S modes is not a bottleneck; at sufficiently high temperatures, the bottleneck will exist if ΔH is constant with temperature while $1/T_1$ increases;

then $1/T_1$ vs T will appear to flatten. The output magnons of the Raman process will tend by further Raman processes and by a four-magnon exchange interaction process[4] to maintain approximately a spin temperature T_{sp}. One probably may not speak of a spin temperature below about 5°K for input power ~1 watt/cm³. Except at low temperature, the spin temperature may be closely equal to the lattice temperature. After a study of the magnon-phonon scattering processes treated by Kaganov and Tsukernik,[5] we conclude that the Čerenkov process is dominant and is probably adequate down to 5°K. If trace amounts of impurities are present which relax the uniform mode (and all other modes) even slowly, then substantial additional powers can be handled, because of the large number of spin wave modes. Thus 1 watt/cm³ can be transferred from the spin system to the lattice at 5°K with a temperature drop ~0.3°K by an impurity mechanism giving every mode a $T_1 = 10^{-5}$ sec. A failure of spin-lattice contact will flatten the measured $1/T_1$ vs T curve at low temperatures.

We have calculated the relaxation rate of the S modes for Raman processes in which, by magnetic dipolar coupling between an S mode and a thermal spin wave, the z component of the magnetic moment changes by $\pm 2\mu_B$. The role of magnetic dipole coupling in the related problem of relaxation averaged over a thermal distribution has been treated by Akhiezer.[4] A calculation similar to that below was made by Kasuya[6] in 1954, before the line-broadening process was understood, so our present note amounts to a numerical refinement, on a firmer physical basis, of his result.

The magnetic field[7] associated with a spin wave $\vec{k}$ of magnetization $\Delta\vec{M}$ is $\vec{H} = -4\pi(\vec{k}\cdot\Delta\vec{M})\vec{k}/k^2$, and the magnetic energy coupling one spin wave to the medium gives terms bilinear, trilinear, and higher in the spin wave operators $a_{\vec{k}}^{\dagger}, a_{\vec{k}}$. The bilinear terms may be diagonalized[8]; the trilinear terms split a spin wave in two and vice versa. The trilinear terms may be written, taking $g=2$ and $\mu = |\mu_B|$,

$$\mathcal{H}_m' = -8\pi\mu(\mu M_s/V)^{1/2}\sum\Delta(\vec{k}_1 - \vec{k}_2 + \vec{k}_3)k_1^{z}k_1^{-}(k_1)^{-2}a_{\vec{k}_1}a_{\vec{k}_2}^{\dagger}a_{\vec{k}_3}^{\dagger} + \text{c.c.} \qquad (2)$$

By standard methods we find, for the relaxation time T_1 of a spin wave k_1 making an angle θ with the z axis,

$$\frac{1}{T_1} = \frac{16\pi\mu^3 M_s(k_B T_{sp})k_1 F(\theta)}{3D\hbar^2\omega_0}, \qquad (3)$$

where $F(\theta) = 1 + (11/2)\sin^2\theta - (23/4)\sin^4\theta$, and D defines the high-frequency dispersion relation $\hbar\omega \cong Dk^2$; ω_0 is the resonance frequency. The angle θ is determined[3] for a sphere by

$$(\hbar\omega_0)^2 = [\hbar\gamma(H - 4\pi M_s/3) + Dk_1^2]\times[\hbar\gamma(H - 4\pi M_s/3) + Dk_1^2 + \hbar\gamma 4\pi M_s\sin^2\theta]. \qquad (4)$$

In the derivation of (3) it was assumed (A) that $Dk_1^2 \ll \hbar\omega_0$; and (B) that $(\hbar\omega_0)^2 \ll 4(k_B T)(Dk_1^2)$.

We take for YIG the values $D \cong 0.55\times10^{-28}$ erg cm² and $M_S \cong 200$. We suppose[9] that in the actual specimen the most important S modes have $k_1 \approx 2\pi/d \approx 3\times10^5$ cm^{-1}, where $d \approx 2\times10^{-5}$ cm is a representative grinding particle diameter; for this k_1, (A) is comfortably satisfied and (B) is satisfied for $T \gg 0.3$°K. For much larger pits the sharp edges on the surface pits will be of major importance, but for small pits and local imperfections the details are fortunately not important. Equation (3) cannot be applied to the larger pits without averaging over the surface details.

We calculate $1/T_1 \cong 0.74\times10^5 T_{sp}$ sec^{-1} on these assumptions, in not bad agreement with (1); here T_{sp} is the spin temperature. For linewidth caused entirely by point imperfections, one calculated $1/T_1 \cong 0.71\times10^5 T_{sp}$ sec^{-1}. We therefore see that M_z is expected to relax by magnetic dipole interaction with thermal spin waves at a rate comparable with observation. This process will also limit the propagation of coherent spin waves which may be generated in the laboratory.

We are indebted to R. C. LeCraw and R. C. Spencer for discussions of the experiments, and to R. Loudon for theoretical conversations.

*Supported in part by the National Science Foundation.
†Professor of Physics in the Miller Institute for

Basic Research in Science.

[1]E. G. Spencer and R. C. LeCraw, Phys. Rev. Letters 4, 130 (1960).

[2]R. C. Fletcher, R. C. LeCraw, and E. G. Spencer, Phys. Rev. (to be published).

[3]A. M. Clogston, H. Suhl, L. R. Walker, and P. W. Anderson, Phys. Chem. Solids 1, 129 (1956); their analysis has been extended by R. Loudon to the effects of surface polish, of major importance in YIG.

[4]A. I. Akhiezer, J. Phys. U.S.S.R. 10, 217 (1946); A. I. Akhiezer, V. G. Bar'yakhtar, and S. V. Peletminskii, J. Exptl. Theoret. Phys. U.S.S.R. 36, 216 (1959) [translation: Soviet Phys.-JETP 36(9), 146 (1959)]; M. I. Kaganov and V. M. Tsukernik, J. Exptl. Theoret. Phys. U.S.S.R. 34, 1610 (1958) [translation: Soviet Phys.-JETP 34(7), 1107 (1958); F. J. Dyson, Phys. Rev. 102, 1217 (1956). From Dyson we find for the collision frequency of a magnon $\vec{k}$ with a thermal equilibrium distribution of magnons:

$$\frac{1}{T_{mm}} \cong \frac{\zeta(3/2)}{2}\left(\frac{g\mu_B}{M_s}\right)^2\left(\frac{k_BT}{4\pi D}\right)^{3/2}\frac{Dk^3}{\hbar},$$

which $\approx 5\times10^3$ sec^{-1} for YIG at 5°K, taking $k\approx 2\times10^6$ cm^{-1} as a typical magnon produced in the process leading to Eq. (3).

[5]M. I. Kaganov and V. M. Tsukernik, J. Exptl. Theoret. Phys. U.S.S.R. 36, 224 (1959) [translation: Soviet Phys.-JETP 36(9), 151 (1959)].

[6]T. Kasuya, Progr. Theoret. Phys. (Kyoto) 12, 802 (1954).

[7]C. Herring and C. Kittel, Phys. Rev. 81, 869 (1951).

[8]T. Holstein and H. Primakoff, Phys. Rev. 58, 1098 (1940).

[9]R. Loudon (private communication).

ELECTRON NUCLEAR DOUBLE RESONANCE EXPERIMENTS WITH RUBY*

R. W. Terhune, J. Lambe,† G. Makhov, and L. G. Cross
Willow Run Laboratories, The University of Michigan, Ann Arbor, Michigan
(Received January 14, 1960)

The polarization of nuclear spins throughout a crystal by saturation of an electron spin resonance of paramagnetic ions present as impurities has recently been reported.[1,2] We have observed an apparent inverse of this effect in ruby (Al_2O_3:0.05% Cr^{+++}), i.e., when the induced nuclear polarization is partially removed by saturating an aluminum nuclear spin resonance transition, a large decrease in the power absorbed by the electron spin resonance of the Cr^{+++} ions is observed. We have also observed effects associated with inducing transitions between the hyperfine levels of the chromium-53 ions.

Magnetic field modulation at 5 kc/sec was used to observe the edge of the $(+\frac{1}{2}\rightleftarrows-\frac{1}{2})$ electron spin resonance absorption line of ruby with a microwave power level about 20 db above saturation. The spectrum shown in Fig. 1 was then obtained by scanning the frequency of a low-power rf oscillator connected to a single turn of wire around the ruby sample. The five lines in the 3-Mc/sec region correspond very well with the nuclear magnetic resonance spectrum of the host aluminum nuclei in the crystal. The same dependence of the splitting between lines upon the angle of dc magnetic field and line width were observed both here and in the nuclear magnetic resonance spectra.

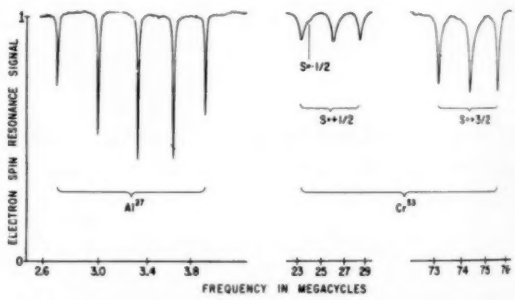

FIG. 1. Spectrum obtained by observing the $(+\frac{1}{2}\rightleftarrows-\frac{1}{2})$ electron spin resonance signal from ruby under saturation conditions and scanning the frequency of an rf generator connected to a coil around the crystal. ($H \cong 3285$ gauss, $\theta = 0°$, $\nu = 9160$ kMc/sec, $T = 4.2$°K.)

The lines near 25 and 75 Mc/sec are associated with the $\vec{I}\cdot\vec{S}$ splitting of the chromium-53 ions[3] which have a nuclear spin of 3/2 and a natural abundance of 9.5%. The other isotopes of chromium all have zero nuclear spin. The +1/2 and +3/2 electron spin states are very close together at our operating point. As a result they interact strongly as the angle of the dc magnetic field is varied, causing large changes in the hyperfine splitting (Fig. 2). Also, the second order correction to their hyperfine splitting is appre-

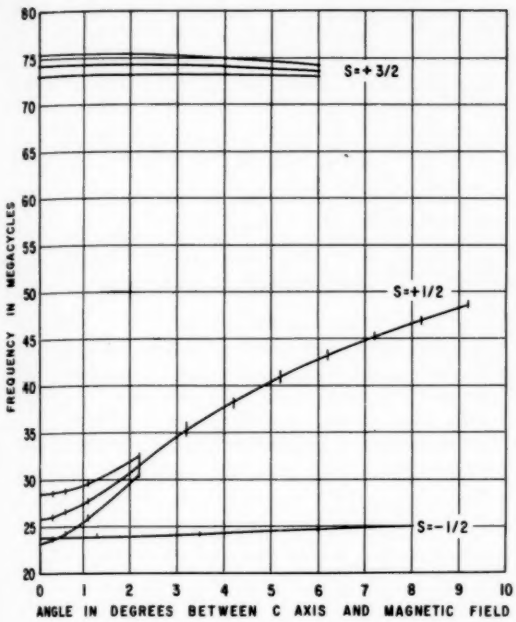

FIG. 2. Experimental data on angular dependence of the hyperfine splittings of the electron spin states of the Cr^{53} ion in ruby. The change in frequency with angle results from the mixing of electron spin states. (ν=9160 kMc/sec, T=4.2°K.)

ciable, leading to the observed triplets. The strength of the lines reduced very rapidly with departure from zero degrees. A weak triplet associated with $S=-3/2$ was also observed with the lines falling at 71.93, 72.15, and 72.37 Mc/sec at zero degrees. It is interesting to note that while all the Cr^{53} data were taken by observing the $S=-1/2$ to $+1/2$ transition, saturation of the hyperfine levels in the $S=+3/2$ state caused the largest changes in the electron spin resonance signal.

The strong effect of nuclear polarization on the electron spin resonance can easily be observed in ruby without applying rf. At microwave power level well above saturation, if one rapidly moves from one part of the resonance line to another a large transient with a decay time of about 5 seconds is observed. The same decay time is observed for the transient following removal of rf power sufficient to saturate one of the aluminum nuclear transitions. Further, the observed decay time of the aluminum nuclear polarization is also 5 seconds while T_1 for the electron spin resonance transition is approximately 0.2 second. The decay time of the effects associated with the chromium-53 nuclei was also near 5 seconds.

The effects of nuclear polarization upon the electron spin resonance signal were only observable when microwave power levels of the order of or greater than that needed to saturate the electron spin transition were used. When the electron spin resonance signal was observed at low microwave powers, the application of rf had no effect upon the signal. Further, when the signal was observed during the nuclear polarization relaxation time following a quick reduction in the microwave power level from above to well below saturation, only a 0.2-second time constant transient was observed. The application of rf power had no effect upon the transient, indicating that T_1 is independent of the nuclear polarization.

A decrease in microwave power absorption with the application of rf power was always observed. As a check, some observations were made using amplitude modulation of the microwaves rather than magnetic field modulation. Also, the amplitude of the magnetic field modulation was varied over a wide range with no significant effects being observed.

It does not seem that the effects reported here can be explained by any of the mechanisms proposed by Feher[4] to explain his observations in doped silicon. The slow relaxation after the removal of rf power would seem to indicate that the host nuclei play an important role in either the induced transition probabilities or relaxation mechanisms between electron spin states. If such were the case, in order to get an appreciable percentage effect in the electron system by saturating the nuclei, one would have to reduce the relative electronic polarization (N_i/N_j) to the same order as the nuclear polarization (n_k/n_l), i.e., $N_i/N_j \cong n_k/n_l$. This idea is consistent with our experimental results as the nuclear polarizations are increased by about a factor of[1] 40 and the electronic polarizations are decreased by about a factor of 100 under our experimental conditions, making the two comparable.

We have also studied the effect of rf upon maser action in ruby,[5] and have observed a number of additional very weak lines.

We wish to thank Professor C. Kikuchi for many helpful discussions.

*This work was supported by Project Michigan (administered by the U. S. Army Signal Corps), and

by the Air Force Office of Scientific Research.

†Now with the Scientific Laboratory, Ford Motor Company, Dearborn, Michigan.

[1]J. A. Cowen, R. W. Schafer, and R. D. Spence, Phys. Rev. Letters 3, 13 (1959).

[2]M. Abraham, M. A. H. McCausland, and F. N. H. Robinson, Phys. Rev. Letters 2, 449 (1959).

[3]A. A. Manenkov and A. M. Prokhorov, Zhur. Eksp. i Teoret. Fiz. 31, 346 (1956) [translation: Soviet Phys.-JETP 4, 288 (1957)].

[4]G. Feher, Phys. Rev. 114, 1219 (1959); G. Feher and E. A. Gere, Phys. Rev. 114, 1245 (1959).

[5]G. Makhov, L. G. Cross, R. W. Terhune, and J. Lambe, J. Appl. Phys. (to be published).

THERMAL EQUILIBRIUM BETWEEN *F* AND *M* CENTERS IN POTASSIUM CHLORIDE

C. Z. van Doorn
Philips Research Laboratories, N. V. Philips' Gloeilampenfabrieken, Eindhoven, Netherlands
(Received February 3, 1960)

Various models have been proposed for the M centers in alkali halides. According to Seitz[1] an M center consists of an F center associated with a neutral vacancy pair. A modification, having inversion symmetry, was put forward by Knox.[2] Van Doorn and Haven[3] have proposed a model consisting of a pair of associated F centers (F_2 model). From these models it is clear that the formation of M centers from F centers requires one F center for each M center formed in the case of the Seitz-Knox model and two in the case of the F_2 model.

It might be possible to distinguish between these cases by investigating (a) the kinetics of the reaction $F \rightarrow M$ and (b) the thermal equilibrium $F \rightleftharpoons M$. For the Seitz-Knox center the equilibrium can be written as

$$F + \text{vacancy pair} \rightleftharpoons M,$$

$$K = [M]/[F][\text{vac. pairs}];$$

and for the F_2 center as

$$2F \rightleftharpoons M, \qquad K' = [M]/[F]^2.$$

In the first case the M concentration will be proportional to the F concentration at a fixed temperature (the concentration of vacancy pairs being constant), whereas in the second case the M concentration will vary quadratically with the F concentration.

Theisen and Scott[4] found the thermal bleaching of F centers at about 300°C to be a second-order reaction, indicating that two F centers combine to form a new center. The thermal equilibrium between F and M centers was studied by Smith and Scott.[5] They colored a KCl crystal inhomogeneously by heating for a short time in potassium vapor in order to obtain a range of F concentrations. It was assumed that the attainment of the equilibrium between F and M centers is rapid compared with the diffusion of the centers in the crystal. The F and M concentrations in different regions of the crystal were measured optically, using a thin beam of monochromatic light. A linear dependence between F and M centers was found up to a concentration of 10^{17} F centers/cm^3. This experiment is, however, not conclusive because (a) no true equilibrium existed and (b) the high M/F ratio found indicates that the crystals were not properly quenched. Therefore, the following experiment was performed. KCl was purified by crystallizing it twice according to the Kyropoulos method. From the single crystal thus obtained, plates were cut having the dimensions $4 \times 5 \times 1.3$ mm^3. These were colored by heating to 697°C in potassium vapor of various pressures in a nickel tube. A heating time of 10 minutes was found to be sufficient to obtain equilibrium, as no further increase in optical absorption was observed with longer heating times. After quenching in carbon tetrachloride to room temperature, which was done in the dark to avoid photochemical reactions, the relative F and M concentrations were determined by measuring the extinction of the absorption bands at 77°K. With the apparatus used for coloring (to be described in a forthcoming publication) it took less than one second to transfer the crystal from the furnace to the quenching bath, thus ensuring freezing-in of the high-temperature equilibrium. All crystals had the same dimensions in order to obtain equal quenching rates.

The results are shown in Fig. 1. It is seen that the M concentration varies quadratically with the F concentration, which is inconsistent with the Seitz-Knox model but agrees well with the F_2 picture.

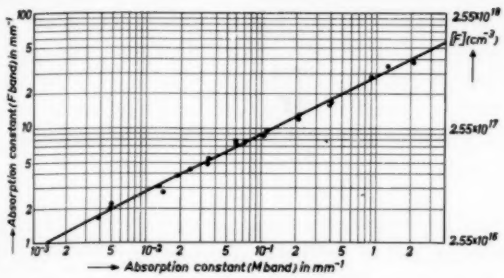

FIG. 1. Double-logarithmic plot of the concentrations of F and M centers in equilibrium at 697°C, expressed as absorption constants at 77°K of the F and M bands, respectively. The number of F centers per cm^3 is calculated from the Smakula formula with $f = 0.81$ and a half-value width 0.195 ev.

A rough determination of the equilibrium constant K' at other temperatures showed the temperature dependence to be small, corresponding to a heat of formation of the M center of about 0.01 ev.

I would like to thank Mr. A. T. Vink for his assistance.

[1]F. Seitz, Revs. Modern Phys. 18, 384 (1946).
[2]R. S. Knox, Phys. Rev. Letters 2, 87 (1959).
[3]C. Z. van Doorn and Y. Haven, Philips Research Rept. 11, 479 (1956). C. Z. van Doorn, Philips Research Rept. 12, 309 (1957).
[4]F. E. Theisen and A. B. Scott, J. Chem. Phys. 20, 529 (1952).
[5]W. A. Smith and A. B. Scott, J. Chem. Phys. 21, 2096 (1953).

NUCLEAR RESONANCE FLUORESCENCE IN Au^{197}†

D. Nagle, P. P. Craig, J. G. Dash, and R. R. Reiswig
Los Alamos Scientific Laboratory, University of California, Los Alamos, New Mexico
(Received February 1, 1960)

We have observed the Mössbauer effect[1] in the 77-kev gamma-ray line of Au^{197}. A resonance curve from which the level lifetime may be deduced was obtained by moving a Pt^{197} source relative to a Au absorber. Resonance was found using as sources either the β^- parent, Pt^{197}, or the electron capture parent, Hg^{197}. We also find that the effect can be either enhanced or diminished by placing the source and/or absorber atoms in suitable crystal lattices. All measurements were performed at a temperature of 4°K.

The shape of the resonance line was determined using a Pt^{197} source prepared by neutron activation of 60 mg of natural Pt. Pulse-height spectra taken at intervals for several days following activation showed a prominent gamma line at 77 kev, decaying with the mean life of about 26 hours, which is characteristic of Pt^{197}. Figure 1 shows the counting rate (corrected for source decay during measurement) versus the velocity of the source relative to a 200-mg/cm^2 Au absorber. No distinction between positive and negative velocities was made. The velocity half-width obtained is 3.5 ± 0.5 mm/sec. No evidence of subsidiary resonances was seen up to the highest velocity used, 24 mm/sec. The total resonance absorption effect is 5.5 ± 0.5% after a correction (not shown in the figure) is made for background in the gamma-ray spectrum.

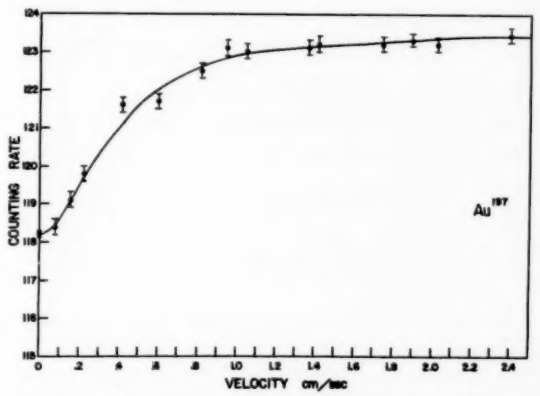

FIG. 1. Nuclear resonance absorption vs the magnitude of the source velocity in the 77-kev gamma ray of Au^{197}.

Using a source prepared by activation of enriched Pt (65.9% Pt^{198}), measurements of resonance absorption were made on three Au absorber foils of thickness 100, 200, and 400 mg/cm^2. The net absorptions were, after correction for background (including the unresolved 60-kev x ray), 4.0 ± 0.6%, 7.7 ± 0.5%, and 11.5 ± 0.7%, respectively. The velocity curve was similar

to that of Fig. 1. Ascribing this nonexponential dependence upon absorber thickness to preferential absorption of the center of the line, we determine the probability f for emission of photons in no-phonon processes, and the probability f' of resonant absorption from an incident beam of uniform energy spectrum,[2] namely, $f = 23 \pm 7\%$ and $f' = 3 \pm 1\%$. The calculation of f' is based upon a resonance cross section which includes the value[3] 3.5 for the internal conversion coefficient of the 77-kev Au^{197} line. An earlier value[4] of 5.9 would raise f' to $4.6 \pm 1.5\%$.

f and f' are intimately related to the phonon spectra of the source and absorber. In the limit of low temperatures, Visscher[5] has shown that for monatomic isotropic crystals this relation takes the simple form of a weighted integral over the phonon spectrum. We feel that values of these weighted integrals are the major results of transmission measurements using the Mössbauer effect. We define an effective temperature,

$$\Phi = \left[\frac{k}{3N\hbar}\int_0^{\nu_m}[g(\nu)/\nu]d\nu\right]^{-1},$$

where $g(\nu)d\nu$ is the number of phonon states in a frequency range $d\nu$, N is the number of atoms in the solid, and k is the Boltzmann constant. Then for the source, Φ is related to f by $\Phi = R/\ln(1/f)$, where R is the classical recoil energy of a source atom of energy E and mass m, $R = E^2/2kmc^2$. The same relation relates the absorber phonon spectrum to f'.

We find that for Au, $\Phi = 54^{+5}_{-6}$ °K; for Pt, $\Phi = 127^{+27}_{-24}$ °K. Our earlier results[2] on Os and Ir yield $\Phi = (200 \pm 17)$°K for Os and $\Phi = (174 \pm 20)$°K for Ir.

The simplified Debye model of phonon excitations in solids yields $\Phi = \frac{3}{5}\theta$, where θ is the Debye characteristic temperature. On this model, $\Phi = 123$°K for Au and $\Phi = 155$°K for Pt, using $\theta = 185$°K for Au and $\theta = 233$°K for Pt,[6] in significant disagreement with our results. However, one should not place too much reliance on the predictions of the Debye model in this instance.

By using the above transmission results, the resonance curve of Fig. 1 may be corrected for broadening caused by selective absorption in the 200-mg/cm² absorber. For this absorber the corrected mean life may be written[7]

$$\tau = \frac{\hbar(1+3.8f')c}{uE} = 2.57\left(\frac{1+3.8f'}{u}\right)\ \text{m}\mu\text{sec},$$

where E is the gamma-ray energy (77 kev) and u is the velocity half-width in mm/sec. Using our determination of f' we find $\tau = 0.82 \pm 0.15$ mμsec. The mean life obtained by conventional techniques is 1.9 ± 0.2 mμsec.[4]

There is some indication of hyperfine structure which is less than the natural linewidth and which is slightly asymmetric about zero velocity. We are at present investigating this point. Such an asymmetry would broaden the observed resonance curve and decrease f' below the value expected from the Debye model, in agreement with our observations.

In an effort to understand the influence of the lattice binding upon the resonance, several experiments were performed in which the source or the absorber was modified. An absorber was prepared of the compound $AuAl_2$, containing 208.5 mg/cm² of Au. The Lindemann formula[8] was used to compute roughly the Debye temperature of this compound. With the enriched Pt source, a nuclear resonance effect of about 21% was to be expected. We were able to observe only a marginal effect of about $0.3 \pm 0.3\%$.

The source lattice may be drastically altered through the use of the electron capture parent, Hg^{197}. Such a source was prepared by neutron activation of natural Hg. On the Debye model, taking $\theta = 69$°K, the total resonance absorption expected with a 200-mg/cm² Au absorber is 1.1%. The spectrum has, however, unresolved 60-kev x rays from K capture in Hg which we estimate to be 2.5 times as intense as the 77-kev line of interest. The effect observed was $(0.14 \pm 0.12)\%$ before correcting for x rays, and after correction $(0.49 \pm 0.42)\%$.

The small effect in this case may be attributed to a low value of the effective temperature Φ for the mercury, and to a lack of symmetry between the crystallographic environments of emitting and absorbing Au^{197} nuclei. Accordingly, we tried to enhance the absorption by adding active mercury to compacted gold powder in the proportion 10% Hg and 90% Au. The amalgam was then diffusion annealed for 70 min at 430°C under a helium atmosphere. One day later the resonance effect was measured and found not to differ from the result with pure Hg. Previous x-ray work had shown that samples of this type were homogeneous after 24 hours at 430°C. Therefore the sample was given an additional 24 hours heat treatment at 430°C. The resonance was now found to be $(0.46 \pm 0.04)\%$ before background correction and $(1.6 \pm 0.5)\%$ after correction. It appears that placing the emitting atoms in a lattice which is mostly Au has resulted in a

substantial enhancement of the resonance.

We wish to thank A. D. McGuire for help in the early portion of this experiment. We would like to thank M. Goldhaber for a helpful discussion. We take pleasure in acknowledging the help of the Omega reactor group in preparing sources.

---

†Work performed under the auspices of the U. S. Atomic Energy Commission.

[1]R. L. Mössbauer, Z. Physik 151, 124 (1958); Naturwissenschaften 45, 538 (1958); Naturforsch. 14a, 211 (1959).

[2]P. P. Craig, J. G. Dash, A. D. McGuire, D. Nagle, and R. D. Reiswig, Phys. Rev. Letters 3, 221 (1959).

[3]E. M. Bernstein and H. W. Lewis, Phys. Rev. 100, 1345 (1955).

[4]A. W. Sunyar, Phys. Rev. 98, 653 (1955).

[5]W. Visscher, Ann. Phys. (to be published).

[6]American Institute of Physics Handbook (McGraw-Hill Book Company, Inc., New York, 1957).

[7]W. Visscher (unpublished).

[8]F. A. Lindemann, Physik. Z. 11, 609 (1910).

SPACE-TIME CORRELATION FUNCTION FORMALISM FOR SLOW NEUTRON SCATTERING

P. Schofield

Theoretical Physics Division, Atomic Energy Research Establishment, Harwell, England

(Received January 29, 1960)

Van Hove[1] has shown that the partial differential cross section for the coherent scattering of neutrons by an assembly of atoms is related to the space-time correlation function, $G(\vec{r}, t)$, by

$$\frac{\partial^2\sigma}{\partial\Omega\,\partial\epsilon} = \frac{a^2}{2\pi\hbar}\frac{k'}{k}\Gamma(\vec{\kappa}, \omega), \tag{1}$$

$$\Gamma(\vec{\kappa}, \omega) = \iint \exp[i(\vec{\kappa}\cdot\vec{r} - \omega t)]\, G(\vec{r}, t)\, d\vec{r}\, dt, \tag{2}$$

where a is the appropriate scattering length, $\vec{k}$ and $\vec{k}'$ the wave vectors of the incident and outgoing neutron, $\hbar\vec{\kappa}$ the momentum transfer, and $\epsilon = \hbar\omega$ the energy lost by the neutron. The spatial part of the transform (2), $\gamma(\vec{\kappa}, t)$, is given by

$$\gamma(\vec{\kappa}, t) = N^{-1}\Big\langle \sum_{l,j=1}^{N} \exp[-i\vec{\kappa}\cdot\vec{r}_l(0)] \times \exp[i\vec{\kappa}\cdot\vec{r}_j(t)]\Big\rangle_T, \tag{3}$$

where $\langle\cdots\rangle_T$ denotes a thermal average over the states of the scattering system, and $\vec{r}_j(t)$ is the Heisenberg operator for the position of the jth atom at time t.

Now it can easily be verified, by writing the thermal average and $\vec{r}_j(t)$ in terms of the Hamiltonian of the system, that $\gamma(\vec{\kappa}, t + i\hbar/2k_BT)$ is a real function of t. Let this function be denoted by $\gamma'(\vec{\kappa}, t)$. The Fourier transform of $\gamma'(\vec{\kappa}, t)$ with respect to t then defines a function $\Gamma'(\vec{\kappa}, \omega)$ which is related to $\Gamma(\vec{\kappa}, \omega)$ by

$$\Gamma'(\vec{\kappa}, \omega) = \Gamma(\vec{\kappa}, \omega)\, \exp[\hbar\omega/2k_BT]. \tag{4}$$

From the properties of $\gamma'(\vec{\kappa}, t)$ it follows that $\Gamma'(\vec{\kappa}, \omega)$ is even in both $\vec{\kappa}$ and ω. Thus (4) expresses the condition of detailed balance, which we know a priori must be satisfied by the scattering cross section.

By inverting the transform (2) and using (4), it is possible to obtain a dispersion relation relating the real and imaginary parts of $G(\vec{r}, t)$. This may be written in integral form:

$$\mathcal{I}\{G(\vec{r}, t)\} = (k_BT/\hbar) \times \int_{-\infty}^{\infty} \csc(\pi k_BTt'/\hbar)\,\mathcal{R}\{G(\vec{r}, t - t')\}\, dt', \tag{5}$$

or, more conveniently, in operator form:

$$\mathcal{I}\{G(\vec{r}, t)\} = -\tan\left(\frac{\hbar}{2k_BT}\frac{\partial}{\partial t}\right)\mathcal{R}\{G(\vec{r}, t)\}. \tag{6}$$

This can be regarded as a constraint imposed upon the correlation function as a consequence of the thermal equilibrium of the system.

Vineyard[2] has suggested that in many systems it is possible to replace $G(\vec{r}, t)$ in (2) by its classical equivalent $G_c(\vec{r}, t)$. Since the classical correlation function is real, the resulting cross section does not satisfy the detailed balance condition. The above analysis suggests that $G_c(\vec{r}, t)$ should be used to define $\Gamma'(\vec{\kappa}, \omega)$, rather than $\Gamma(\vec{\kappa}, \omega)$, so that this condition is satisfied. Although in the limit $\hbar \to 0$, $\gamma'(\vec{\kappa}, t)$ and $\gamma(\vec{\kappa}, t)$ are identical, since the variable of transformation is the energy transfer divided by $\hbar$, the transforms are not identical.

The use of the classical correlation function in this way takes some account of the recoil of the

scattering atom, and, as may be seen by considering the simple examples of the monatomic gas and the isotropic oscillator, gives a cross section which is formally correct to first order in $\hbar$.

Another case discussed by Vineyard[2] is that in which the atoms diffuse according to the Langevin equation. By means of the real function $\gamma'(\vec{\kappa}, t)$ it is possible to obtain an explicit expression for the cross section:

$$\Gamma'(\vec{\kappa}, \omega) = \frac{2}{\eta} e^{\alpha} \sum_{n=0}^{\infty} \frac{(-1)^n}{n!} \alpha^{n+1} \times \left[\frac{1}{(\alpha+n)^2+\beta^2} - \frac{1}{(\alpha+n+1)^2+\beta^2} \right], \quad (7)$$

where η is the coefficient of viscous damping, and

$$\alpha = k_B T \kappa^2 / M \eta^2, \quad \beta = \omega/\eta.$$

The result obtained if the simple diffusion equation is used to derive $G(\vec{r}, t)$ corresponds to the first part of the first term in (7) so that unless both α and β are small, this approximation is not valid. In fact, (7) gives a width for the scattered energy distribution less than that given by both the simple diffusion model and the gas model. This is in agreement with the observations of Pelah et al.[3] on liquid lead. However, (7) does not give a width sufficiently small to explain the results of Turberfield[4] on lead with cold neutrons. These experiments indicate that the atoms of the liquid must make many vibrational oscillations between diffusive jumps, and the results cannot be interpreted on a basis of continuous diffusion.

[1]L. Van Hove, Phys. Rev. 95, 249 (1954).
[2]G. H. Vineyard, Phys. Rev. 110, 5 (1958).
[3]I. Pelah, W. L. Whittemore, and A. W. McReynolds, Phys. Rev. 113, 767 (1959).
[4]K. C. Turberfield (to be published).

LEAD K ABSORPTION EDGE FOR μ-MESON MASS DETERMINATION

Alan J. Bearden*
Department of Physics, The Johns Hopkins University, Baltimore, Maryland
(Received January 26, 1960)

The recent accurate determination of the f_μ/f_p ratio for the μ meson[1] and the comparison of the magnetic moment of the μ meson based on this measurement with the value predicted by quantum electrodynamics[2] depends critically on the mass of the μ meson. It has been shown experimentally that the $3D$-$2P$ transition in μ-mesonic phosphorus lies near the Pb K edge energy.[3] In fact, when considered in detail, it appears that the fine structure splitting of the $3D$-$2P$ transition in phosphorus will cause the lines to straddle the Pb K edge energy.[4] Therefore, it seems possible that one may use the variation of the mass-attenuation coefficient in lead as a function of energy in the K edge region as a very accurate measurement of the mesonic x-ray energy. The detailed shape of the lead K edge must be known precisely both in energy scale and mass-attenuation coefficient. Knowing these transition energies, and accounting for corrections due to vacuum polarization, nuclear size effects, etc., it would be possible to make a precise determination of the μ-meson mass. The transition energies for the mesonic phosphorus lines under discussion are given by[4]

$3D_{3/2} - 2P_{3/2}$: 425.42 m_μ/m_e, relative intensity = 1;

$3D_{5/2} - 2P_{3/2}$: 425.65 m_μ/m_e, relative intensity = 9;

$3D_{3/2} - 2P_{1/2}$: 427.75 m_μ/m_e, relative intensity = 5.

From the quoted "best value" of the μ-meson mass,[5] $m_\mu/m_e = 206.86 \pm 0.11$, the $3D_{3/2} - 2P_{3/2}$ transition would lie at 88 041 ev. The best estimate of the inflection point of the Pb K edge is at 88 014 ev,[6] and its width is of the order of 100 ev. The intent of this Letter is to present then an accurate measurement of the Pb K absorption edge.

A two-crystal spectrometer using the $20\bar{2}3$ planes of quartz as diffracting surfaces was constructed. Angles were measured by use of the precision circle of the Societé Genevoise goniometer of the Johns Hopkins x-ray laboratory.[7] In order to gain comparative freedom from scattering, distances of one meter were used between x-ray source, first crystal, second crys-

tal, and detector. With this arrangement the signal to background ratio was never worse than one hundred to one. A commercial high kilovoltage x-ray tube[8] was used as an x-ray source, and a NaI(Tl) scintillation counter with single-channel pulse-height discrimination detected the radiation. The full width of the (1-1) rocking curve at the Pb K edge wavelength was 5.5''. The use of this narrow window allowed the determination of the edge shape without any appreciable interference due to window width. The "thickness effect" as previously reported[9,10] is negligible in this case, as was shown by measuring the mass-attenuation coefficient near the high side of the edge and varying the thickness of the absorbing foil. No change of mass-attenuation coefficient of more than two percent was detected over an absorber thickness from one-quarter to five absorption lengths. This absence of "thickness effect" is a distinct advantage of the high-resolution two-crystal instruments, and is due to the smaller unbent crystal diffraction widths and the larger dispersion obtainable by the two-crystal method.

The crystal spacing was determined by measuring the diffraction angles for Mo $K_{\alpha 1}$, Ag $K_{\alpha 1}$, and W $K_{\alpha 1}$ radiation. The lattice spacing for the $20\bar{2}3$ planes in quartz at 25°C was found to be (1372.117 ± 0.010) xu.

The Pb K edge determination was made with the diffracted x-ray beam passing through the crystals. As a check, the W $K_{\alpha 1}$ line was measured with: (1) the diffracted beam passing through the crystal; and (2) the diffracted beam in "reflection." No significant difference in diffraction angle could be detected, once the diffraction angle in case (2) was corrected for refraction in the crystal.

The measured shape of the Pb K edge for 98% purity lead foil[11] appears in Fig. 1. The energy scale is known to ±3 ev and the value of the mass-attenuation coefficient at any point is stated with a probable error of two percent. Since the $3D_{3/2}$-$2P_{1/2}$ transition probably lies entirely on the high absorption side of the Pb K edge, the mass-attenuation coefficient of lead was measured at 88 450 ev and found to be (7.30 ± 0.1) cm^2/gram.

As the two-crystal spectrometer measures the mass-attenuation coefficient for an extremely "good geometry," the mass-attenuation coefficient includes both photoelectric absorption and scattering cross sections. For any particular mesonic x-ray experiment, it is necessary to

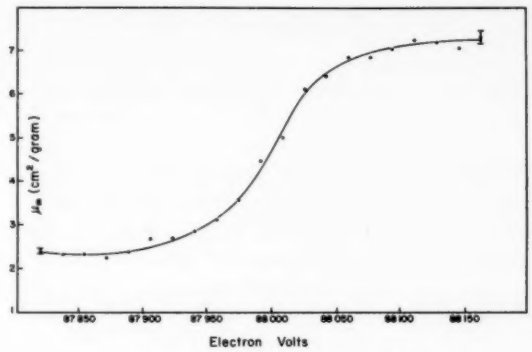

FIG. 1. Pb K absorption edge.

ascertain the amount of scattered radiation which enters the detector in order to arrive at the appropriate mass-attenuation coefficients for the unavoidable "poor geometry." Unfortunately, present measurements of the attenuation of $3D$-$2P$ mesonic x rays of phosphorus in lead[3] are not suitable for use in a precise determination of the μ-meson mass. Therefore, new experiments are essential to determine with high precision the attenuation in lead for these mesonic x-ray transitions.

The author is indebted to Dr. R. L. Garwin and Dr. S. Penman for discussions of this problem, and to the Nevis Cyclotron Laboratory of Columbia University for supplying the high-voltage x-ray tube. Many helpful discussions as to the measurements were had with Professor L. Madansky and Professor J. A. Bearden.

---

*Now at the Department of Physics, University of Wisconsin, Madison, Wisconsin.

[1]R. L. Garwin, D. P. Hutchinson, S. Penman, and G. Shapiro, Phys. Rev. Letters 2, 213 (1959); 2, 516 (1959).

[2]C. Sommerfield, Phys. Rev. 107, 328 (1957).

[3]S. Koslov, V. Fitch, and J. Rainwater, Phys. Rev. 95, 291 (1954).

[4]A. Petermann and Y. Yamaguchi, Phys. Rev. Letters 2, 359 (1959).

[5]K. Crowe, Nuovo cimento 5, 541 (1957).

[6]A. E. Sandstrom, Handbuch der Physik, edited by S. Flügge (Springer-Verlag, Berlin, 1957), Vol. 30, p. 214.

[7]J. A. Bearden and C. H. Shaw, Phys. Rev. 48, 18 (1935).

[8]A 260-kv, 5-ma unit supplied by the Picker X-Ray Corporation.

[9]L. G. Parratt, Revs. Modern Phys. 31, 616 (1959).

[10]O. Beckman et al., Arkiv Fysik 15, 567 (1959).

[11]Foils supplied by the Revere Copper and Lead Brass Company, Brooklyn, New York.

$\pi^{\pm}$-p TOTAL CROSS SECTIONS IN THE RANGE 450 Mev TO 1650 Mev*

Thomas J. Devlin, Barry C. Barish, Wilmot N. Hess, Victor Perez-Mendez, and Julius Solomon
Lawrence Radiation Laboratory, University of California, Berkeley, California
(Received February 8, 1960)

A series of counter experiments is being carried out at the Berkeley Bevatron and 184-inch cyclotron to measure total and differential scattering cross sections for pions at energies above the first resonance.[1-3] In this Letter we report the results of measurements of the total cross section for positive and negative pions on protons in the energy range from 450-Mev to 1650-Mev pion kinetic energy (lab).

The experimental arrangement is shown in Fig. 1. The pions were produced in an internal Pt target, plunged into the circulating proton beam of the Bevatron. The Pt target was located in the field-free tangent tank, allowing us to examine both positive and negative pions with the same experimental setup. Our magnet system consisted of an 8-in.-bore focusing quadrupole doublet, an 18×36-in. bending magnet which deflected the particles through an angle of 23 deg, and a 4-in.-bore focusing quadrupole triplet, used as a field lens. The absorber was a 48-in. target of liquid hydrogen.[4]

The beam incident on the liquid hydrogen target was monitored by coincidence of a set of plastic scintillation counters, M (1.5 and 2 in. in diameter), and a gas Čerenkov counter,[5] for discrimination against protons in the positive beam. In the energy range in which protons of the same momentum had a velocity less than $0.8c$, a liquid nitrogen Čerenkov counter was used in place of the gas counter. The transmission of pions was measured by a set of scintillation counters, S_1 to S_6, in coincidence with the monitor telescope. The scintillation counter, S_0, was placed in coincidence with S_1 to S_6 to reduce the accidental background. Counters S_1 to S_6 subtended different solid angles from the target, ranging from 1.5 to 7.1 millisteradians. The cross section was determined for each of these counters and extrapolated to zero solid angle. Eight transmission measurements were made at each energy, four with the hydrogen target empty and four with it full.

The momentum of the pion beam was determined by deflection through the bending magnet. It was measured by the current-carrying-wire method at four different times, before, during, and after the experiment. The consistency of these measurements was of the order of 1%. The momentum was also measured with a gas Čerenkov counter pressure curve. This gave the same result, but with somewhat less accuracy. The momentum spread determined by the counter telescope and the uncertainty in momentum were both 1.5%.

It was necessary to make several corrections to the data. Several species of accidental counts were monitored continuously during the experiment. These were negligible for negative pions. A fairly significant accidental rate was observed

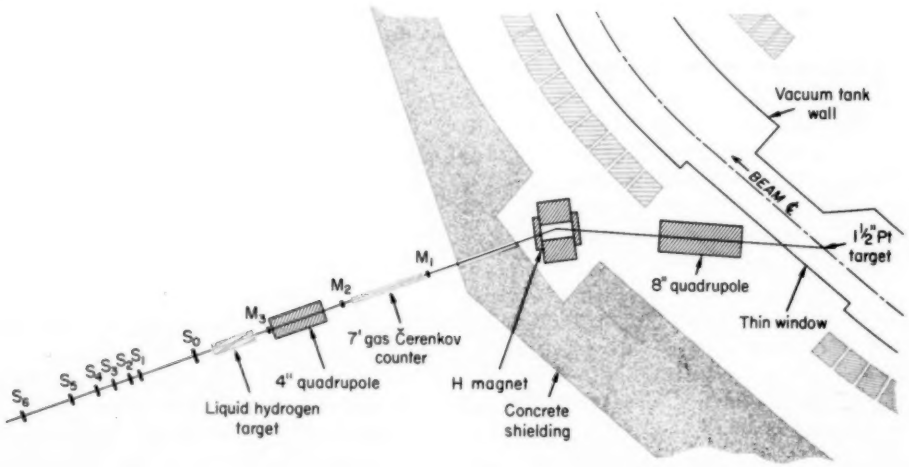

in the monitor telescope for positive pions. This was due to the high flux of protons in the beam, and can be corrected for with the known proton-proton cross section.

The beam is also contaminated by muons from π decay, and by electrons. The muon contamination originates from two regions: before the bending magnet, and after it. The contribution from pion decays before the bending magnet was measured directly by means of a gas Čerenkov counter pressure curve. An exact calculation of this contribution is difficult, and we were forced to make some simplifying approximations. The measured contamination agreed very well with the approximate calculations. The contribution from decays after the bending magnet was not measurable by the pressure-curve method, but it is calculable in a simple straightforward manner. The total muon contamination varied from $2.5 \pm 1.0\%$ at 1650 Mev to $9.5 \pm 1.0\%$ at 450 Mev. The electron contamination was also measured by the pressure curves, and it was estimated to be less than 1%.

The effect of Coulomb scattering in the hydrogen target was taken into account in the extrapolation of the cross section to zero solid angle. At higher energies, the effect was negligible at all solid angles; at lower energies, the smaller solid angles were affected. Where necessary, the cross sections were corrected by a method similar to that of Sternheimer.[6]

The number of counts taken in each measurement gave a statistical uncertainty of 1% or less in the cross section at each solid angle. The fluctuations in the series of eight transmission measurements for each particular cross section were consistent with this. The errors on the points in Fig. 2 include the systematic errors due to muon, Coulomb, and accidentals corrections in addition to counting statistics.

The total cross sections for positive and negative pions on protons are shown in Fig. 2. Our results show peaks in the π^- cross section at 600 ± 15 Mev and at 900 ± 15 Mev. These are somewhat lower energies than indicated earlier by the MIT experiment,[7] but they are in substantial agreement, within statistics, with the measurements of the group at Saclay,[8] which are also plotted in Fig. 2. The existence of a maximum in the π^+ cross section was indicated earlier by an experiment at Brookhaven.[9] Our results, in this and in a previously reported experiment,[2] confirm its existence and show it to be centered about 1350 Mev.

We wish to acknowledge our indebtedness to Professor Burton J. Moyer and Professor A. C. Helmholz for their constant help and encouragement, to Michael Longo and John Atkinson for

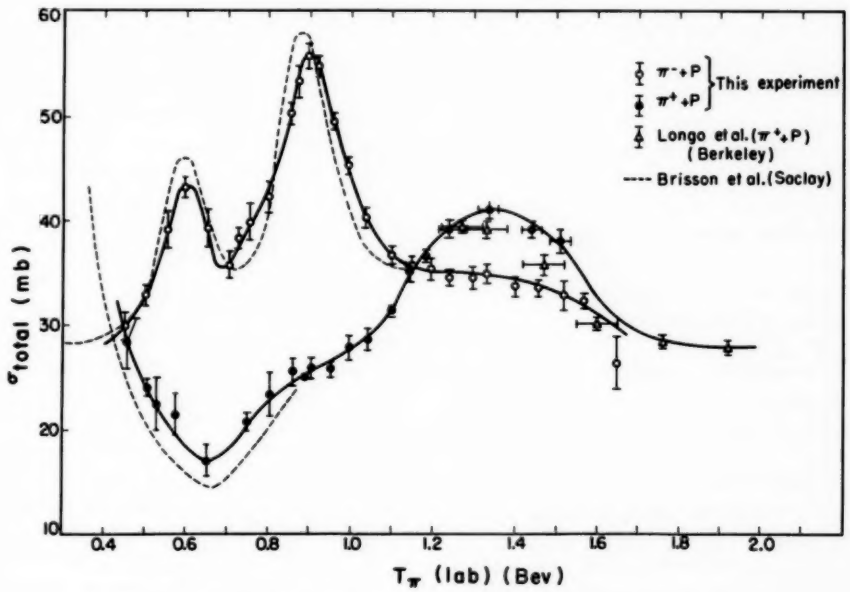

FIG. 2. Total $\pi^{\pm}-p$ cross sections vs pion kinetic energy.

their valuable aid in all phases of the experiment, and to the Bevatron staff and crew.

*Work done under the auspices of the U. S. Atomic Energy Commission.

[1]Victor Perez-Mendez, Bull. Am. Phys. Soc. 8, 451 (1959).

[2]M. J. Longo, J. A. Helland, W. N. Hess, B. J. Moyer, and V. Perez-Mendez, Phys. Rev. Letters 3, 568 (1959).

[3]L. K. Goodwin, R. W. Kenney, and V. Perez-Mendez, Phys. Rev. Letters 3, 522 (1959).

[4]Duane B. Newhart, Victor Perez-Mendez, and William H. Pope, Lawrence Radiation Laboratory Report UCRL-8857, August, 1959 (unpublished).

[5]John H. Atkinson and Victor Perez-Mendez, Rev. Sci. Instr. 30, 865 (1959).

[6]R. M. Sternheimer, Rev. Sci. Instr. 25, 1070 (1954).

[7]H. C. Burrowes, D. O. Caldwell, D. H. Frisch, D. A. Hill, D. M. Ritson, R. A. Schluter, and M. A. Wahlig, Phys. Rev. Letters 2, 119 (1959).

[8]J. C. Brisson, J. Detoef, P. Falk-Vairant, L. van Rossum, G. Valladas, and L. C. L. Yuan, Phys. Rev. Letters 3, 561 (1959).

[9]R. Cool, O. Piccioni, and D. Clark, Phys. Rev. 103, 1082 (1956).

QUESTION OF THE EXISTENCE OF A STRANGENESS 2 MESON*

D. J. Prowse
Department of Physics, University of California, Los Angeles, California
(Received February 3, 1960)

Recently Yamanouchi[1] has suggested that there is strong evidence for the existence of a strangeness 2 meson with a mass of about 720 Mev. Among several events enumerated by Yamanouchi in support of this contention is the Bristol anomalous K^+-meson decay reported by Prowse and Evans.[2]

Yamanouchi points out that if the identity of the primary particle in this event is unknown one could set up a scheme, $D^+ \rightarrow \pi^+ + K^0$ rather than $K^+ \rightarrow \pi^+ + \pi^0 + \gamma$ or $K^+ \rightarrow \pi^+ + x^0$, because the identities of all the neutral particles involved are unknown. The argument on whether or not the decay involves two or three bodies is based upon the fact that in a similar event found by the Columbia group,[3] the π^+-meson energy was the same (approximately 60 Mev). If the existence of two decays giving the same π^+-meson energy can be considered as possible evidence of a unique π^+ energy, then one is justified in postulating the decay mode $K^+ \rightarrow \pi^+ + x^0$ or, if the nature of the primary particle is undetermined, $D^+ \rightarrow \pi^+ + K^0$ also. The purpose of this Letter is to point out that the mass of the primary particle is known in the Bristol event and it is not consistent with the mass value of 720 Mev.

The event in question was found during a systematic study of the interactions of K^+ mesons with nuclei.[4] In the course of this work it appeared of interest to determine the decay modes of those K^+ mesons which had interacted and to compare them with the decay modes of those K^+ mesons which had not interacted.[5] The decay particles of the K^+ mesons which had been followed to rest in the search for interactions were therefore examined. Details of the pickup criteria used for finding and following these tracks are given in reference 4; the details of the measurements on the secondary particles are given in reference 5. In the course of the grain density measurements on these secondaries it became important to normalize the values obtained very carefully in each pellicle utilized. The normalization used was the grain density of the beam π mesons ($1.01 \times$minimum); this value was carefully determined in each plate as outlined in reference 5 and shown in Fig. 2 of reference 2. A number of K^+-meson identities were established by g^* vs R measurements because not all secondaries were visible owing to the low minimum grain density in the stack. In particular the identity of the primary of the anomalous event was established in this way. Grain density measurements were made at three residual ranges and the values were normalized using the minimum-ionization results mentioned above. The K^+-meson track was quite flat (1.4 cm/pellicle) and so no difficulties were encountered because of steepness. The three values obtained are shown graphically in Fig. 1. The expected variations of g^* vs R are shown for π mesons, K mesons, D particles, and protons. The mass of the primary is thus determined to be 532 ± 24 Mev. The identity can be seen to be well established.

The high strangeness number of 2 suggested by Yamanouchi for the new particle is sufficient to

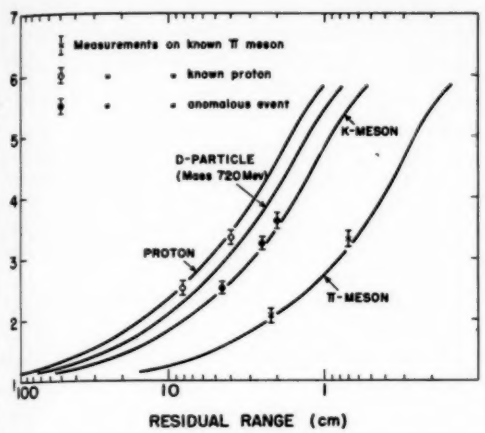

FIG. 1. Grain density measurements plotted against residual range (R). The expected variations of g^* (normalized to minimum) with R for the various particles are computed from the curves of G. Alexander and R. H. W. Johnston [Nuovo cimento 5, 363 (1957)] for g^* values below 2.9. Above this value the curves are computed from the values of $(g^*)_{F.P.}$ given by P. H. Fowler and D. H. Perkins [Phil. Mag. 46, 587 (1955)].

explain the apparent absence of conclusive proof of its existence. It is likely to be removed from any mass-separated beam which has been used heretofore and the energies of the separated strange-particle beams have not been high enough to produce it. The only experiments which might have detected the particle are those involving momentum-separated beams only. The emulsion stack in which the Bristol anomalous K^+ meson was found was exposed to such a beam (of positive sign) of 375 Mev/c momentum. During the systematic scan for K^+ particles, a search was also made in this stack for stopping particles of mass $500m_e$ and mass $1480m_e$; this search was inspired by previous reports of particles of this mass. No particles were found stopping and decaying in the regions of the emulsion stack corresponding to these mass values. If the particles have the same lifetime as the K^+ meson, the ratio of $(D^+$ or $X^+)/K^+$ at production is less than 0.5%.

The evidence for the existence of the particle, $D^\pm$, is partially listed by Yamanouchi. The results given in this paper show, however, that the 2 anomalous events[6] have to be deleted from this list. This is unfortunate for two reasons: (a) The exact mass value is not now known, and (b) it materially decreases the probable lifetime of the particle. Both of these factors will make it harder to detect.

The interpretation of the Wisconsin events[7] which are also listed as supporting evidence for the particle is not convincing. In each of these events a K^- meson of 40 Mev is produced alone by a singly charged particle which may be at rest. The K mesons are arrested in the stack and they give rise to ρ endings. Yamanouchi proposes that they are due to an interaction of D^- mesons according to the scheme,

$$D^- + n_{\text{bound}} \rightarrow \Lambda^0 + K^-.$$

Such an interpretation does not explain the equality of the K-meson energy in each event because the momentum of the bound neutron would considerably broaden the spectrum; evaporation prongs would also be expected. A better interpretation is that they are due to the decay of a heavy particle as originally suggested by the authors.[7]

There have been reports of other mass 1450 particles; in 1955 Menon reported the result of Fowler and Perkins at the Rochester Conference.[8] Mass determinations by grain density and scattering measurements on flat particles from cosmic-ray stars gave some indication of a peak at $1480m_e$. When these measurements became more accurate, however, in larger stacks where the particle ranges could be determined, these mass values were not confirmed.

An event which can be interpreted as a $D^\pm$-meson decay according to the scheme suggested by Yamanouchi has been observed by Sen Gupta and Sinha[9] in a cloud chamber.

In conclusion we may say that although a number of hitherto unexplained events can be interpreted if such a particle is postulated, concrete evidence for its existence is lacking and is certainly not provided by the anomalous K^+ decays.

We are grateful to Professor H. K. Ticho, Dr. J. H. Mulvey, Professor J. Orear, and Professor E. C. G. Sudarshan for many discussions. We also wish to thank Professor J. Orear for prepublication information on the mass value of the Columbia anomalous K^+ decay.

---

*Partially supported by the U. S. Atomic Energy Commission.

[1]T. Yamanouchi, Phys. Rev. Letters 3, 480 (1959).
[2]D. J. Prowse and D. Evans, Nuovo cimento 8, 856

(1958).

[3]G. Harris, J. Lee, J. Orear, and S. Taylor, Phys. Rev. 108, 1561 (1957).

[4]B. Bhowmik, D. Evans, S. Nilsson, D. J. Prowse, F. Anderson, D. Keefe, A. Kernan, and J. Losty, Nuovo cimento 6, 440 (1957).

[5]B. Bhowmik, D. Evans, D. J. Prowse, F. Anderson, D. Keefe, and A. Kernan, Nuovo cimento 8, 147 (1958).

[6]J. Orear has informed us that the mass value of the primary particle in the Columbia event is also consistent with the K^+-meson mass [private communication, and Bull. Am. Phys. Soc. 5, 12 (1960)].

[7]W. F. Fry, J. Schneps, and M. Swami, Phys. Rev. 97, 1189 (1955) and Nuovo cimento 2, 346 (1955).

[8]M. G. K. Menon, Proceedings of the Fifth Annual Rochester Conference on High-Energy Nuclear Physics (Interscience Publishers, New York, 1955), p. 77; work of P. H. Fowler and D. H. Perkins. Preliminary results were also reported by P. H. Fowler, Proceedings of the Fourth Annual Rochester Conference on High-Energy Nuclear Physics (University of Rochester Press, Rochester, 1954), p. 80; and by D. H. Perkins, Proceedings of the Third Annual Rochester Conference on High-Energy Nuclear Physics (University of Rochester Press, Rochester, 1952), p. 42.

[9]S. N. Sen Gupta and M. S. Sinha, Phil. Mag. 2, 936 (1957).

PARTIAL-WAVE DISPERSION RELATIONS FOR MESON-NUCLEON SCATTERING*

Reinhard Oehme

Enrico Fermi Institute for Nuclear Studies and Department of Physics, University of Chicago, Chicago, Illinois

(Received February 3, 1960)

It is of interest to compute the implications for the pion-nucleon scattering amplitude of possible resonance effects in the two-pion system.[1] In this note we propose a form of the π-N partial-wave dispersion relations[2] which is suitable for this purpose. Our formulas can be easily generalized for amplitudes involving other particles with unequal mass.

We write the covariant π-N amplitude in the form[3] $F = A - i\gamma\cdot\frac{1}{2}(k+k')B$, where $A_{\alpha\beta} = A^+\delta_{\alpha\beta} + A^-\frac{1}{2}[\tau_\alpha, \tau_\beta]$, etc. and $k+p = k'+p'$, $k^2 = k'^2 = -\mu^2$, $p^2 = p'^2 = -m^2$. In the following we discuss explicitly only the invariant amplitudes $A^\pm$; the extension to $B^\pm$ and to center-of-mass quantities is straightforward. Let us first consider the $A^\pm$ as functions of the invariant variables $z = -(k+p)^2$, $\zeta = -(k-k')^2$. We assume that they are analytic in both variables except for the absorptive singularities[4] due to the possible intermediate states of the three physical reactions associated with the π-N Green's function. Then we have the branch lines[3]

$$z = s \geq (m+\mu)^2, \quad \bar{z} = \bar{s} \geq (m+\mu)^2, \quad \text{and } \zeta = t \geq (2\mu)^2, \tag{1}$$

where $\bar{z} = 2m^2 + 2\mu^2 - z - \zeta$. The single nucleon poles $z = m^2$, $\bar{z} = m^2$ appear only in the amplitudes $B^\pm$. The variables z and ζ may be expressed in terms of q^2 (q = c.m. momentum) and θ (c.m. angle) by

$$z = m^2 + \mu^2 + 2q^2 + 2[(q^2+m^2)(q^2+\mu^2)]^{1/2}, \tag{2a}$$

$$\zeta = -2q^2(1-\cos\theta). \tag{2b}$$

Note that the complex z plane is mapped into a Riemann surface with two leaves which are connected through the cut $-m^2 \leq q^2 \leq -\mu^2$. We define sheet I (II) by the requirement that the root in Eq. (2a) is positive (negative) for real $q^2 > -\mu^2$. In the z plane, the exterior of the circle $|z| = m^2 - \mu^2$ corresponds to sheet I and the interior to sheet II.

Let us now consider the amplitude A as an analytic function of q^2 for $-1 \leq \cos\theta \leq +1$. It is regular on the Riemann surface mentioned above except for cuts along the real axes in both sheets. In particular, the partial-wave amplitudes,

$$A_J(q^2) = \tfrac{1}{2}\int_{-1}^{+1} d\cos\theta\, P_J(\cos\theta) A(q^2, \cos\theta), \tag{3}$$

have the following cuts: (πN) from 0 to $+\infty$ in I, due to $s \geq (m+\mu)^2$; $(\bar{\pi}N)$ from 0 to $+\infty$ in I and from $-\infty$ in II up to $-m^2$ and then down to $-\infty$ in I, both due to $\bar{s} \geq (m+\mu)^2$; $(\pi\bar{\pi})$ from $-\mu^2$ to $-\infty$ in I and II, due to $t \geq (2\mu)^2$. The weight functions associated with the unphysical branch lines $(\bar{\pi}N)$ and $(\pi\bar{\pi})$ can be expressed in terms of the absorptive parts $N(\alpha,\beta)$ and $M(\alpha,\beta)$ (α,β being the squares of energy momentum transfer), cor-

responding to the reactions $\pi+N\to\pi+N$ and $\pi+\bar{\pi}\to N+\bar{N}$, respectively. In the physical sheet I we can write partial-wave dispersion relations in the simple form

$$A_J(q^2)=\frac{1}{\pi}\int_0^\infty dq'^2\frac{\mathrm{Im}A_J(q'^2)}{q'^2-q^2}+\frac{1}{\pi}\int_{-\infty}^{-\mu^2}dq'^2\frac{\mathrm{Im}A_J(q'^2)}{q'^2-q^2},\qquad(4)$$

which should be amended by the usual substractions. However, in the interval $-m^2\le q^2\le-\mu^2$ the real weight $\mathrm{Im}A_J$ can be expressed in terms of the absorptive parts N and M only indirectly by writing a similar dispersion formula in sheet II. Dispersion relations involving both sheets can be easily written down, but it seems to be advantageous to use the invariant variable z for those portions of the cuts which map onto the real axis in the z plane, and to retain the variable q^2 for that part of the branch line $(\pi\bar{\pi})$, which maps onto the circle $|z|=m^2-\mu^2$. Omitting again appropriate subtractions, we can write

$$A_J(z)=\frac{1}{\pi}\int_{(m+\mu)^2}^\infty ds\frac{\mathrm{Im}A_J(s)}{s-z}+\frac{1}{\pi}\int_{-\infty}^{(m-\mu)^2}ds\frac{\mathrm{Im}A_J(s)}{s-z}+F_J(z)+F_J^*(z^*),\qquad(5)$$

where

$$F_J(z)=-\frac{1}{\pi}\int_{-m^2}^{-\mu^2}d\lambda\frac{2s(\lambda)}{s(\lambda)-m^2-\mu^2-2\lambda}\frac{M_J(s(\lambda))}{s(\lambda)-z},\qquad(6)$$

with

$$s(\lambda)=m^2+\mu^2+2\lambda+2i[(\lambda+m^2)(-\lambda-\mu^2)]^{1/2},\qquad(7)$$

and, for $s\le(m-\mu)^2$,

$$\mathrm{Im}A_J^{\pm}(s)=\theta(-s)\epsilon(s+m^2-\mu^2)N_J^{\pm}(s)\mp M_J^{\pm}(s).\qquad(8)$$

The functions M_J and N_J are given in terms of the absorptive parts $M(\alpha,\beta)$ and $N(\alpha,\beta)$ by

$$M_J(s)=-\frac{1}{4q^2}\int_{4\mu^2}^{-4q^2}dt\,P_J(1+t/2q^2)M(t,s),$$

$$N_J(s)=-\frac{1}{4q^2}\int_{2m^2+2\mu^2-s}^{c(s)}d\bar{s}\,P_J\left(1+\frac{2m^2+2\mu^2-s-\bar{s}}{2q^2}\right)N(\bar{s},2m^2+2\mu^2-s-\bar{s}),\qquad(9)$$

where $q^2=q^2(s)$ is given by the inverse of Eq. (2a) with $z=s$; and $c(s)=(m^2-\mu^2)^2/s$ for $0_+\le s\le(m-\mu)^2$, $c(s)=(m+\mu)^2$ for $s\le0_-$. The term $F_J+F_J^*$ in Eq. (5) contains the low-energy properties of the 2π system. Using Eqs. (6) and (9), it can be easily written in terms of real and imaginary parts of $M(t,s)$.[5] The latter quantity is complex due to the appearance of $s(\lambda)$ given by Eq. (7). In a partial-wave expansion of $M(t,s)$ the variable s will appear only in the argument of the spherical harmonics.

*Supported in part by the U. S. Atomic Energy Commission.

[1]W. R. Frazer and J. R. Fulco, Phys. Rev. Letters 2, 365 (1959).

[2]Partial wave relations have been discussed also by S. W. MacDowell, Phys. Rev. 116, 774 (1959).

[3]See, for example, G. F. Chew, Annual Reviews of Nuclear Science (Annual Reviews, Inc., Palo Alto, 1959), Vol. 9, p. 29; this paper contains further references.

[4]R. Oehme, Nuovo cimento 13, 778 (1959).

[5]The absorptive parts $M(\alpha,\beta)$ and $N(\alpha,\beta)$ can also become complex for large negative values of β. The contributions from the corresponding imaginary parts cancel each other in Eq. (5).

CLASSICAL ELECTRODYNAMIC EQUATIONS OF MOTION WITH RADIATIVE REACTION*

Gilbert N. Plass
Aeronutronic, Ford Motor Company, Newport Beach, California
(Received November 5, 1959)

The classical relativistic equations of motion of a charged particle including the force of radiative reaction have been derived by Dirac[1] and by Wheeler and Feynman.[2] The existence of divergent solutions of these equations which increase exponentially with time has been discussed extensively in the literature.[1,3] The existence of these solutions has been the basis for the fairly widespread belief that these equations provide only an approximate description of the behavior of a classical radiating charged particle. Eliezer[3] has claimed that no physical solutions for these equations exist for (1) the field of a thin infinite charged plate, (2) an attractive Coulomb force, and (3) a repulsive Coulomb force. On the contrary it can be shown that a physically reasonable solution for these equations exists for any force field that satisfies certain conditions given below.

For simplicity consider first the one-dimensional, nonrelativistic equation of motion,

$$ma - mb^{-1}\dot{a} = f(t), \tag{1}$$

where

$$b^{-1} = 2e^2/3mc^3, \tag{2}$$

$f(t)$ is the force acting on the particle, a is the acceleration of the particle, and dots signify differentiation with respect to time.

The exact nondivergent solution of Eq. (1) is

$$ma(t) = b\int_0^\infty e^{-bt'} f(t+t')dt'. \tag{3}$$

Since Eq. (1) contains a third derivative with respect to the position of the particle, the appropriate physical boundary conditions require that the initial acceleration as well as the initial velocity and position be specified. The initial value of the acceleration is obtained by setting $t=0$ in Eq. (3). It is seen from Eq. (3) that the acceleration at a given time is determined by the force that will act on the particle over a time interval of the order of b^{-1} (which is approximately 10^{-23} sec) in the future. This phenomenon of pre-acceleration has been shown[1,2] not to violate our ordinary causal concepts over time intervals greater than b^{-1}.

From the theory of Laplace transforms it follows that a nondivergent, physical solution of Eq. (1) for the position, velocity, and acceleration of the particle exists whenever (1) $f(t)$ is continuous or piecewise continuous; (2) $t'^n|f(t+t')|$ is bounded near $t'=0$ for some number n, where $n<1$; (3) $e^{-bt'}|f(t+t')|$ is bounded for large values of t'. The solution for the three-dimensional nonrelativistic equation has the same form as Eq. (3) with a and f replaced by the corresponding vector quantities.

A general solution cannot be given for a space-dependent force. Whenever a solution exists of Eq. (3) for $f[r(t)]$, it is nondivergent provided that the above conditions on the force are satisfied. The existence of such a solution cannot be proved in general; however, nondivergent solutions have been obtained for a number of particular space-dependent forces, some of which are listed below.

An alternative solution to Eq. (1) is

$$ma(t) = \sum_{n=0}^{\infty} b^{-n} f^{(n)}(t), \tag{4}$$

where $f^{(n)}(t)$ is the nth derivative of f. Thus, the acceleration at the time t can also be obtained from all of the derivatives of the force evaluated at the same time t. This solution is usually very rapidly convergent, since a physical force seldom changes appreciably over a time interval b^{-1}.

Physically acceptable solutions exist for relativistic particles whenever a similar solution exists for the same force field at nonrelativistic velocities. The one-dimensional relativistic equation of motion is

$$\dot{u} - \frac{1}{b}\ddot{u} + \frac{1}{b}\frac{u\dot{u}^2}{c^2+u^2} = \frac{1}{m}\left(1+\frac{u^2}{c^2}\right)^{3/2} f(\tau), \tag{5}$$

where u is the derivative of position with respect to the proper time, τ, and dots in this equation indicate differentiation with respect to τ. The exact, nondivergent solution of this equation is

$$u = c\,\sinh\{\sinh^{-1}(u_0/c) + (mc)^{-1}\int_0^\tau f(\tau')d\tau'$$

$$+ (mc)^{-1}\int_0^\infty e^{-b\tau'}[f(\tau+\tau') - f(\tau')]d\tau'\}, \tag{6}$$

where u_0 is the value of u at $\tau = 0$. The first two terms on the right side of Eq. (6) are the solution of the relativistic equation of motion without radiative reaction, while the last term represents the effect on the motion of radiative reaction.

The exact, nondivergent solutions of these equations of motion have been obtained for a number of particular force fields including the cases where (1) $f = C(t-t_0)^n$, $n \geq -1$; (2) $f = C \sin\omega t$; (3) $f = C \exp[-(t-t_0)^2/2\sigma^2]$; (4) $f = C$, $x_0 < x < x_1$; $f = 0$ otherwise; (5) crossed, oscillating electric and magnetic fields; (5) constant magnetic field; (6) harmonic oscillator; (7) field of a thin charged plate. Furthermore, by numerical procedures, nondivergent solutions have been obtained for three-dimensional motion under the influence of attractive and repulsive Coulomb forces.

Thus, when the proper boundary condition is used to specify the initial acceleration of a charged particle, nondivergent solutions exist for most force fields of interest in physics. Therefore, there no longer appears to be any reason for not accepting these equations of motion. To the best of our knowledge, they provide an exact description of the motion of a charged particle within the framework of classical theory.

The author wishes to thank Sylvan Katz for several valuable discussions during which the present method for obtaining the mathematical solutions for the equations of motion was formulated. Professor John Wheeler made many useful suggestions during the early stages of this work.

---

*This research was supported by the Office of Naval Research.

[1]P. A. M. Dirac, Proc. Roy. Soc. (London) A167, 148 (1938). P. Langevin and M. de Broglie, La théorie du rayonnement et les quanta (Gauthiers-Villars, Paris, 1912), record (pp. 41-46) the back and forth discussion at the Solvay conference of 1911 between Langevin and Lorentz concerning pre-acceleration.

[2]J. A. Wheeler and R. P. Feynman, Revs. Modern Phys. 17, 157 (1945).

[3]C. J. Eliezer, Revs. Modern Phys. 19, 147 (1947).

ABSTRACTS

In this section are printed the abstracts of Articles that have been forwarded to The American Institute of Physics for publication in THE PHYSICAL REVIEW. In quoting information obtained from this section before the appearance of the corresponding Article, reference should be made to "Physical Review (to be published)" rather than to this Journal.

SIGNIFICANCE OF POTENTIALS IN QUANTUM THEORY. W. H. Furry and N. F. Ramsey, Lyman Laboratory of Physics, Harvard University, Cambridge, Massachusetts (Received November 16, 1959).

The effects of the scalar and vector potentials in quantum mechanics, which were pointed out recently by Aharonov and Bohm, are discussed from the point of view of the consistency of the quantum-mechanical description of interference experiments. A well-known requirement for this consistency is that if any measuring device is introduced that can be used to determine which path the particle has taken, it must have the effect of eliminating the interference phenomenon. Two conceptual experiments are discussed corresponding to the two phase effects noted by Aharonov and Bohm. In each case it is found that the phase effect is of just the magnitude required to destroy the interference pattern when the circumstances are such that no pattern should be observed.

RELATION BETWEEN INELASTIC NEUTRON SCATTERING AND THERMODYNAMIC FUNCTIONS OF LIQUID HELIUM. Michael Cohen, University of Pennsylvania, Philadelphia, Pennsylvania (Received October 26, 1959).

A model of liquid helium is analyzed, in which the liquid is regarded as a collection of excitations ("rotons" only with energy $\geq\Delta$) with an arbitrary pairwise number-conserving interaction. The entropy and normal fluid density of the liquid and the energy distribution of scattered neutrons are computed as power series in the density of excitations $\exp(-\Delta/kT)$. The first terms containing effects of the interactions are studied. When the interactions are weak, the entropy [through order $\exp(-2\Delta/kT)$] is simply related to the neutron scattering, the connection being correctly given by the formula of Bendt, Cowan, and Yarnell. For strong interactions there appears to be no simple connection. Even when interactions are weak, the first correction to the normal fluid density involves information which is not contained in the neutron scattering.

A method due to Bloch and de Dominicis is used in the analysis, and leads to a new form for the second virial coefficient. This is closely related to a curious new form for the level shift of a particle in a large spherical box, under the influence of a central potential.

ELECTRIC FIELD DISTRIBUTIONS IN AN IONIZED GAS. II. Bernard Mozer* and Michel Baranger, Carnegie Institute of Technology, Pittsburgh, Pennsylvania (Received November 23, 1959).

A method previously described is used to calculate the probability distribution of the low-frequency component of the electric field at a neutral point, the distribution of the low-frequency component at an ion, and that of the high-frequency component at an electron. The results are compared with those obtained by other authors.

*Now at Brookhaven National Laboratory, Upton, New York.

SELF-CONSISTENT FIELD AND MOTION OF ELECTRONS WHICH HAVE A RANGE IN CANONICAL ANGULAR MOMENTUM IN A UNIFORM MAGNETIC FIELD. Lewi Tonks, Lawrence Radiation Laboratory, University of California, Livermore, California (Received November 2, 1959).

The self-consistent theory of relativistic electrons circulating in a uniform impressed magnetic field, the "Astron problem," has been generalized to the extent that a range of canonical angular momentum among monoenergetic electrons has been treated. For simplicity, the density distribution in phase space has been chosen to be uniform over a finite momentum range. Just as in the single-momentum case, field reversal is found, but new field and spatial density configurations appear. The uniform distribution is found to be consistent with isotropic regions of constant spatial density and constant magnetic field. The thickness of transition layer between vacuum and such a region conforms, within limits, to an empirical relation previously

found. The limit to the number of electrons per unit axial length of layer still exists. The curves relating the ratio of internal to external field to the layer strength still show multiple values of both ratio and strength in certain ranges. Trajectories have been calculated and plotted for several cases.

GROUND-STATE ENERGY OF A MANY-FERMION SYSTEM. W. Kohn, Carnegie Institute of Technology, Pittsburgh, Pennsylvania, and J. M. Luttinger, University of Pennsylvania, Philadelphia, Pennsylvania (Received October 19, 1959).

This paper contains a critique of the Brueckner-Goldstone perturbation series for the ground-state energy of an interacting gas of Fermions. We have calculated this energy by first constructing the grand partition function at finite temperature, and then carefully taking the limit as $T \to 0$. In general this leads to a series which differs from that of Brueckner and Goldstone. An exception is the case where both the unperturbed single-particle energy as well as the interaction potential have spherical symmetry. Reasons for the breakdown of the Brueckner-Goldstone formalism are briefly discussed.

QUANTUM STATISTICS OF NONIDEAL SYSTEMS. Frank H. Stillinger, Jr.,* and John G. Kirkwood,† Department of Chemistry, Yale University, New Haven, Connecticut (Received October 23, 1959).

A new cluster development for the logarithm of the grand partition function of a system of interacting particles is derived. The leading term in this expansion is the pressure exerted by an ideal Bose or Fermi gas at the same temperature and absolute activity Z as the actual system. Succeeding terms involve quantum cluster integrals which themselves depend upon Z, unlike their classical analogs. The definition of these cluster integrals follows in a natural fashion using techniques illustrated by construction (in closed form) of the successive Z derivatives of the Bose and Fermi ideal gas grand partition functions. It is not possible (except in the classical limit) to eliminate Z explicitly between the pressure and density series, so that the equation of state must remain in parametric form.

*Present address: Bell Telephone Laboratories, Murray Hill, New Jersey.

†Deceased.

TRANSPORT PHENOMENA IN SLIGHTLY IONIZED GASES: HIGH ELECTRIC FIELDS. Mahendra Singh Sodha, Physics Division, Armour Research Foundation, Chicago, Illinois (Received November 9, 1959).

Starting with the electron velocity distribution obtained by Chapman and Cowling for a Lorentzian gas, in the presence of an electric field, the author has investigated the variation with electric field of a number of transport properties, arising from a magnetic field, perpendicular to the electric field and temperature gradient in the gas. The applicability of the results to semiconductors has also been pointed out. A constant mean free path has been assumed, which is validated by experiments for helium.

LOW-LYING EXCITATIONS IN A BOSE GAS OF HARD SPHERES. F. Mohling, Department of Physics, Columbia University, New York, New York, and A. Sirlin, Department of Physics, New York University, New York, New York (Received November 2, 1959).

The pseudopotential method is used to calculate the low-lying excitation energies of a Bose gas of hard spheres at $T = 0$ to an order beyond that previously calculated by this technique. The results are in agreement with those obtained by Beliaev using a different approach. The phonon velocity is found to be equal to the velocity of compressional waves to the order of approximation considered.

STATISTICAL MECHANICAL THEORY OF FERROMAGNETISM: HIGH-DENSITY LIMIT. R. Brout, Laboratory for Atomic and Solid State Physics and Department of Physics, Cornell University, Ithaca, New York (Received November 30, 1959).

The partition function of the Ising model of ferromagnetism is examined in the limit of high density in the anticipation that in the limit of in-

finite density one recovers the Weiss molecular field. The formal parameter of expansion is $1/z$, where z is the number of spins in the range of the exchange potential (not restricted to nearest neighbor interactions). In the absence of long-range order, only ring diagrams in the cluster expansion contribute. These give a divergence in the specific heat at $kT_C = \sum_{j \neq i} v_{ij}$, where v_{ij} is the exchange potential. This is the molecular field value for the Curie point T_C. In the presence of a magnetic field the partition function is evaluated for fixed magnetic moment M in the same approximation, M being determined by minimization. This results in a susceptibility differing from the molecular field theory and hence an inconsistency in the theory.

The inconsistency is traced back to the observation that the acceptance of ring diagrams is equivalent to the Gaussian model of Kac and Berlin which violates the sum rule $\sum_{i=1}^{N} (\mu_i^2) = N$. μ_i is the "spin" per particle and N is the total number of particles. This condition is reinstated by insuring the sum rule. The result leads to the spherical model. Thus, a consistent high-density approximation to the Ising model is the spherical model. Below the Curie point or for fixed magnetic field, M is again held fixed and only the Fourier components of the spin density with nonvanishing wave vector are "spherically." The result leads to a physically acceptable model which becomes the molecular field theory at low temperatures or high fields and deviates in $O(1/z)$ in general. Formally, the results are simply expressed in terms of a temperature-dependent Weiss field. These results differ from the ordinary spherical model which is physically unacceptable below the Curie point. However a molecular field modification of the spherical model due to Lax yields the same result when properly interpreted.

It is shown that the above results are also valid (to the same approximation) in the quantum mechanical Heisenberg model, for temperatures above the Curie point.

EXCITATION OF SPIN WAVES IN FERROMAGNETS: EDDY CURRENT AND BOUNDARY CONDITION EFFECTS.

P. Pincus, Department of Physics, University of California, Berkeley, California (Received November 16, 1959).

The boundary condition for the transverse magnetization is derived when there is a surface anisotropy field H_S. Writing the transverse magnetization as $\alpha \sin kz + \beta \cos kz$, we have

$$\alpha/\beta = -\tfrac{1}{2}ka + (H_s/H_e ak),$$

where H_e is the exchange field and a the lattice constant. A similar result is found when there is an antiferromagnetic surface layer. For $H_S \neq 0$ spin-wave modes can be excited by a uniform rf field in a ferromagnet. The power absorbed in each mode in an insulator is calculated as a function of the surface anisotropy field. The excitation of the exchange modes is calculated for a metal with eddy-current damping. The eddy currents are found to have a large effect only on long-wavelength spin waves. The line shape in a thick metal plate is calculated for H_0 normal to the plate.

NUCLEAR QUADRUPOLE AND ELECTRONIC HEAT CAPACITIES OF BISMUTH.

Norman E. Phillips, Department of Chemistry and Lawrence Radiation Laboratory, University of California, Berkeley, California (Received November 17, 1959).

The heat capacity of bismuth has been measured from 0.1 to 2.0°K and found to be represented by $C = 2.8 \times 10^{-7} T^{-2} + 2.1 \times 10^{-5} T + 1944 (T/\theta)^3$ joules/mole deg with $\theta = 120.4 - 0.67^2$. The T^{-2} term in the heat capacity is assumed to be associated with the alignment of the nuclear electric quadrupole moment in the electric field gradient of the crystal and is used to obtain the value 25 Mc/sec for the quadrupole coupling constant. The linear term is used, together with known parameters for the electrons in the conduction band, to obtain an average effective mass for the holes in the valence band of 0.9 times the free electron mass.

EFFECT OF OXIDATION ON THE CHARACTERISTIC LOSS SPECTRA OF ALUMINUM AND MAGNESIUM.

C. J. Powell* and J. B. Swan,† Department of Physics, University of Western Australia, Nedlands, Western Australia (Received October 26, 1959).

Measurements of the characteristic electron energy loss spectra of aluminum and magnesium were made (in a reflection experiment) during oxidation of a fresh evaporated layer of either

metal. It was found that surface oxidation results in the rapid disappearance of the low-lying energy losses (10.3 ev in aluminum and 7.1 ev in magnesium) and the appearance of modified low-lying losses of 7.1 ev in aluminum and 4.9 ev in magnesium. The general changes in the loss spectra and the particular changes in the spectrum of aluminum were in good agreement with the predictions of Ferrell and Stern.

*Now at the Imperial College of Science and Technology, London, England.
†Now on leave at Brookhaven National Laboratory, Upton, New York.

LIMITING PROPERTIES OF NUMBERS OF SELF-AVOIDING WALKS. J. M. Hammersley, Institute of Statistics, Oxford, England (Received November 16, 1959).

A counter-example is given to a conjecture of Fisher and Sykes [Phys. Rev. 114, 45 (1959)] on the number of self-avoiding walks arising in the excluded-volume problem in the Ising model of ferromagnetism.

NUCLEAR QUADRUPOLE SPIN-LATTICE RELAXATION IN ALKALI HALIDES. E. G. Wikner,* W. E. Blumberg,† and E. L. Hahn, Department of Physics, University of California, Berkeley, California (Received November 25, 1959).

Nuclear quadrupole spin-lattice relaxation times have been measured in alkali halide crystals by the pulsed magnetic resonance technique. Measurements were made on Na^{23} in NaCl, NaBr, and NaI; Cl^{35} in NaCl and KCl; $Br^{79,81}$ in NaBr, KBr, RbBr, and CsBr; Rb^{87} in RbCl and RbBr; and I^{127} in NaI, KI, and CsI. Over a temperature range of 298°K to 195°K the relaxation times are inversely proportional to the square of the absolute temperature. The data are compared to relaxation times calculated from an ionic crystal model of Van Kranendonk and a covalent model of Yosida and Moriya. The ionic model is modified to include the interaction between the nuclear quadrupole moment and the electric field gradient due to electric dipole moments associated with optical modes of vibration. Neither of these models alone predicts the experimental relaxation times for all cases, but a combination of the two effects is required. The modified ionic model applies reasonably well to crystals which contain the lighter ions.

*Present address: General Atomics, San Diego, California.
†Present address: Bell Telephone Laboratories, Murray Hill, New Jersey.

CRYSTAL STRUCTURE OF FERROELECTRIC $LiH_3(SeO_3)_2$. K. Vedam, Y. Okaya, and R. Pepinsky, Department of Physics, Crystal Research Laboratory, The Pennsylvania State University, University Park, Pennsylvania (Received November 30, 1959).

The structure of the room-temperature ferroelectric $LiH_3(SeO_3)_2$ has been determined by x rays, using the heavy-atom method, and refined on the IBM 704. The crystals are monoclinic, with space group Pn and $a = 6.25_8$ A, $b = 7.88_6$ A, $c = 5.43_3$ A, $\beta = 105.2°$. Fairly strong O-H···O bonds with distances 2.52, 2.56, and 2.57 A are found, nearly perpendicular to the polar direction. The O-Se-O angles in one of the two selenite ions are rather similar; in the other ion these angles are unequal, as in the structure of H_2SeO_3. Possible positions for the Li ions are given based on crystal-chemical considerations.

SPIN RESONANCE OF CHARGE CARRIERS IN GRAPHITE. G. Wagoner, Research Laboratory, National Carbon Company, Cleveland, Ohio (Received November 25, 1959).

The observations reported here of the electron spin resonance in quite perfect single crystals of graphite clearly establish that the resonance arises from mobile charge carriers. The line shape is of the Dyson form which is characteristic of conduction electron spin resonance in metals. The intensity of the spin resonance agrees, both in absolute magnitude and in temperature dependence, with values calculated from the band model of graphite by McClure. The g value of the resonance shows a remarkably large anisotropy which depends strongly on temperature and on the position of the Fermi level with respect to the band edge. At room temperature in pure graphite, g varies from 2.0026 ± 0.0002 to 2.0495 ± 0.0002 as the magnetic field is shifted from perpendicular to parallel to the c axis. The g-value anisotropy increases

with decreasing temperature; $g_{\parallel}$ becomes 2.127 at 77°K while $g_{\perp}$ remains constant. The line width of the resonance is a few gauss ($T_2 = 2.0 \times 10^{-8}$ sec) which is extremely narrow in comparison with the field shifts caused by changes of anisotropy with temperature. This indicates that for conduction states in graphite, the g value is a strong function of the wave vector and that the line is narrowed by an averaging process in k space. This averaging is similar to that which occurs in motional and exchange narrowing.

NORMAL MODES OF A LATTICE OF OSCILLATORS WITH MANY RESONANCES AND DIPOLAR COUPLING. U. Fano, National Bureau of Standards, Washington, D. C. (Received November 2, 1959).

The normal modes of a lattice of coupled dipoles are studied as a model of the collective excitations of electrons in condensed materials. Two types of oscillations are found, in which electrostatic coupling has a dominant influence. One of them is analogous to the oscillation of an electron plasma and has a high dipole moment. Other collective oscillations have a low net dipole moment, owing to destructive interference between out-of-phase components. These two types of oscillation occur in systems with a sufficiently high density of oscillator strength in space and in spectrum. A simple estimate indicates that most condensed materials fulfill this condition.

PULSED NUCLEAR RESONANCE SPECTROSCOPY. M. Emshwiller,* E. L. Hahn, and D. Kaplan,† Department of Physics, University of California, Berkeley, California (Received November 2, 1959).

A technique for the detection of weak nuclear resonance interactions in solids is carried out by a pulsed method which obtains nuclear double resonance. The resonance of the unknown species to be detected does not require a Boltzmann population difference in spin orientation, but must have a sufficient dipole-dipole interaction with a second spin species. At resonance, a single 180° pulse reorients the unknown spins at the time of the 180° pulse in the 90°-180° pulse sequence necessary to obtain the observed spin-echo signal of the second species. A reduction of the spin-echo signal signifies double resonance due to changes in local dipolar fields, coupled to the observed spins, which scrambles their precessional phases. Nuclear quadrupole coupling interactions of K, Cs, and Rb isotopes are measured in the chlorates of these ions, where the Cl^{35} nucleus provides the observed nuclear quadrupole echo. An analysis is presented for the case of low concentration of unknown spin species. Double quantum transitions and special properties of nuclear quadrupole spectra are observed.

*Present address: Bell Telephone Laboratories, Whippany, New Jersey.

†Present address: Lockheed Missile Systems Division, Palo Alto, California.

INTERNAL FIELD EMISSION AT NARROW SILICON AND GERMANIUM p - n JUNCTIONS. A. G. Chynoweth, W. L. Feldmann, C. A. Lee, R. A. Logan, and G. L. Pearson, Bell Telephone Laboratories, Murray Hill, New Jersey, and P. Aigrain, Ecole Normale Supérieure, Paris, France (Received November 5, 1959).

A detailed study has been made of the reverse characteristics of several silicon and germanium alloyed p - n junctions with breakdown voltages in the range of about 0.1 to 0.8 volt. In these junctions the reverse current is generated almost entirely by internal field emission (tunneling). The reverse bias characteristics are insensitive to the dislocation density present so that the tunneling current occurs mainly in undistorted material. From capacitance studies it is established that these narrow junctions are very close to being ideal step junctions. The room temperature reverse characteristics are analyzed in terms of the usual tunneling probability expressions and in particular, good agreement, both qualitative and quantitative, is found between experiment and theory. The tunneling probability $\exp(-\alpha\epsilon^{3/2}/E)$, when compared with experiment, yields values for $\alpha\epsilon^{3/2}$ in agreement with the theoretical ones to within a factor of less than 2 for both silicon and germanium.

The critical voltage (the reverse bias voltage necessary to maintain a constant tunneling current) was measured as a function of temperature from 4.2°K up to temperatures as high as 700°K. In germanium, the critical voltage drops mono-

tonically as the temperature increases whereas in silicon, there is considerable structure in the curve. This is shown to be consistent with the tunneling being by direct transitions in germanium and by indirect transitions (involving phonon emission and absorption) in silicon. In germanium, the temperature dependence of the critical voltage arises from that of the direct energy gap while in silicon, it is determined, primarily, by the available phonon density. From an analysis of the temperature data for silicon that invokes the transverse acoustic phonons, the estimate of $\alpha\epsilon^{3/2}$ that is obtained is in excellent agreement with that found, independently, from the analysis of the reverse characteristics.

THERMOELECTRIC POWER OF DILUTE COPPER ALLOYS. F. J. Blatt and R. H. Kropschot,* Physics Department, Michigan State University, East Lansing, Michigan (Received October 12, 1959).

The thermoelectric power of dilute binary copper alloys containing one atomic percent Zn, Ge, Cd, In, Sn, and Sb was determined over the temperature range extending from about 8°K to 320°K. The thermoelectric powers were obtained by measuring the thermoelectric emf's of thermocouples formed of the alloys and pure copper. The absolute thermoelectric power of pure copper was obtained from measurements on a pure copper versus lead thermocouple.

The results are analyzed in terms of the Friedel theory. It is found that above 40°K satisfactory agreement with that theory can be obtained only if it is assumed that phonon drag makes a significant contribution to the thermoelectric power in the pure material below room temperature. The magnitude and temperature dependence of this assumed phonon drag contribution are in satisfactory agreement with theoretical estimates. Moreover, the effect of alloying on this phonon drag contribution also agrees with theoretical estimates based on reasonable models. In the temperature range below about 40°K we have not been able to give a satisfactory interpretation of our results. Our measurements show that near 40°K the absolute thermoelectric power of pure copper reverses sign, becoming negative, and attains an anomalously low minimum of about -1.8 microvolts/degree near 10°K. If this behavior is due to the presence of minute amounts of impurities in the pure copper which give rise to a thermoelectric anomaly associated with the appearance of a resistivity minimum, then our results can be interpreted without much difficulty. However, the residual resistivity of the pure copper was so low that we do not believe that the low-temperature thermoelectric anomaly can be attributed to the presence of impurities.

A research program on thermoelectric properties of dilute alloys which should shed further light on these questions is outlined.

*Present Address: National Bureau of Standards, Cryogenics Laboratory, Boulder, Colorado.

LOW-TEMPERATURE IMPURITY CONDUCTION IN n-TYPE SILICON. K. R. Atkins, R. Donovan,* and R. H. Walmsley, Department of Physics, University of Pennsylvania, Philadelphia, Pennsylvania (Received November 12, 1959).

Hall coefficients and electrical resistivities were measured down to liquid helium temperatures for silicon specimens containing about 10^{17} phosphorus impurities per cm^3 and about 10^{15} boron impurities per cm^3. The density of minority impurities was determined during the preparation of the ingots, rather than deduced from the electrical measurements themselves. The results are extremely sensitive to the density of minority impurities. They are discussed in relationship to the theories of Conwell, Mott, and Price.

*Now at Molecular Engineering Section, Westinghouse Air Arm, Blatimore, Maryland.

LOW-TEMPERATURE INTERNAL FRICTION IN FACE-CENTERED CUBIC AND BODY-CENTERED CUBIC METALS. L. J. Bruner,* Department of Physics and Institute for the Study of Metals, University of Chicago, Chicago, Illinois (Received November 2, 1959).

Data on the anelasticity produced by plastic deformation in various face-centered cubic and body-centered cubic pure metals and alloys are reported. Face-centered cubic materials studied at temperatures from 4.2°K to 300°K include Cu, Al, and Al - 0.25 at. % Cu. Body-centered cubic systems are Fe, Nb, and β brass. Bordoni peaks are observed in Cu and Al in agreement with previous work, but are not found in either

strain aged Al-Cu alloys or pure Fe. A peak observed in Nb at 173°K is not believed to be a Bordoni type. Unexplained low-temperature internal friction peaks are also observed in β brass. A new mechanism is proposed for dislocation relaxation in which the essential feature is the thermally activated motion of paired partial dislocations between vacancy-pinning points. It is in general qualitative accord with experiment, and permits semiquantitative evaluation of all essential parameters.

*Now at International Business Machines Watson Laboratory at Columbia University, New York, New York.

PROPERTIES OF p-TYPE InSb IN PULSED HIGH ELECTRIC FIELDS. M. C. Steele and M. Glicksman, RCA Laboratories, Princeton, New Jersey (Received November 6, 1959).

The results of high electric field experiments on p-type InSb at 77°K are described. It is shown that electron-hole pair creation occurs at electric fields greater than 700 volts/cm. When a sufficient number of pairs are created the Hall coefficient changes from positive to negative. The question of whether holes or possible injected electrons initiate the pair creation is examined in detail. An incipient negative resistance effect in transverse magnetic fields and the absence of any self-pinch effects are also discussed.

DIFFUSION AND IONIC CONDUCTIVITY IN CESIUM BROMIDE AND CESIUM IODIDE. David W. Lynch,* Department of Physics, University of Illinois, Urbana, Illinois (Received November 9, 1959).

The diffusion coefficients of the constituent ions were measured in CsBr and CsI single crystals between 300°C and 550°C by means of radioactive tracers and were compared with electrical conductivity measurements. Approximate satisfaction of the Nernst-Einstein equation indicates that the conductivity is nearly completely ionic and the diffusion measurements show that the halogen ion defects are the more mobile. Attempts to identify the mechanisms for ionic transport by means of the Bardeen-Herring correlation factor are discussed. Schottky defects seem likely but the assumption of an additional mechanism for cationic transport is required. If Schottky defects are predominant, their formation enthalpies are 2.0 ev and 1.9 ev in CsBr and CsI, respectively, and the activation enthalpies for halogen vacancy motion are 0.27 ev and 0.3 ev, respectively, while the cesium vacancy activation enthalpy is about 0.58 ev for both salts.

*Present address: Institute for Atomic Research and Department of Physics, Iowa State University, Ames, Iowa.

TEMPERATURE DEPENDENCE OF EDGE EMISSION IN CADMIUM SULFIDE. D. C. Reynolds, Aeronautical Research Laboratory, Wright-Patterson Air Force Base, Ohio (Received November 12, 1959).

The temperature dependence of the blue and the green emission in cadmium sulfide has been investigated in the temperature range from 77°K to 300°K. The blue emission shifts to longer wavelengths as the temperature is increased above 77°K with a temperature coefficient of 4.9×10^{-4} ev/°C. The intensity of the green emission falls off exponentially above 77°K with very little shift in the spectral position of the green peaks.

SPIN-PHONON INTERACTION IN PARAMAGNETIC CRYSTALS. R. D. Mattuck* and M. W. P. Strandberg, Department of Physics and Research Laboratory of Electronics, Massachusetts Institute of Technology, Cambridge, Massachusetts (Received November 16, 1959).

A general theory of the spin-phonon interaction, which is applicable to any iron group spin not in an S state, is developed. The theory employs a perturbation treatment that has a more direct physical meaning than techniques previously used and that leads to more accurate results. These results are presented in the form of an equivalent spin-phonon interaction Hamiltonian involving sums over products of spin operators and phonon creation-annihilation operators. The interaction between any two spin levels can then be calculated by using the spin wave functions associated with the usual "spin Hamiltonian." It is shown that, owing to the dominant role played by the quadratic term in the above interaction, odd half-integer iron group spins ($S>\frac{1}{2}$) obey quadrupole selection rules. A formula is derived for order-of-magnitude cal-

culations of the interaction strength. It is shown that acoustic experiments should provide the ideal way to test this theory in detail, and two methods of checking the quadrupole rule are proposed. Experimental results are reported on observed acoustic saturation in MgO doped with Cr^{+++}, on the absence of saturation between low-field Kramers doublets in ruby, and an apparent saturation effect in F-center quartz.

*Now at Royal Institute of Technology, Stockholm, Sweden.

GALVANOMAGNETIC EFFECTS IN n-TYPE SILICON. W. E. Krag, Lincoln Laboratory, Massachusetts Institute of Technology, Lexington, Massachusetts (Received November 3, 1959).

The galvanomagnetic effects in n-type silicon have been investigated experimentally and theoretically at 77°K and 300°K. The samples ranged in resistivity from 0.2 to 27 ohm-cm (at room temperature). Measurements of the field dependence from 0.5 to 22 kilogauss of the Hall coefficient and the magnetoresistance for several orientations are presented, as well as measurements of the angular dependence of the magnetoresistance and planar Hall effects at similar fields. A number of theoretical calculations using a constant relaxation time in the manner of Gold and Roth are presented which show the effect on the coefficients of a change in the mass anisotropy K_m. The Boltzmann transport equation, and collision times of the form

$$\nu_l = I_l \mathcal{E}^{-3/2} + L\mathcal{E}^{1/2} + N,$$

$$\nu_t = I_t \mathcal{E}^{-3/2} + L\mathcal{E}^{1/2} + N,$$

where ν_l and ν_t are the longitudinal and transverse collision times, I_l, I_t, L, and N are constants, and $\mathcal{E}$ is the energy, have been used to calculate the galvanomagnetic coefficients for different amounts of lattice, ionized-impurity, and neutral-impurity scattering, and for different anisotropies of the ionized-impurity scattering. The various components of the collision frequency were taken from available theoretical work. Detailed comparisons of the experimental data and the theoretical calculations are presented which show that the assumption of a constant collision frequency allows one to predict qualitatively all the field dependencies and symmetries which are found experimentally. It is also shown that with an anisotropic, energy-dependent collision frequency the quantitative agreement with experiment is considerably improved, especially with regard to the behavior of samples of different resistivities.

SPIN RELAXATION AND LINE WIDTH IN ALKALI METAL VAPORS. Arnold L. Bloom, Varian Associates, Palo Alto, California (Received November 16, 1959).

Relaxation constants T_1 and T_2 have been computed for experiments involving optical pumping and optical detection in alkali metal vapor. The calculations have been performed for several possible spin relaxation mechanisms; namely, magnetic dipole, electric quadrupole, spin exchange, and the optical pumping process itself. For all of these mechanisms a reorientation experiment will approximately predict a spin resonance linewidth (equivalent to the statement $T_1 \approx T_2$ for spin-1/2 particles). However, a spin reorientation experiment of the type originally performed by Dehmelt, employing circularly polarized light, gives ambiguous results because of the nonexponential character of the reorientation. A more suitable experiment is one employing hyperfine population differences and unpolarized light.

CALCULATION OF THE MAGNETIC HYPERFINE STRUCTURE COUPLING CONSTANTS OF NO. Hélène Lefebvre-Brion and C. M. Moser, Centre de Mécanique Ondulatoire Appliquée, Paris, France (Received November 18, 1959; revised manuscript received January 21, 1960).

A calculation of the magnetic hyperfine structure (hfs) coupling constants of NO has been made using an ab initio configuration interaction wave function built from LCAO-MO-SCF orbitals. The constants predicted by this wave function are in good agreement with experiment for the two constants related to the quantities $\langle L_z/r^3 \rangle_{av}$ (constant a) and $\langle \sin^2\theta S^-/r^3 \rangle_{av}$ (constant d). The direct calculation of $\langle (3\cos^2\theta - 1)S_z/r^3 \rangle_{av}$ (constant c) gives a value which is about 25% less than that predicted by an approximation which implies that unpaired l and s are associated with the same electron. From this calculated value of c the quantity $\langle \psi^2(0) \rangle_{av} - \frac{1}{3}c$

(constant b) now is found to be about 40 Mc/sec instead of 68.91 Mc/sec which has been previously used by experimentalists.

The same wave function has been used to calculate the fine structure constant (spin-orbit coupling) for the $^2\Pi$ ground state of NO. The agreement with experiment is quite satisfactory.

The calculation of the nuclear quadrupole coupling constant q gives about 73% of the observed electronic part assuming that $Q(N^{14}) = 0.02 \times 10^{-24}$ cm^2.

ELECTRON-HYDROGEN SCATTERING AT LOW ENERGIES. Takashi Ohmura* and Haruko Ohmura,* Division of Pure Physics, National Research Council, Ottawa, Canada (Received October 23, 1959).

The effective range in the singlet system has been evaluated as 2.646 ± 0.004 atomic units by using the asymptotic amplitude of the 202-parameter H^- wave function of Pekeris. This value of the effective range, together with the value of the electron affinity of H^-, determines the scattering length in the singlet system as 6.167. The effective range in the triplet system is calculated to be 1.219 atomic units by a Hartree-Fock approximation. It is shown that the effective-range approximation is very good for all energies at which only elastic scattering is allowed. The photo-ionization of H^- is briefly discussed on the basis of the effective-range theory.

*On leave of absence from Department of Physics, University of Tokyo, Tokyo, Japan.

RELATIVISTIC SELF-CONSISTENT SOLUTIONS FOR ATOMS OF LARGE ATOMIC NUMBER. Stanley Cohen, The RAND Corporation, Santa Monica, California, and Lawrence Radiation Laboratory, University of California, Berkeley, California (Received November 2, 1959).

Relativistic self-consistent solutions, without exchange, have been obtained for several atoms of large atomic number by use of a general program for a high-speed computing machine. A short description of this program and of the self-consistent calculation is given. Eigenvalues for the individual electron subshells of the self-consistent mercury, tungsten, platinum, and uranium atoms are presented. A comparison of the calculation with previous results for the mercury atom is also included.

MAGNETIC HYPERFINE STRUCTURE OF THE GROUND STATE OF LITHIUM. R. K. Nesbet,* Lincoln Laboratory, Massachusetts Institute of Technology, Lexington, Massachusetts (Received November 30, 1959).

The magnetic hyperfine splitting of the ^2S ground state of the lithium atom is calculated. It is shown that the discrepancy between experiment and the value calculated in the traditional Hartree-Fock approximation can be accounted for quantitatively by the exchange polarization effect, which distorts one 1s orbital relative to the other. The present calculation obtains a value within one percent of the experimental value. A general procedure is proposed for evaluating operators that do not commute with the Hamiltonian, when approximate variational methods must be used.

*Present address: Department of Physics, Boston University, Boston, Massachusetts.

POSITRON ANNIHILATION IN AQUEOUS SOLUTIONS. Georg Trumpy,* Institutt for Atomenergi, Lillestrøm, Norway (Received November 30, 1959).

The angular correlation of 2-quantum emission from the annihilation of positrons in different materials has been measured in an apparatus with 8 photon counters providing coincidences for 16 output channels. As positron targets were chosen indium, water, and aqueous solutions of 5 paramagnetic salts and 10 other substances. It was confirmed that the amount of singlet positronium formed is influenced by two processes: a reduction of positronium due to electron capture by oxidizing substances and an increase of the triplet → singlet conversion due to the electron exchange with paramagnetic ions.

The oxidation potential of positronium is found to be very nearly zero. The conversion rate seems to be proportional to the number of unpaired electrons on the dissolved ions. A discrepancy with the interpretation of Green and Bell for their lifetime experiments is discussed.

*Now at A. B. Atomenergi, Studsvik, Tystberga, Sweden.

SHELL-MODEL ASSIGNMENTS FOR THE ENERGY LEVELS OF C^{14} AND N^{14}. E. K. Warburton and W. T. Pinkston,* Palmer Physical Laboratory, Princeton University, Princeton, New Jersey (Received November 24, 1959).

Electromagnetic transition widths, reduced widths, and inelastic scattering cross sections are calculated for the following states of N^{14} and C^{14}: (1) the levels arising from the ground-state configuration, s^4p^{10}; (2) the odd-parity levels arising from excitation of a $1p$ nucleon into the degenerate $2s_{1/2}$ and $1d_{5/2}$ shells; (3) the even-parity group of levels formed by excitation of two $1p$ nucleons into the $2s$ and $1d$ shells. The calculations for the s^4p^{10} configuration are carried out using the wave functions of Elliott and of Visscher and Ferrell, and in jj coupling. The calculations for the odd-parity levels are done in the jj-coupling scheme. For the even-parity excited configuration an inert C^{12} core is assumed and $M1$ radiative widths are calculated for states arising from s^2+d^2+sd. The calculations are compared to the existing data. On the basis of this comparison, shell-model assignments are proposed for 19 of the 27 known levels below 11-Mev excitation in N^{14} and for all the known levels in C^{14} below 9-Mev excitation.

*Present address: Department of Physics and Astronomy, Vanderbilt University, Nashville, Tennessee.

ENERGY LEVEL PARAMETERS FROM NUCLEAR RESONANCE FLUORESCENCE AT 7 Mev. K. Reibel and A. K. Mann, University of Pennsylvania, Philadelphia, Pennsylvania (Received November 17, 1959).

The recoil-broadened photon spectrum from the reaction $F^{19}(p, \alpha\gamma)O^{16}$ has been used to measure the elastic photon scattering cross sections at 7 Mev of 31 elements. The observed angular distributions are consistent with dipole transitions. A plot of the cross sections versus mass number shows definite peaks around the closed shell regions near $Z=50$, $N=82$ (Sn, Te, and Ba), and $Z=82$, $N=126$ (Pb and Bi). For six medium and heavy elements self-absorption measurements were made which, when analyzed in terms of a number of nonoverlapping Breit-Wigner resonances, yield values of the average partial radiation widths to the ground states, the average total radiation widths, and the average level spacings for those elements. The radiation widths are significantly larger than those determined from slow-neutron scattering and capture experiments and, excepting Pb and Bi, the average level spacings are also appreciably greater than would be expected from the neutron data. The observed widths and spacings are in order-of-magnitude agreement with the recent interpretation of the modified single-particle calculation of Blatt and Weisskopf.

GAMMA-RAY INTENSITIES IN THE THORIUM ACTIVE DEPOSIT. Guy T. Emery* and Walter R. Kane,* Lyman Laboratory of Physics, Harvard University, Cambridge, Massachusetts (Received November 24, 1959).

The relative intensities of the gamma rays of the descendants of radiothorium have been studied by measuring the photoelectron spectra from thorium and platinum foils. The relative sensitivity of the arrangement at different energies was found by using other sources having gamma rays of known relative intensity. Comparison of the measured gamma-ray intensities with the measurements by others of internal conversion intensities allows internal conversion coefficients to be computed and the multipolarities of several transitions to be determined. An electric monopole transition was found in Po^{212}. The gamma-ray intensities are used to find the intensities of beta-ray branches. Gamma-ray intensities are compared with the known intensities of long-range alpha particles from Po^{212} and transition probabilities are estimated for some electromagnetic transitions between states of that nucleus. The level schemes of Po^{212} and Pb^{208} are discussed in the light of the information found here and of other recent information.

*Now at Brookhaven National Laboratory, Upton, New York.

SLOW-NEUTRON SCATTERING BY THE TITANIUM ISOTOPES. C. G. Shull* and M. K. Wilkinson, Oak Ridge National Laboratory, Oak Ridge, Tennessee, and M. H. Mueller, Argonne National Laboratory, Lemont, Illinois (Received November 17, 1959).

Neutron diffraction studies are reported on isotopically enriched samples of TiO_2 from which are evaluated the coherent scattering amplitudes

of the titanium isotopes. Scattering amplitudes of +0.48, +0.33, -0.58, +0.08, and $+0.55\times10^{-12}$ cm were established for the titanium isotopes of mass 46, 47, 48, 49, and 50, respectively. The major isotope Ti^{48} is thus responsible for the anomalous scattering amplitude, -0.34×10^{-12} cm, characteristic of the normal element. Pronounced nuclear scattering resonance effects on the observed neutron scattering are suggested to occur for the most of the isotopes.

*Present address: Massachusetts Institute of Technology, Cambridge, Massachusetts.

SLOW-NEUTRON RESONANCE SPECTROSCOPY. I. U^{238}. J. L. Rosen, J. S. Desjardins, J. Rainwater, and W. W. Havens, Jr., Department of Physics, Columbia University, New York, New York (Received November 20, 1959).

The results of time-of-flight measurements of U^{238} resonances in the region 90 - 1300 ev are presented and resonance parameters for levels up to 1000 ev are obtained. Neutron widths for the 55 observed levels and radiation widths for 32 of the stronger levels are deduced. The reduced neutron width distribution is found to be in good agreement with the theoretical prediction of Porter and Thomas for a single channel process, while the level spacing distribution agrees with the "repulsion" formula suggested by Wigner. The average value of the radiation widths was found to be $(24.6\pm0.8)\times10^{-3}$ ev, while the average reduced neutron width and level spacing were found to be $(1.76\pm0.26)\times10^{-3}$ ev and 18.5 ±1.3 ev, respectively. These values are in good agreement with earlier results reported by other workers. A strength function of $(0.95\pm0.15)\times10^{-4}$ is obtained.

It appears on the basis of their size and number, that several of the weaker levels may be due to p-wave neutrons.

PRECISION MEASUREMENT OF THE TOTAL NEUTRON CROSS SECTION OF U^{233} BETWEEN 0.000818 AND 0.0818 ev. G. J. Safford, W. W. Havens, Jr., and B. M. Rustad, Columbia University, New York, New York, and Brookhaven National Laboratory, Upton, New York (Received November 20, 1959).

The absolute value of the total neutron cross section of U^{233} was measured at neutron energies between 0.000818 ev and 0.0818 ev for two types of samples, a metallic foil and D_2O solutions of uranium nitrate. Balanced solutions of $U^{233}O_2(NO_3)_2$ and $U^{238}O_2(NO_3)_2$ were used to determine the difference between the total cross sections of U^{233} and U^{238}. This value, when combined with the relatively small known value of the total cross section for U^{238}, gives $\sigma_T(U^{233}) = 587\pm5$ barns at 0.0253 ev. The measurements on the metallic U^{233} foil agreed with the measured total cross section determined from the liquid solution data to better than 1%, yielding $\sigma_T(U^{233}) = 586\pm2$ barns at 0.0253 ev.

SLOW-NEUTRON TOTAL AND FISSION CROSS SECTIONS OF U^{233}. M. S. Moore, L. G. Miller, and O. D. Simpson, Atomic Energy Division, Phillips Petroleum Company, Idaho Falls, Idaho (Received November 25, 1959).

The slow-neutron total and fission cross sections of U^{233} have been measured from 0.02 ev to 200 ev on the MTR (Materials Testing Reactor) fast chopper. The strong resonances are resolved below a neutron energy of 15 ev, and show marked interference effects in the fission cross section. No resonances are observed in the total cross section which are not also present in the fission cross section, except for those attributed to the known contaminants in the samples. An estimate of the neutron strength function $\langle\Gamma_n^0/D\rangle$, made by an area analysis, gives the value $(1.0\pm0.2)\times10^{-4}$ for this energy region in U^{233}.

MULTILEVEL ANALYSIS OF THE SLOW-NEUTRON CROSS SECTIONS OF U^{233}. M. S. Moore and C. W. Reich, Atomic Energy Division, Phillips Petroleum Company, Idaho Falls, Idaho (Received November 25, 1959).

A multilevel analysis of the slow-neutron total and fission cross sections of U^{233} from thermal energies to 11 ev has been carried out, under the assumption that in one of the two spin states the nucleus undergoes fission primarily through a small number of channels. The cases of one and of two fission channels for this spin state have been investigated in detail. Although the analysis does not yield an exact value for the number of available fission channels, the data are adequately fit with a two-fission-channel formula.

it is not necessary to invoke any negative-energy resonances in the analysis. The presence of a noninterfering component in the cross sections, having a $1/v$ energy variation, is indicated. At thermal energies, this component accounts for approximately 80% of the total and fission cross sections. An interpretation of this component as being due to one spin state of the compound nucleus is presented. Under this assumption, the fission characteristics of the two spin states of the compound nucleus formed by s-wave neutrons are quite different.

LOW-ENERGY NEUTRON CROSS SECTIONS OF FISSIONABLE NUCLEI. Erich Vogt, Atomic Energy of Canada Limited, Chalk River, Ontario, Canada (Received November 30, 1959).

The method of analysis developed in a previous paper is applied to the low-energy neutron cross sections of the common fissionable isotopes. Further evidence is presented to show that U^{235} possesses the unusual negative-energy level required by the previous analysis. However, good fits are obtained for the cross sections of both U^{233} and Pu^{239} without such an unusual bound level, suggesting that the neutron resonance cross sections of the fissionable isotopes do not exhibit a basic anomaly. The size of the level interference effects in each of the isotopes implies that the fission process involves more than one but no more than a few fission channels.

MONTE CARLO CALCULATIONS OF NUCLEAR EVAPORATION PROCESSES. IV. THE SPECTRA OF NEUTRONS AND CHARGED PARTICLES FROM NUCLEAR REACTIONS. Israel Dostrovsky and Zeev Fraenkel, The Weizmann Institute of Science, Rehovoth, Israel, and Lester Winsberg, Lawrence Radiation Laboratory, University of California, Berkeley, California, and The Weizmann Institute of Science, Rehovoth, Israel (Received November 20, 1959).

The calculation of spectra of neutrons and charged particles and of cross sections for their production from nuclear reactions is compared with experimental values. A compound-nucleus mechanism followed by nuclear evaporation is assumed for the reactions Zr, Ta, Bi(14.1-Mev n,n'); Ni(13.4-17.5-Mev n,p); Cu, Pd(23-Mev p,α); and Ni(162-Mev O^{16},α). The production of neutrons and charged particles from the interaction of 190-Mev protons with Ni, Ag, and Au is analyzed in terms of a nucleon cascade, followed by particle evaporation. The calculation of the nuclear evaporation is based on Weisskopf's statistical theory. Fairly good agreement is obtained for the values of the cross sections for producing these particles with an appropriate set of radius and level-density parameters in each case. There are serious discrepancies, however, in the comparison of the experimental and calculated spectra; many of the latter are deficient in low-energy neutrons and charged particles. Possible improvements in the calculation are discussed.

MONTE CARLO CALCULATIONS OF NUCLEAR EVAPORATION PROCESSES. V. THE EMISSION OF PARTICLES HEAVIER THAN He^4. I. Dostrovsky, Z. Fraenkel, and P. Rabinowitz, The Weizmann Institute of Science, Rehovoth, Israel (Received November 20, 1959).

Previous Monte-Carlo calculations of nuclear evaporation reactions have been extended to include the emission of He^6, Li^6, Li^7, Li^8, and Be^7 from Cu, Ag, Au, and Bi targets bombarded with high-energy protons (340-2000 Mev). Comparison with available experimental results shows good agreement in most cases. A discrepancy has been observed between the calculated and observed variation of Be^7 formation cross section with the mass of the target nucleus, but even here the agreement is within a factor of two. It is shown that, for the usually chosen parameters of the calculation, a level density parameter of $a=A/10$ is necessary.

TOTAL NEUTRON CROSS SECTIONS OF HELIUM, NEON, ARGON, KRYPTON, AND XENON. F. J. Vaughn, W. L. Imhof, R. G. Johnson, and M. Walt, Lockheed Missiles and Space Research Laboratory, Palo Alto, California (Received November 30, 1959).

The total neutron cross sections of the noble gases helium, neon, argon, krypton, and xenon have been measured for neutron energies from 120 kev to 6.2 Mev and from 12.1 Mev to 19.8 Mev by a transmission experiment. The neutrons were produced using the $Li^7(p,n)Be^7$, the $T(p,n)He^3$, the $D(d,n)He^3$, and the $T(d,n)He^4$ reactions in the appropriate energy intervals.

A Van de Graaff accelerator was the source of the protons or deuterons. In general, the results obtained agree with previous work where such work exists. A previously unobserved S-wave scattering resonance was found in neon at about 500 kev, indicating the presence of an excited state in Ne^{21} with $J=1/2$ and even parity. The results for argon, krypton, and xenon exhibit general agreement with the cross sections of neighboring elements, as would be expected from the previously observed smooth variation of the $\sigma(A,E)$ surface.

HALF-LIFE OF Pb^{210}. W. R. Eckelmann,* W. S. Broecker, and J. L. Kulp, Lamont Geological Observatory, Columbia University, Palisades, New York (Received February 19, 1959).

A new determination of the half-life of Pb^{210} has been made by the geological method. $PbCl_2$ extracted from uranium minerals in secular equilibrium was used to calibrate a thick-source scintillation counter for Po^{210} alpha particles. Using this calibration, the absolute activity of Po^{210} in partial equilibrium with a known number of Pb^{210} atoms prepared from the decay of a measured quantity of radon was determined. From these data a half-life of 21.4 ± 0.5 years was obtained for Pb^{210}.

*Present address: Jersey Production Research Company, Tulsa, Oklahoma.

DECAY OF Be^{9*} (2.43-Mev STATE). E. M. Henley* and P. D. Kunz, Department of Physics, University of Washington, Seattle, Washington (Received July 13, 1959).

The decay of the 2.43-Mev state of Be^9 is treated theoretically. Of the open two-body decay channels all but one involve a nuclear state, the energy of which is not well defined. The usual formalisms have been generalized to take this into account. The estimate of the decay rates is made by means of a variational internal wave function for the Be^{9*} state, based upon the alpha-particle model. It is found that the principal mode of decay is to He^5+He^4. Model-independent arguments are given to show that decay to the ground state of Be^8 should be inhibited. Furthermore, the momentum and angular distributions of alphas emitted in the decay through several two-particle decay modes are computed. These latter calculations do not assume any specific nuclear model, but depend on the weak assumption that the state is excited by a direct reaction. Comparison with recent measurements indicates that in addition to the He^5 - He^4 decay, approximately 7% of the decay occurs to the ground state of Be^8, which is consistent with our calculations.

*Presently on leave at the Institute for Theoretical Physics, Copenhagen, Denmark.

CROSS SECTIONS FOR THE $(n,2n)$ REACTION IN N^{14}, P^{31}, Cu^{63}, AND Pr^{141}. J. M. Ferguson and W. E. Thompson, U. S. Naval Radiological Defense Laboratory, San Francisco, California (Received October 12, 1959).

The $(n,2n)$ cross sections have been measured for N^{14}, P^{31}, Cu^{63}, and Pr^{141}, for neutron energies from 12.5 to 18 Mev. The annihilation radiation emitted from the product nuclides was counted with two NaI(Tl) crystals in coincidence. In the energy range measured, the cross sections were found to vary, as follows: N^{14}, 3.03 to 11.67 mb; P^{31}, 0 to 74 mb; Cu^{63}, 186 to 836 mb; Pr^{141}, 1231 to 1737 mb. The results are generally in agreement with those of others. The data are compared with curves plotted from Weisskopf's theoretical expression for $(n,2n)$ cross sections.

NUCLEAR ENERGY LEVELS OF Na^{24}. Carl T. Hibdon, Argonne National Laboratory, Lemont, Illinois (Received November 5, 1959).

The neutron cross-section data up to 350 kev show a number of relatively large peaks and many smaller ones among the 86 peaks observed, the widths ranging from 0.2 to 6 kev. Approximately 50 small peaks were observed between 60 and 200 kev. Above 200 kev, each of the previously known peaks was resolved into two or more peaks and between these large peaks many narrower peaks were observed. The analyses show 9 s-wave levels and 46 p-wave levels, the remainder being d- and f-wave levels. A plot of the number of levels having energies $\leq E_n$ as a function of the neutron energy E_n shows an essentially linear distribution of the levels. As obtained from the reduced widths averaged over both values of J, the value of the strength function for $l=0$ is 0.06; averaged over all values of

J for $l=1$ it is 0.65; and for higher values of l it is too large in comparison with the p-wave strength function.

DIFFERENTIAL CROSS SECTIONS FOR NEUTRON RESONANCE SCATTERING FROM Na^{23}. R. O. Lane and J. E. Monahan, Argonne National Laboratory, Lemont, Illinois (Received November 12, 1959).

The differential scattering cross section for neutrons on sodium has been measured with an energy spread of ~25 kev for neutron energies between 200 kev and 800 kev. The data are presented in the form of Legendre polynomial coefficients.

NEUTRON PRODUCTION BY HEAVY-ION BOMBARDMENTS. Edward L. Hubbard, Robert M. Main,* and Robert V. Pyle, Lawrence Radiation Laboratory, University of California, Berkeley, California (Received September 11, 1959).

Neutron yields from C^{12}, N^{14}, and Ne^{20} bombardments of a number of target elements have been measured by an activation method. The maximum bombarding energies were 10.4 Mev per nucleon of the incident ion. Neutron yields have been calculated by assuming complete fusion of the two nuclei, with an interaction radius of $r_0 \approx 1.5\times10^{-13}$ cm, followed by deexcitation of the compound nuclei by neutron emission only. Calculated neutron yields are a factor of about two higher than experiment in the case of heavy target nuclei, with greater differences for light targets. Some possible refinements of the theory that could bring the results closer to agreement with experiment are mentioned.

*Now at Tracerlab Inc., Richmond, California.

PHOTONEUTRON CROSS SECTIONS OF Li, N, AND A. R. W. Fast, P. A. Flournoy, R. S. Tickle, and W. D. Whitehead, University of Virginia, Charlottesville, Virginia (Received November 13, 1959).

Using a Halpern-type photoneutron detection system, the photoneutron yields from Li, N^{14}, and A^{40} have been measured as a function of the maximum bremsstrahlung energy from threshold to approximately 50 Mev. The method of Penfold and Leiss was used to extract from the yield curves the total neutron cross section: $\sigma_T = \sigma(\gamma, n) + \sigma(\gamma, pn) + 2\sigma(\gamma, 2n) + \ldots$. The results are compared with previous findings of other laboratories. No gross structure was detected in the lithium cross section in the giant resonance region. The data indicate that lithium has a high-energy tail on the cross section of considerable magnitude.

TOTAL CROSS SECTIONS OF THE $O^{18}(p,\alpha)N^{15}$ AND $O^{18}(p,n)F^{18}$ REACTIONS. J. M. Blair and J. J. Leigh, School of Physics, University of Minnesota, Minneapolis, Minnesota (Received November 9, 1959).

The angular distribution of the α particles from the $O^{18}(p,\alpha)N^{15}$ reaction and the total cross section for the $O^{18}(p,n)F^{18}$ reaction have been measured for proton energies between 2600 and 3000 kev. Comparison of the total cross sections for the two reactions eliminate the previously observed differences in resonance energies in these reactions. At most energies the α particles are preferentially emitted in the forward and backward directions and the angular distributions are rapid functions of proton energy.

ENERGY SPECTRA OF PROTONS FROM (d,p) REACTIONS IN HEAVY ELEMENTS. B. L. Cohen, J. B. Mead, R. E. Price, K. S. Quisenberry, and C. Martz, Radiation Laboratory, University of Pittsburgh, Pittsburgh, Pennsylvania (Received July 27, 1959).

Surveys of proton energy distributions from (d,p) reactions were made on nuclei with $Z>30$ using resolutions of 500 and 80 kev. The gross structure shows broad peaks due to the major nuclear shells, as expected from the fact that (d,p) stripping reactions excite single-particle states; peaks due to the subshell structure can be seen in some cases, especially in the heavier nuclei. The energies of the various peaks do not shift from element to element in the manner expected from simple theory; it is shown that this is not in conflict with neutron cross-section evidence, and possible explanations are proposed. The energy spacing between major shells derived from these measurements allows cal-

culation of the reduced mass for nucleons in nuclei; the result is very different from the predictions of Brueckner's theory, but explanations for this discrepancy are advanced. The results and their interpretation given here are in direct conflict with the Wilkinson theory of gamma-ray giant resonances. The energy spectra are very similar at different angles, which indicates that the stripping process is predominant at all angles. Deviations from Butler's angular distribution theory at large angles must therefore be due to difficulties in that theory rather than due to the onset of a competing process.

POLARIZATION OF 9-Mev PROTONS ELASTICALLY SCATTERED FROM MAGNESIUM. A. B. Robbins, University of Birmingham, Birmingham, England, and Rutgers University, New Brunswick, New Jersey, and G. W. Greenlees, University of Birmingham, Birmingham, England (Received November 30, 1959).

The polarization as a function of angle has been measured for protons elastically scattered from a 1-Mev thick magnesium target with a mean energy of 9.1 Mev. The resulting polarization distribution is compared to a differential cross-section measurement with the same target.

DEVIATIONS FROM THE $\Delta T = 0$ ISOTOPIC SPIN SELECTION RULE IN FERMI TRANSITIONS. Claude C. Bouchiat, Palmer Physical Laboratory, Princeton University, Princeton, New Jersey (Received September 23, 1959).

Experimental deviations from the $\Delta T = 0$ isotopic spin selection rule have been observed experimentally in $J \to J$ beta transitions. In the theory of a vector interaction with a conserved current these deviations have to be explained only in terms of isotopic spin impurities, while in the conventional theory exchange mesonic currents may also induce Fermi transitions with $\Delta T \neq 0$. In this paper an attempt is made to estimate the contribution of the isotopic spin impurities arising from the Coulomb interaction between the protons. The j-j coupling shell model is used to calculate the relevant Coulomb matrix elements. When all the nucleons outside the core are in the same orbit, the main contribution comes from the Coulomb interaction between the protons outside the core. A comparison between the empirical Fermi matrix element and the calculated one is performed in the case of Mn^{52}, Sc^{44}, Na^{24}. The two quantities agree fairly well for manganese-52. No such an agreement is found in the two other cases, the predicted M_F being too large for sodium-24, too small for scandium-44, at least by a factor ten. This discrepancy may reflect the inadequacy of the j-j shell model to describe the Coulomb effects or the presence of mesonic effects. More experiments are needed to make a choice between these two possibilities.

DIRECT DETERMINATION OF INTERNAL CONVERSION COEFFICIENTS. Paresh Mukherjee, Saha Institute of Nuclear Physics, Calcutta, India (Received November 24, 1959).

Using the same source and instrument geometry, both the external as well as internal conversion lines of the 1.17- and 1.33-Mev gamma rays of Co^{60} are scanned in a Siegbahn-Slätis spectrometer. From the known internal conversion coefficients of these gamma rays, the instrument is calibrated for the direct determination of the internal conversion coefficient of any other gamma rays having energy near 1.3 Mev. As an example, the internal conversion coefficient of the 1.408-Mev gamma ray, in the decay of Eu^{152}, is measured. The value obtained is 4.99×10^{-4}.

FISSION OF Ra^{226} BY DEUTERONS AND HELIUM IONS. R. C. Jensen* and A. W. Fairhall, Departments of Chemistry and Physics, University of Washington, Seattle, Washington (Received November 30, 1959).

Fission induced in Ra^{226} by 14.5- and 22-Mev deuterons, and by 23.5-, 31-, and 43-Mev He ions has been studied using radiochemical techniques. The mass distributions of fission products for deuteron-induced fission is triple-humped, corresponding to separate symmetric and asymmetric fission modes. The symmetric mode dominates at the higher bombarding energy. The mass distributions observed for fission products from He ion-induced fission look more "normal": asymmetric at the lowest bombarding energy, becoming a single broad peak at the

highest bombarding energy. These results are interpreted in terms of a symmetric fission mode which increases strongly with increasing excitation energy, and an asymmetric fission mode which occurs mainly at low excitation energies following neutron evaporation from highly excited compound nuclei. Asymmetric fission is interpreted to be disappearing as a fission mode for nuclei of lower atomic number than thorium.

*Now at the Department of Chemistry, San Diego State College, San Diego, California.

NUMERICAL EVALUATION OF THE PION-NUCLEON FORWARD SCATTERING AMPLITUDE. James W. Cronin, Palmer Physical Laboratory, Princeton University, Princeton, New Jersey (Received July 13, 1959; revised manuscript received January 7, 1960).

The real part of the forward elastic scattering amplitude for $\pi^{\pm}$-proton scattering has been evaluated from experimental cross sections by means of dispersion relations. Recent measurements indicate two peaks in the π^{-}-proton total cross section at 590 and 870 Mev incident pion kinetic energy. Tables of the real part of the forward scattering amplitude for $\pi^{\pm}$-proton scattering are presented as a function of incident pion kinetic energy in the laboratory. The forward scattering amplitudes obtained from some recent $\pi^{\pm}$ scattering experiments are compared with the calculations. Measurement of the forward charge exchange cross section appears to be the most suitable way of investigating the predictions of the dispersion relation at high energies. The possibility of detecting Coulomb interference at small angles is also discussed.

NUCLEAR INTERACTIONS IN CARBON PRODUCED BY COSMIC RAYS WITH ENERGIES BETWEEN 10^{10} AND 10^{12} ev. Luisa F. Hansen and W. B. Fretter, Department of Physics, University of California, Berkeley, California (Received November 16, 1959; revised manuscript received February 3, 1960).

An experiment is described in which high-energy nuclear interactions in the range of energies 10^{10} - 10^{12} ev were analyzed by means of a cloud chamber in a magnetic field. Measurements of ionization and momentum made possible the identification of electrons and π mesons to about 20 Bev/c. Protons, K mesons, and hyperons could not be identified unambiguously among themselves, except in very limited regions of momentum. The primary particles were cosmic-ray nucleons and a possible fraction of pions, the target nuclei were carbon, and the velocities of the primaries were determined from balance of momentum in the center-of-mass system. A total of 41 events were analyzed, and the results compared to previous experimental work and the predictions of the theories of Heisenberg and Landau. The measurements made included the transverse momenta of the secondaries and their average energy in the center-of-mass system, the energy and angular distribution of the pions and heavy particles (protons, K mesons, hyperons) in the center-of-mass system, the inelasticity of the collision, the multiplicity of the showers, the percentage of strange particles, and the positive excess of the secondaries.

HIGH-ENERGY K^{-}-MESON INTERACTIONS AND DECAYS. Stanley C. Freden, Francis C. Gilbert, and R. Stephen White, Lawrence Radiation Laboratory, University of California, Livermore, California (Received October 20, 1959).

The interactions of 20- to 300-Mev K^{-} mesons on free protons and on emulsion nuclei have been studied and their decays analyzed. The K^{-}-meson mean lifetime is found to be $(1.38 \pm 0.24) \times 10^{-8}$ sec. Examples of the decay modes $K_{\mu 2}$, $K_{\pi 2}$, $K_{\mu 3}$, τ, and τ' are identified. The branching ratios are found to be in agreement with those for K^{+} mesons. The $(K^{-}p, K^{-}p)$ elastic scattering cross section is found to be 35 ± 16 mb and the $(K^{-}p, \Sigma^{\pm}\pi^{\mp})$ cross section 27 ± 13 mb in the energy region of 150 to 300 Mev. The mean free path for K^{-}-meson captures and inelastic scatters on emulsion nuclei, except hydrogen, can be represented by $\Lambda(\mathrm{cm}) = (17.2 \pm 3.4) + (0.081 \pm 0.027)T_K$, for K^{-}-meson energies from 20 to 300 Mev. This increase in the mean free path with K^{-}-meson energy is explained in terms of the decreasing nucleon cross section. The fraction of the interactions of K^{-} mesons on nuclei which are inelastic scatters increases from 2% at low K^{-}-meson energies to about 15% at 150 Mev. This increase in inelastic scat-

tering with energy is additional evidence that the nucleus is becoming partially transparent to K^- mesons at about 150 Mev. Data are presented for the fraction of events with observed π mesons, Σ hyperons, and π meson-Σ hyperon pairs. The data are discussed in terms of the model which was previously presented to explain K^--meson captures at rest on nucleons bound in nuclei.

π^+-p INTERACTIONS PRODUCING Σ^+-K^+ IN A PROPANE BUBBLE CHAMBER. W. H. Hannum,* H. Courant, E. C. Fowler, H. L. Kraybill, J. Sandweiss, and J. Sanford, Yale University, New Haven, Connecticut (Received November 13, 1959).

Seven cases of production of Σ^+-K^+ by 1.0-Bev π^+-p interactions have been identified in the Yale propane bubble chamber. In six of these cases, the Σ^+ direction was forward in the center-of-momentum system. The cross section derived from these is 0.08 mb. The decay of the Σ^+ is equally divided between the pion and proton decay modes.

*Now at Westinghouse Atomic Power Laboratory, Pittsburgh, Pennsylvania.

FURTHER SEARCH FOR THE DECAY $\mu^+ \to e^+ + \gamma$. S. Frankel, V. Hagopian, J. Halpern, and A. L. Whetstone, University of Pennsylvania, Philadelphia, Pennsylvania (Received November 4, 1959).

A new experiment for determining the upper limit for the branching ratio R of the process $\mu^+ \to e^+ + \gamma$ relative to the normal decay mode $\mu^+ \to e^+ + \nu + \bar{\nu}$ yields a value of R of less than 1.2×10^{-6} with a 90% confidence level.

EVIDENCE FOR A FORBUSH TYPE OF DECREASE IN THE INTENSITY OF HEAVY NUCLEI OF THE PRIMARY COSMIC RADIATION. S. Biswas,* P. J. Lavakare,† K. A. Neelakantan, and P. G. Shukla, Tata Institute of Fundamental Research, Bombay, India (Received November 13, 1959).

In an emulsion stack flown on March 13, 1956, from Iowa, the flux of heavy nuclei with $Z \geq 6$ in the primary cosmic radiation was measured as 15.8 and 4.7 particles/m^2 sec sr for particles of kinetic energy ≥ 0.23 and ≥ 1.55 Bev/nucleon, respectively. The measured flux of energy ≥ 1.55 Bev/nucleon was 45 ± 11% lower than the normal flux. It is shown that almost the entire part of the reduction must be attributed to a large Forbush decrease of the cosmic radiation that occurred at the same time. The exponent of the integral energy spectrum of heavy nuclei ($Z \geq 6$) was measured as 1.7 ± 0.25 in the energy interval 0.23 to 9 Bev/nucleon. As this value is not significantly different from its normally measured value, it appears that the large reduction in the primary flux was not accompanied by any significant change in the energy spectrum.

*Now at the University of Minnesota, Minneapolis, Minnesota.

†Now at the University of Rochester, Rochester, New York.

ANGULAR DISTRIBUTION OF FRAGMENTS FROM THE FISSION OF BISMUTH BY 450-Mev PROTONS. M. V. Ramaniah* and Nathan Sugarman, Enrico Fermi Institute for Nuclear Studies, University of Chicago, Chicago, Illinois (Received November 4, 1959).

Test experiments on the "bead-cone" method used for the measurement of the angular distribution of fission fragments from the 450-Mev proton fission of bismuth have been performed. These experiments make doubtful the conclusions of the previous measurement.

*Present address: Radiochemistry Laboratory, Atomic Energy Establishment, Trombay, Bombay, India.

SMALL-ANGLE PROTON SCATTERING AT 3 Bev. W. M. Preston, Richard Wilson, and J. C. Street, Cyclotron Laboratory, Harvard University, Cambridge, Massachusetts (Received November 2, 1959).

The differential cross section for elastic scattering of 3-Bev protons has been measured from targets of hydrogen, carbon, copper, and lead over the angular range 0.5 to 4 degrees in the laboratory coordinate system. Within our limits of error, no evidence of Coulomb-nuclear interference was found. In the case of hydrogen, the real component of the nuclear scattering amplitude (if any) is not over one-tenth the imaginary;

less stringent limits can be set for the other elements because of experimental uncertainties. For carbon, the differential nuclear scattering cross section at zero degrees agrees with that predicted by the optical theorm for a purely imaginary scattering amplitude; the lack of such agreement found for hydrogen may be evidence for a spin-dependent term. A derived value of the rms radius for p-p scattering exceeds that found in electron-proton scattering by a factor $\sqrt{2}$.

INTERACTION OF K^+ MESONS WITH PROTONS. T. F. Kycia,* L. T. Kerth, and R. G. Baender, Lawrence Radiation Laboratory, University of California, Berkeley, California (Received September 11, 1959).

The total K^+-p cross section was measured at the three K^+-meson energies 175 ± 25, 225 ± 25, and 275 ± 25 Mev, and the differential scattering cross section was measured at 225 Mev. The K^+-p nuclear force was shown to be repulsive, from the observed constructive interference with Coulomb scattering. The differential cross section was otherwise isotropic and could arise from either pure S-wave or pure P-wave scattering.

Subtracted dispersion relations were applied to these data and the rest of the available K-proton scattering data. The statistical errors in the data were found to be too large to determine the K-hyperon relative parity. On the assumption that the $K\Lambda$ and $K\Sigma$ relative parities are the same, then for scalar coupling, $g^2/4\pi$ would be less than 0.6; for pseudoscalar coupling, it would be less than 10.

*Present address: Brookhaven National Laboratory, Upton, New York.

NEUTRON FORM FACTORS FROM HIGH-ENERGY INELASTIC ELECTRON-DEUTERON SCATTERING. S. Sobottka,* Department of Physics and High-Energy Physics Laboratory, Stanford University, Stanford, California (Received November 30, 1959).

The inelastic electron-deuteron scattering cross section has been measured for incident electron energies between 300 Mev and 650 Mev and for final electron energies primarily at the maxima of the inelastic continuua. The data were interpreted in terms of neutron form factors by employing the impulse approximation calculations of Goldberg. The results indicate that $F_{2n}{}^2$ is nearly equal to the proton form factor $F_p{}^2$ for $2.65 < q^2 < 15.1$ (fermi)$^{-2}$ but may be 20% or 30% higher than $F_p{}^2$ for the lowest of these q values. Uncertainties, primarily in the theory, make it impossible to determine whether the difference is real. The results also indicate that $-2.5 < F_{1n}/F_{2n} < 0.5$ for $5.1 < q^2 < 12.8$ f^{-2}.

*Now at Boeing Scientific Research Laboratories, Boeing Aircraft Company, Seattle, Washington.

COSMIC-RAY HEAVY NUCLEI AT THE GEOMAGNETIC EQUATOR. D. D. Kerlee and O. K. Krienke, Jr., Seattle Pacific College Institute for Research, Seattle, Washington, J. J. Lord, Department of Physics, University of Washington, Seattle, Washington, and M. E. Nelson, Department of Physics, College of Puget Sound, Tacoma, Washington (Received October 16, 1959).

The flux of primary cosmic-ray heavy nuclei has been measured with a sandwich of C-2 and G-5 emulsions near the island of Guam, magnetic latitude 4°N. The emulsions were exposed at about 101 000 ft for 7.3 hours and the calculated fluxes at the top of the atmosphere in particles/m^2-sec-sr were found to be:

Li, Be, B	(L nuclei)	0.26 ± 0.05,
C, N, O, F	(M nuclei)	0.66 ± 0.10,
$Z \geq 10$	(H nuclei)	0.37 ± 0.09.

This flight took place on February 12, 1957, about a year prior to the sun spot maximum; however, there is no evidence within statistical error for any changes in the composition of the primary heavy nuclei.

HIGH ORBITAL S-STATE CAPTURE OF π^- MESONS BY PROTONS. T. B. Day, G. A. Snow, and J. Sucher, Department of Physics, University of Maryland, College Park, Maryland (Received November 30, 1959).

The consequences of the very short capture time for π^- mesons in liquid hydrogen, recently measured by Fields, Yodh, Derrick, and Fetkovich, are discussed. It is pointed out that colli-

sional de-excitation mechanisms, even including the Stark effect enhancement of capture, are inadequate to explain the experiment. Alternative possibilities are discussed.

MUON CAPTURE IN He^3. Akihiko Fujii, Department of Physics, Purdue University, Lafayette, Indiana (Received November 20, 1959).

The hard-core wave function for a three-nucleon system is used to calculate the capture rate of the reaction $\mu^- + He^3 \rightarrow H^3(\text{ground state}) + \nu$. It is found to be 1.66×10^3 sec^{-1}.

INTERFERENCE PHENOMENA IN NUCLEAR SCATTERING OF NEUTRAL K MESONS. Nripendra N. Biswas, Lawrence Radiation Laboratory, University of California, Berkeley, California (Received November 16, 1959).

The scattering of neutral K mesons has been treated phenomenologically. The scattered beam, in general, contains both K_0 and $\overline{K}_0$ components having different amplitudes. These amplitudes interfere with each other in the generation of K_1 and K_2 components in the scattered beam. The relative sign of the two amplitudes may then be determined from the analysis of K_1, K_2 decays. The leptonic decay rates of the scattered beam show a dependence on ΔM, the mass difference between K_1 and K_2, in such a way that the sign of ΔM can, in principle, be determined experimentally.

LIFETIME MATRIX IN COLLISION THEORY. Felix T. Smith, Stanford Research Institute, Menlo Park, California (Received October 16, 1959).

The duration of a collision is usually a rather ill-defined concept, depending on a more or less arbitrary choice of a collision distance. If the collision lifetime is defined as the limit, as $R \rightarrow \infty$, of the difference between the time the particles spend within a distance R of each other and the time they would have spent there in the absence of the interaction, a well-defined quantity emerges which is finite as long as the interaction vanishes rapidly enough at large R.

In quantum mechanics, using steady-state wave functions, the average time of residence in a region is the integrated density divided by the total flux in (or out), and the lifetime is defined as the difference between these residence times with and without interaction. Transformation properties require construction of the lifetime matrix, Q. If the wave functions ψ_i are normalized to unit total flux in and out through a sphere at $R \rightarrow \infty$, the matrix elements are

$$Q_{ij} = \lim_{R\to\infty}\left[\int^{r<R} \psi_i \psi_j^* d\tau - R(v_i^{-1}\delta_{ij} + \sum_k S_{ik} v_k^{-1} S_{jk}^*)\right]_{\text{av}},$$

where the average value is taken to eliminate oscillating terms at large R. Here, S_{ik} is an element of the unitary scattering matrix, S, and v_i is the velocity in the ith channel. Q is Hermitian; a diagonal element Q_{ii} is the average lifetime of a collision beginning in the ith channel. As a function of the energy, Q is related to S: $Q = -i\hbar S dS^\dagger dE$; Q and S contain the same information, from complementary points of view. When Q is diagonalized, its proper values, q_{ii}, are the lifetimes of metastable states if they are large compared to $\hbar/E$; for a sharp resonance, the measured lifetime is the average of $q_{ii}(E)$ over a distribution in energy. The corresponding eigenfunctions, Ψ_i, are the proper functions to describe these metastable states. The causality principle appears directly from an inequality involving the integral expression for Q_{ii} or q_{ii}, and it is shown how some of its consequences for inelastic collisions can be deduced.

RADIATIVE PION DECAY INTO ELECTRONS. Sidney A. Bludman and James A. Young, Lawrence Radiation Laboratory, University of California, Berkeley, California (Received June 25, 1959; revised manuscript received January 8, 1960).

The possibility of distinguishing the pion structure-dependent radiation from the conventional inner bremsstrahlung radiation in the radiative decay of pions into electrons is discussed. Calculation of the photon energy spectrum and angular correlation shows that evidence for pion structure would be obtained if any photons of energy less that 70 Mev were detected in 180° coincidence with π-decay electrons. The probability of such events per unit solid angle is ≥ 0.2

$\times 10^{-7}$ relative to ordinary $\pi \to \mu + \nu$ decay, if the assumption of a conserved vector current is made to relate the rate of radiative decay through the weak V interaction to the rate of $\pi^0 \to 2\gamma$ decay.

THEORY OF ALLOWED AND FORBIDDEN TRANSITIONS IN MUON CAPTURE REACTIONS. Masato Morita, Columbia University, New York, New York, and Akihiko Fujii, Brookhaven National Laboratory, Upton, New York (Received November 9, 1959).

A general formula for the transition rate of the muon capture reaction, $\mu^- + (A, Z) \to \nu + (A, Z-1)$, where the final nuclear state has definite spin and parity, is given in terms of the total and orbital angular momenta of the emitted neutrino and of the spins of the initial and final nuclear states. The induced pseudoscalar interaction and the interaction due to the assumption of conserved vector current are taken into account, together with the vector and axial vector interactions. The forbiddenness of the muon capture reaction is defined in a manner analogous to the theory of the beta decay. The spin and parity changes can assume the values (0+, 1+), (0-, 1-, 2-), $[n(-)^n, n+1(-)^n]$ for the allowed, first forbidden, and nth ($n \geq 2$) forbidden transitions, respectively. (+ and - mean the parity change "no" and "yes.") For these transitions, the number of reduced nuclear matrix elements involved is nine, sixteen, and fourteen, respectively. The transition rate of the muon capture reaction is reduced by a factor of 10^3, approximately, for a two-unit increase of the forbiddenness, if the atomic number and the energy of the neutrino are constant. The contribution from the higher order transition to the lower one is less than 0.1% in the medium and light nuclei. Explicit formulas for the transition rate are given for the allowed, first forbidden, and nth forbidden transitions. They are related to the corresponding formulas of beta decay. Our formalism was applied to the calculation of the partial muon capture rate by C^{12} ending in the ground state of B^{12}. The numerical analysis indicates that measurement of this capture rate can determine whether the conserved vector current interaction term exists in nature only if the coupling constant of the induced pseudoscalar interaction and the nuclear wave functions are well known. The transition rates are given for the j-j coupling shell model and harmonic oscillator wave functions. They are 9-13% smaller than those given by Fujii and Primakoff.

ELECTROMAGNETIC STRUCTURE OF THE NUCLEON. Adam M. Bincer, Department of Physics, University of California, Berkeley, California (Received November 16, 1959).

Dispersion relations are proved for the electromagnetic and mesonic nucleon vertex functions considered as a function of the nucleon mass. The results are used to express the isotopic scalar and the isotopic vector electromagnetic form factors of the nucleon in terms of pion electroproduction (or photoproduction) and pion-nucleon scattering amplitudes in the $J = \frac{1}{2}$, $T = \frac{1}{2}$ state.

T, P, C SYMMETRIES IN THE π^0 DECAY. Jeremy Bernstein and Louis Michel,* Ecole Polytechnique, Paris, France (Received November 19, 1959).

An analysis is given of the decay of the π^0 in which allowance is made for possible breakdowns in T, P, and C symmetries. It is shown that experiments, until now, have demonstrated only that the two-photon state is an eigenstate of TP, but not of T and P separately. A discussion of experiments which may verify T and P symmetry for the two-photon state is given.

*Present address: Service de Physique Théorique, Faculté des Sciences, B. P., Orsay (Seine-et-Oise), France.